8-2021

Effect of Obesity on Walking to Running and Running to Walking Transitions

Salvador Baruch Alcorta Bautista
The University of Texas Rio Grande Valley

EFFECT OF OBESITY ON WALKING TO RUNNING AND RUNNING TO WALKING TRANSITIONS

A Thesis

by

SALVADOR BARUCH ALCORTA BAUTISTA

Submitted to the Graduate College of
The University of Rio Grande Valley
In partial fulfillment of the requirements for the degree of

MASTER OF SCIENCE IN ENGINEERING

August 2021

Major Subject: Mechanical Engineering

EFFECT OF OBESITY ON WALKING TO RUNNING AND RUNNING TO WALKING TRANSITIONS

A Thesis
by
SALVADOR BARUCH ALCORTA BAUTISTA

COMMITTEE MEMBERS

Dumitru I. Caruntu, PhD, PE
Chair of Committee

Robert Freeman, PhD
Committee Member

Mircea Chipara, PhD
Committee Member

Javier Ortega, PhD
Committee Member

August 2021

ABSTRACT

Alcorta Bautista, Salvador B., Effect Of Obesity On Walking To Running And Running To Walking Transitions. Master of Science in Engineering (MSE), August, 2021, 112 pp., 9 tables, 162 figures, references, titles.

This work investigates human Walking to Running transition (WRT) and Running to Walking transition (RWT). The focus is to be able to identify the correct WRT and RWT phase jumps. This investigation uses experimental data from the VICON Motion Analysis System (MAS) and of the treadmill WRT and RWT trials. The musculoskeletal model consists of pelvis, femur, tibia, and foot. This investigation uses as reference the work reported in the literature by Diedricj and Warren.. For the calculations in this investigation Excel and Matlab are used to filter the data and calculate the relative phase jumps. This work reports the effects of experimental MAS capture frequency, and subject's level of obesity, on WRT and RWT. Specifically, in order to investigate obesity, the subject's experiments were conducted with no additional weight of the subject, additional weight of the subject of 5 Kg, 10 Kg, and 15Kg.

Keywords:

Walking to Running Transition (WRT), Running to Walking Transition (RWT), Gait Transition,Weight, Biomechanics, Frequency, Vicon, Nexus

DEDICATION

I dedicate my thesis to my mother, Isabel Bautista Magaña, who has always been my base model and inspiration to become the best person I could be, and my grandfather Jose Maria Bautista Perez, who taught me to be patient and focused on my daily life. To my girlfriend Kathia Berenice Aleman Montero, who always motivated me to keep pursuing my dreams. Thank you for your patience, love, and support.

ACKNOWLEDGMENT

I would like to thank Dr. Dumitru Caruntu, chair of my thesis committee for his mentorship and support. Thanks for your patience, comprehension, and support on this research. Thanks for pushing me to investigate, learn and analyze in a different manner. Thanks for accepting me as your student and teach me how to do research and helping me to become a better engineer.

TABLE OF CONTENTS

LIST OF TABLES

LIST OF FIGURES

CHAPTER I

INTRODUCTION

The analysis of human kinematics by recording and analyzing humans has been of great interest for biomechanists, bioengineers, and for rehabilitation purposes. Understanding gait patterns is crucial for identifying abnormalities from disease, disuse, or injuries [1]. This type of analysis understanding is very helpful in sports and rehabilitation analysis, and for improving different sport techniques such as the batting technique from some all-star players to the running technic adopted for Olympic competitors, Fig. 1.

Fig. 1. Example of biomechanical analysis performed on a runner.

1.1. Gait patterns

Legged locomotion is the natural transportation in humans, and walking and running are the two most common gait patterns among them [2]. Humans walk at low speed and switch spontaneously to running when they are moving faster [3]. One of the main differences between walking and running is the existence of a flight phase in the running gait, instead of a double support phase existent in the walking gait [4].

The analysis of gaits typically corresponds to three major objectives in mind: a) To improve understanding of how locomotor system works, b) to bring abnormal gaits closer to normal standards, and c) improve normal or above average gait performance to exceptional levels such as the trainings and analysis made to athletes [1]. In Fig. 2 is shown how the gait walking gait cycle is performed according to Ref. [1].

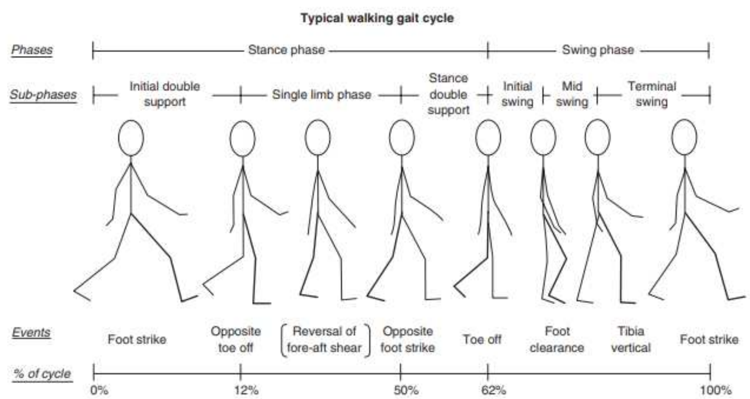

Fig. 2. Walking gait cycle [1]

In order to be able to discern walking from running kinematically, the knee ankle is the preeminent variable. The knee extension is the key to identify the gait pattern: a more extended knee is inherent in walking, and more knee flexion is typical in running [5].

The running to walking gait is a sustained gait that humans can achieve, although not energetically efficiently below the preferred speeds for walking [1]. One of the main differences on the gaits is on the center of mass, which on the running gait behaves like a bouncing ball, that's why the model for the center of mass is represented as a spring [6].

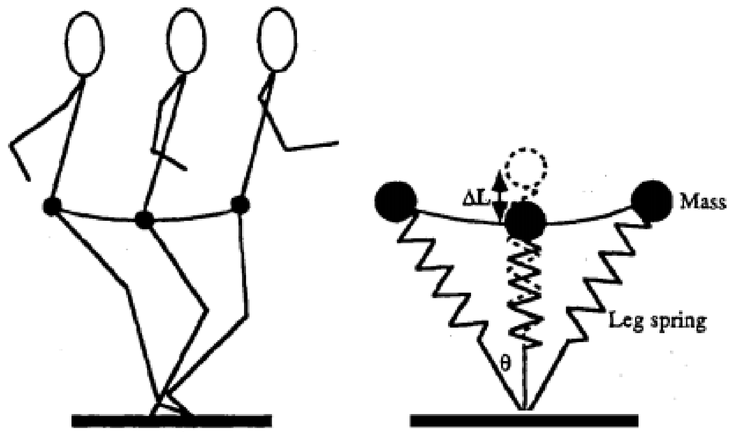

Fig. 3. Spring mass model for the center of mass representing the human running behavior, Farley and Ferris [6].

Another big difference between the walking and running gaits is that running has an aerial phase from the foot. This flight phase or aerial phase consists of none of the feet is in contact with the ground as can be observed on Fig. 4 [6,7].

Fig. 4. Flight phase present during running gait

1.2.Energetic cost for gait transitions.

Hreljac [7] suggested that the Walking to Running Transition (WRT) was determined by the local muscular fatigue in the dorsiflexors. Also he suggested that this local fatigue may be associated with the high angular velocities and accelerations required on the ankle to prevent the toe from dragging at toe-off at high velocity walking. Several studies suggest that the gait transition occurs to avoid energetic cost to keep the gait above certain conditions. Some authors suggest that the energetically optimal transition speed should be the speed where the gait transition should occur. However, has been demonstrated that the transition speed is below the optimal values [7].

CHAPTER II

EXPERIMENTAL PROTOCOL

2.1.Warm up procedure.

A warm-up procedure is proposed [2,9,10].

Fig. 5. Subject on the warm-up period, with the horizontal treadmill.

The subject had a 5 minute for warming-up exercise on the treadmill, Fig. 5. This period is granted to improve blood flow to the legs previous to the Walking to Running Transitions (WRTs) and Running to Walking Transitions (RWTs). Also, the warm-up period helps the subject to familiarize with the dynamics of running on the treadmill.

2.2.Protocol.

2.2.1. Changing frequencies experimental protocol, constant body weight

VICON Motion Analysis cameras have available different capture speeds. According to the manufacturer, the cameras can work for a range up to 360 frames per second (Hz) without compromising the image resolution, thus 4 different capture speeds were defined: 100 Hz (100 frames per second), 150 Hz (150 frames per second), 250 Hz (250 frames per second), and 350 Hz (350 frames per second).

The trial starts with the capture speed at 100 Hz (Standard configuration). On the WRT test, the subject started at 3.0 mph, having a stabilization time of 15 seconds. This time is given to the subject to have a steady pace at that speed. When the stabilization period is over, the recording started, and the speed was set to increase up to 6.0 mph. After the subject reaches the final speed, the treadmill was stopped. After the test, the subject had a 5-minute rest, and the camera capture speed was modified. When the 5-minute rest time was done and the capture speed modified, the trial started over again.

In the RWT, the same experimental technique is used. The capture speed starts at 100 Hz. The subject had a stabilization period of 15 seconds at 6.0 mph. When the stabilization period was over, the recordings started and the speed gradually decreased to 3.0 mph, and the treadmill was stopped. A 5-minute rest is given to the subject and the capture speed is modified to the next defined value.

2.2.2. Constant capture frequency, changing body weight.

The subject was required to perform the warm-up period before starting to record different trials. The warm-up period consisted on the subject walking on the treadmill at 3 mph for a period of 5 minutes. After this first warm-up period, a second warm-up was performed on the treadmill at 6 mph.

The treadmill was placed in a horizontal position, parallel to the ground. Once the warm-up period was over, the WRT trial started. The subject stood on the treadmill walking at 3 mph for a period of 30 seconds, for the subject to stabilize. After the stabilization period, the recording started, and past 5 seconds, the subject changed the speed from the treadmill to 6 mph. The speed was assumed to increase linearly, and the recording stopped 5 seconds after the maximum speed was reached. The subject had a 2-minute rest to avoid fatigue.

On the RWT trials, the same procedure was used. The subject started running at 6 mph on the treadmill before the recording started (Stabilization period) and then, after 5 seconds the recording was started, the velocity was decreased linearly to 3 mph. Once the recording was ended, the treadmill was stopped, and the subject had 2 minutes rest.

The subject had to perform each WRT and RWT trials with a different bodyweight. To do this, the subject carried a weighted vest during the trial. The body weight increments were defined as in Table 1:

Table 1: Additional body weight per trial.

	Additional Body Weight (Kg)
Trial 1	0
Trial 2	5
Trial 3	10
Trial 4	15

Between each trial, the subject had a 3-minute rest period. Once the WRT trials ended, the subject had a 5-minute rest and then the RWT trials started.

2.3.Markers

The reflective markers that are used on the Vicon data acquisition system were placed over previously defined positions in Fig. 6 and were the same on both exercises: changing capture frequency and changing additional body weight. These markers allow us to acquire the required data and be able to analyze the gait transitions from the subject.

The markers' location are on both right and left sides of the body as follows: Anterior Superior Iliac, Greater Trochanter, Trochanter References (1 to 4), Knee (Lateral and medial), Tibial Tuberosity Protuberance, Ankle (Lateral and Medial), Sheen (1 to 4) , Thumb Toe (Hallux), foot (1 to 4), as depicted in Fig. 6.

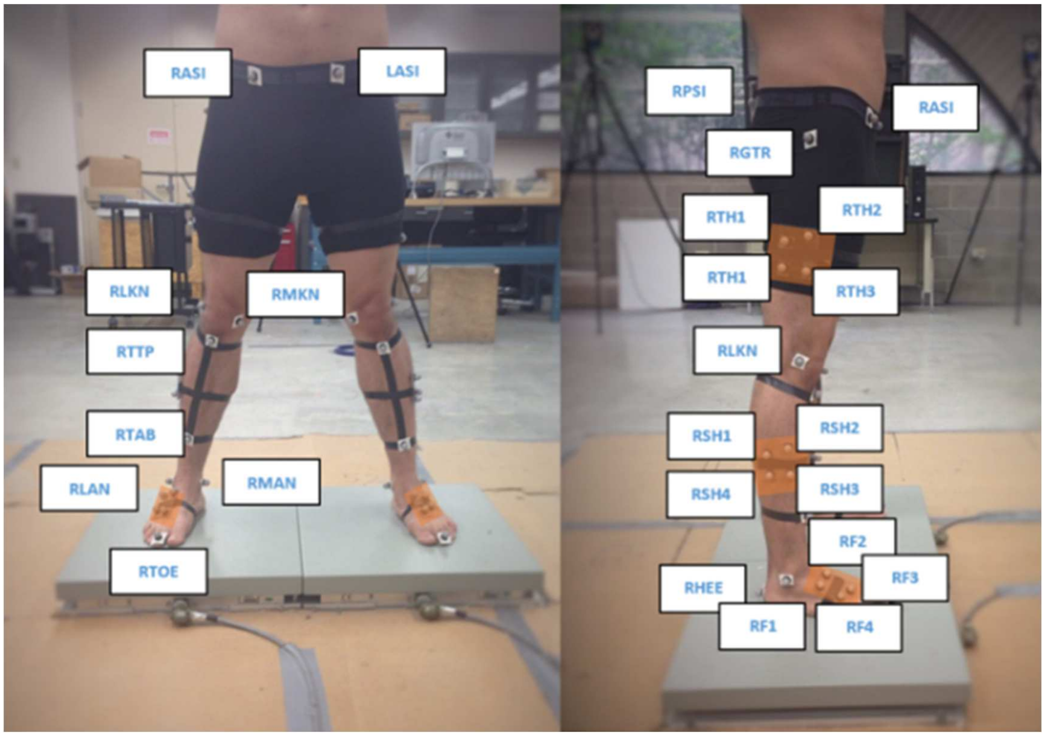

Fig. 6. Markers location on the subject.

CHAPTER III

DATA FILTERING

3.1.Data filtering and cutoff frequency.

The experimental data from the exercises was captured and processed using VICON's software Nexus. The obtained values are X, Y and Z coordinates of the markers referenced to an origin set during the calibration of the system. These coordinates were used to calculate subject's speed as well as the gait transitions. Experimental data contained noise. Thus filtering the noise out of the signal was necessary. This data was exported to a excel spreadsheet and filtered using a double Butterworth Low Pass filter. To filter the data, the used formulas are obtained from Winter [8] :

$$w_c = \frac{\left(\tan\left(\frac{\pi f_c}{f_s}\right)\right)}{C}, where\ fs = 100\ (Signal\ frequency = 100\ hz) \tag{1}$$

$$K = \sqrt{2w_c} \tag{2}$$

$$k2 = {w_c}^2 \tag{3}$$

$$a_0 = \frac{k_2}{(1+k1+k2)} \tag{4}$$

$$a_1 = 2a_0 \tag{5}$$

$$a_2 = a_0 \tag{6}$$

$$k_3 = \frac{2a_0}{k_2} \tag{7}$$

$$b_1 = -2a_0 + k_3 \tag{8}$$

$$b_2 = 1 - a_0 - a_1 - a_2 - b_1 \tag{9}$$

To process the raw data in the time domain the following formula is used:

$$X^1(nT) = a_0X(nT) + a_1X(nT-T) + a_2X(nT-2T) + b_1X^1(nT-T) + b_2X^1(nT-2T) \tag{10}$$

where:

$X^1 = filtered\ output\ coordinates$

$X = Unfiltered\ output\ coordinates$

$nT = nth\ sample$

$(nT-T) = (n-1)th\ sample$

$(nT-2T) = (n-2)th\ sample$

$a_0 \dots b_2 = filter\ coefficients$

The results from using Eq. (10) are the n-th filtered data. This data will be used to calculate the residuals and then to find the cutoff frequency. To find the cutoff frequency, fc, a residual analysis is conducted using the values from the greater trochanter marker with the *x* and *z* displacement values. The residuals are calculated with the formula:

$$R(fc) = \sqrt{\frac{1}{N}\sum_{i=1}^{N}(X_i - \widehat{X}_i)^2} \tag{11}$$

where:

$X_i = raw\ data\ at\ the\ ith\ sample$

$\widehat{X}_i = filtered\ data\ at\ the\ ith\ sample$

When the residuals are obtained, a plot is generated. This plot represents the residuals vs the cutoff frequency. An example of this graph is on Fig. 7.

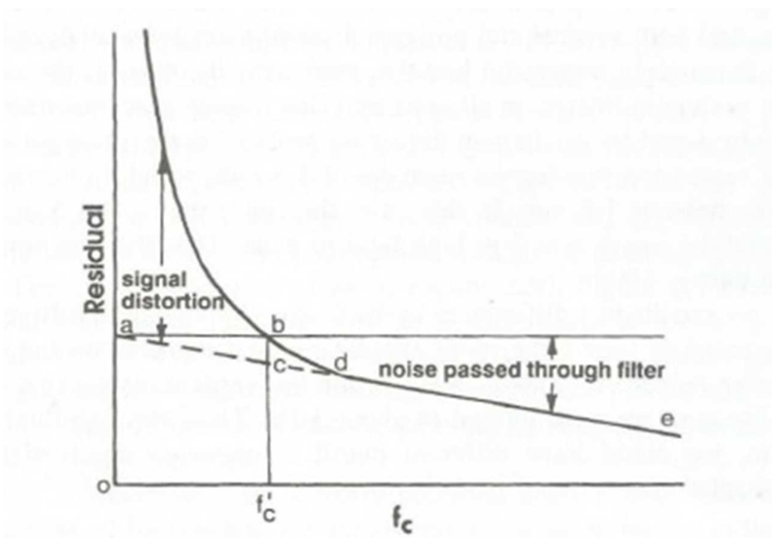

Fig. 7. Cut off frequency graphic method, described by Winter [8]

To find the cutoff frequency, Winter's method is used. Once the residuals are plotted, as in Fig. 7, a straight line is projected from points "d" and "e", and on the intersection with the residual's vertical axis one can find the point "a". Point "a" will be projected horizontally until it intersects the residuals plot. This point is identified as point "b". From point "b" will be projected a vertical line that will intersect the horizontal axis. This intersection of the horizontal axis will be the cutoff frequency. For all presented results, the greater trochanter cut off frequency was calculated, using those values to filter the data from the remaining markers.

CHAPTER IV

ANGLES, SPEED AND RELATIVE PHASE CALCULATION

4.1.Angles calculation

The data obtained from filtering, was used to calculate θ1 and θ2 angles, Fig. 8.

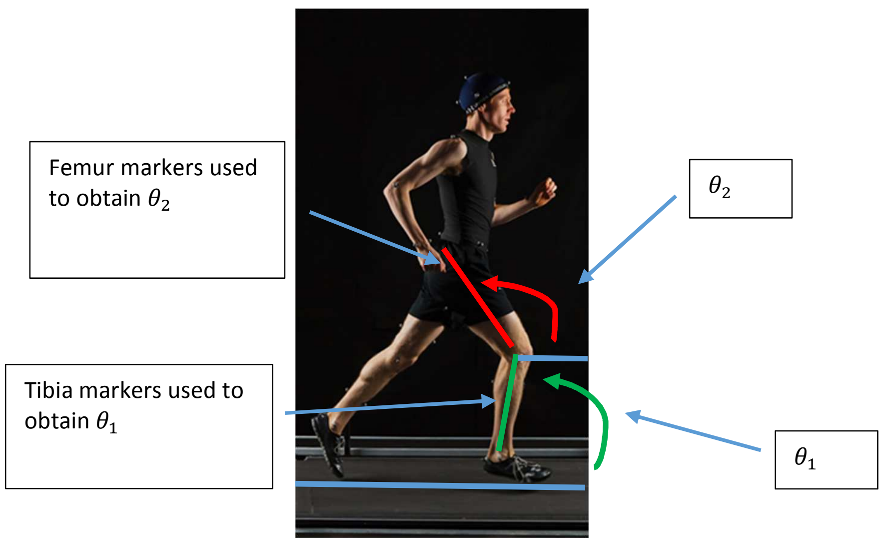

Fig. 8. Angles θ1 and θ2

The formulas used to calculate the θ values are:

$$\theta_2 = tan^{-1}(X\ LGTR - XLLKN, Z\ LGTR - ZLLKN) \tag{12}$$

$$\theta_1 = tan^{-1}(XLTTP - XLLAN, ZLTTP - ZLLAN) \tag{13}$$

$$\Delta\theta = (\theta_2 - \theta_1) \tag{14}$$

where:

XLGTR: Filtered value X from the Left Greater Trochanter marker

XLLKN: Filtered value X from the Left Lateral Knee

ZLGTR: Filtered value Z from the Left Greater Trochanter marker

ZLLKN: Filtered value Z from the Left Lateral Knee

XLTTP: Filtered value X from the Left Tibial Tuberosity Protuberance

XLLAN: Filtered value X from the Left Lateral Ankle

ZLTTP: XLTTP: Filtered value Z from the Left Tibial Tuberosity Protuberance

ZLLAN: Filtered value Z from the Left Lateral Ankle

$\Delta\theta$: Knee flexion angle.

Once all angles have been determined and knee flexion angle $\Delta\theta$ has been calculated, one can graph it, Fig. 9. These plots will allow us to calculate the relative phase. The results for the rest of the trials, are on the Appendix, Fig. 32,Fig. 34,Fig. 36,Fig. 38,Fig. 40,Fig. 42,Fig. 44,and Fig. 46 for the changing frequency trials, and Fig. 48 through Fig. 93 for the changing weight trials.

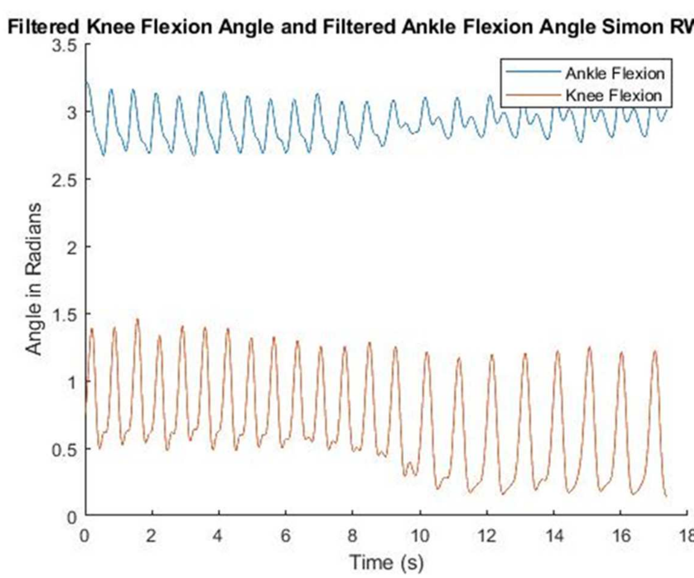

Fig. 9. Filtered knee flexion angle, and ankle flexion angle to be used to calculate relative phase transition speed

4.2. Subject's walking or running speed calculation

It is necessary to calculate the trial speed as the treadmill accelerates if WRT or decelerates if RWT, from the X and Z coordinates of the Right Heel marker. Those coordinates are obtained from the experimental data.

Once the X and Z coordinates are plotted, it is necessary to divide the plot in smaller subplots, in this case, the plots were divided in 200 frames subplots, which purpose is to obtain a more detailed view from the intersection between the minimum Z distance and the X distance.

It is assumed, that when the Z marker has its lowest values, the foot is in contact with the treadmill, thus the speed from the foot would be equal to the speed on the treadmill.

As an example, in Fig. 10 is shown that the Right heel Z coordinate is almost constant, and the distance is minimum.

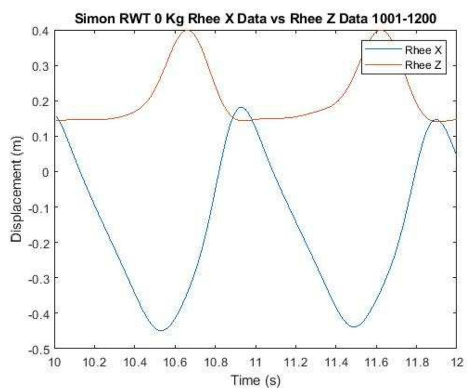

Fig. 10. Subject 1 Simon, RWT, 0 kg, right heel x vs z data, on frames 1001-1200

The speed is calculated using the formula:

$$Speed = \frac{\Delta Distance\ From\ Marker\ Right\ heel\ X(m)}{\Delta Time\ (s)} \tag{15}$$

A numerical example on how the speed is calculated is

$$Speed = \frac{(-.12930m - .1095m)}{(11.19s - 11.01s)}$$

so the speed is:

$$Speed = 1.32\frac{m}{s} \ or \ 2.95 \ Mph$$

This speed indicates that in the selected period, the treadmill speed was 2.95 mph, which corresponds to the trial minimum speed. The speed was calculated for all strides (or cycles) from the leg, by creating the subplots.

Once all plots (Complete Rhee x vs Rhee z) and subplots (Rhee X vs Rhee Z for 200 frames) were obtained, the calculated speeds were plotted in order to identify the trial starting point.

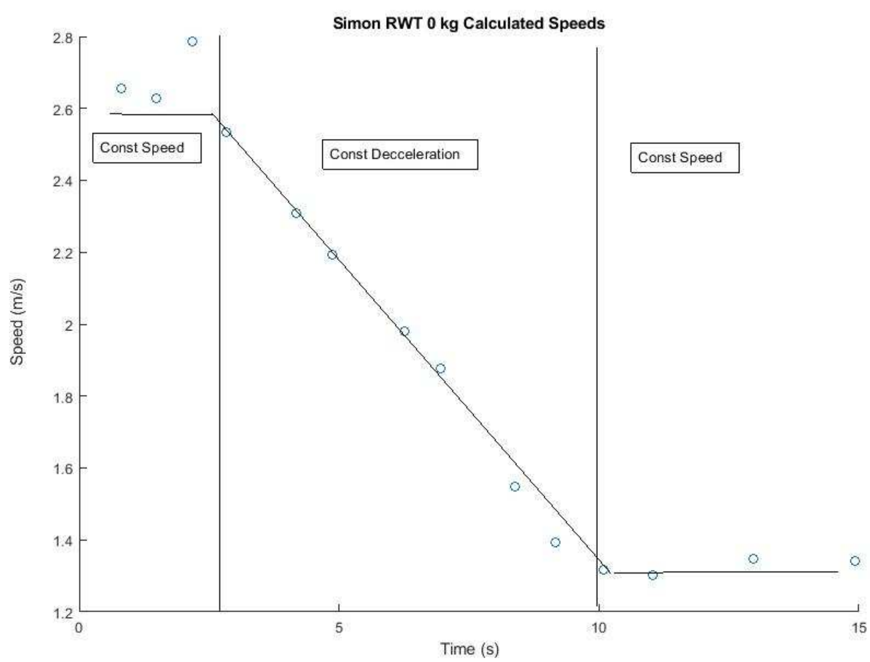

Fig. 11. Constant deceleration identification

In Fig. 11 are plotted the calculated speeds from the complete trial, indicating two constant speed zones, and a constant RWT deceleration (Acceleration on WRT trials) zone. To calculate the linear acceleration/deceleration, the constant acceleration/deceleration time zone was used, and adding 1 second on each side of the deceleration line. Thus, for this example, it was considered to use the speeds from the time from 3.5 thru 11 seconds. Those values were plotted once again, and a linear fitting was calculated.

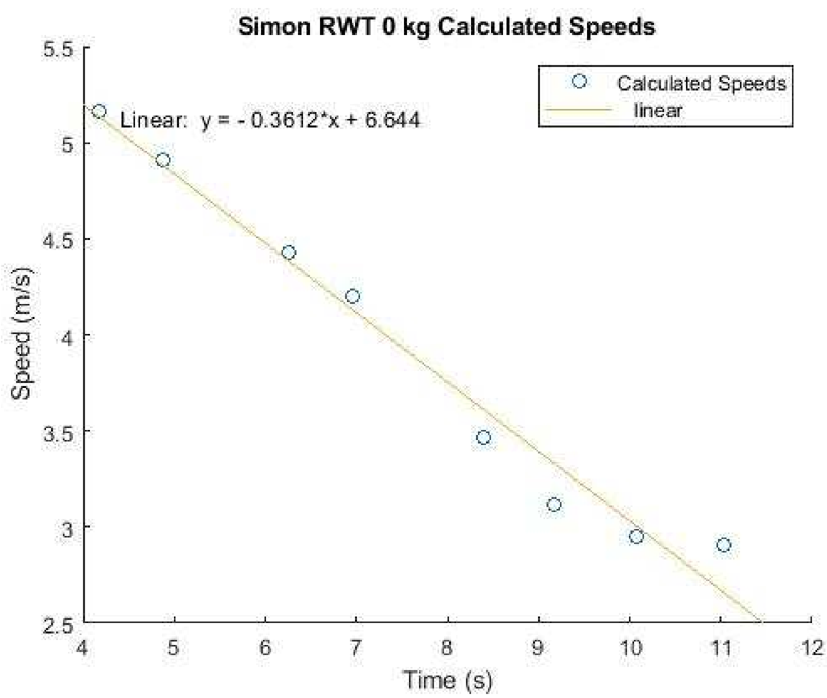

Fig. 12. Linear fitting equation for the RWT trial deceleration (zoom of Fig. 11).

The equation from the linear acceleration best fit line as depicted in Fig. 12 , was used to calculate the speeds of the WRT or RWT Relative Phase Transition Speed Plots, by using the following formula:

$$Subject\ Speed = Time(s) * m + b \tag{16}$$

where m is the linear fitting calculated slope value (Acceleration), in this case, -.3612 m/s^2, and b is the y intercept of the equation (Speed) which is 6.644 m/s. The results for the rest of the Subject Speed calculations, are on the appendix, from Fig. 94 through Fig. 139.

4.3.Relative phase

With the θ_1 and θ_2 values obtained, it is necessary to calculate the knee flexion angle and ankle flexion angle, as follows:

$$Knee\ Flexion = \Delta\theta = \theta_2 - \theta_1 \tag{17}$$

$$Ankle\ Flexion = \theta_1 - foot\ angle + \frac{\pi}{2} \tag{18}$$

$$foot\ angle = \arctan\left(\frac{xtoe - xheel}{ztoe - zheel}\right) \tag{19}$$

Once calculated, the knee flexion angle and the ankle flexion angle are plotted, obtaining a cyclic behavior that can be identified on both angles, Fig. 13.

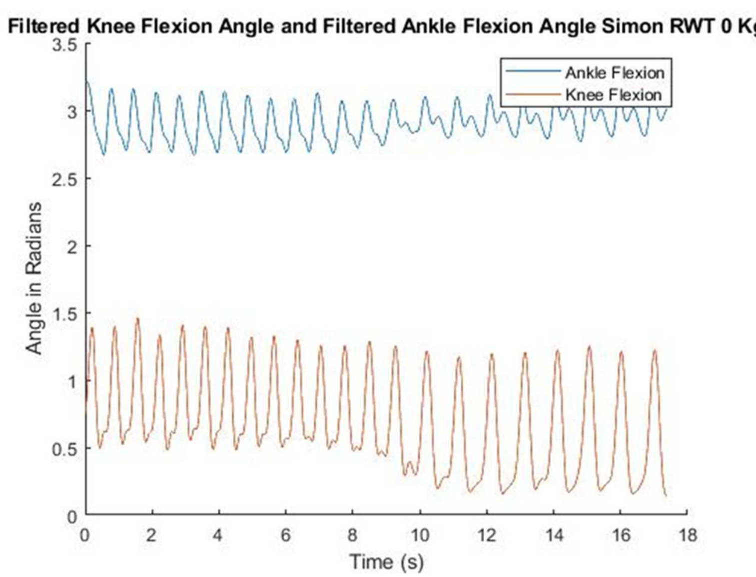

Fig. 13. Ankle and knee flexion angles

From Diedricj [9] is assumed that the period from each cycle represents 360 degrees between the points A and A', and the relative phase is the difference between the points A and B, as shown on Fig. 14.

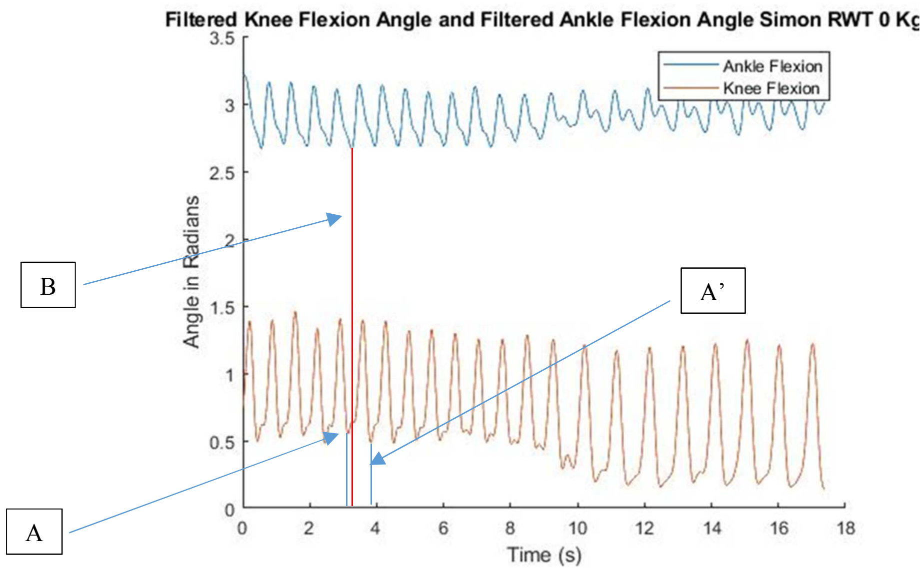

Fig. 14. Relative phase reference values as indicated by Diedricj [9], in the case of subject 1 Simon RWT trial without weight added.

This difference between the points A and B from the knee flexion and ankle flexion angles, is the relative phase angle in radians, and is converted to degrees using the formula:

$$Relative\ Phase\ (Degrees) = \frac{Relative\ Phase\ Radians * 180}{\pi} \tag{20}$$

Relative phase in degrees is plotted versus the Subject Speed, calculated with Eq. (16). This plot will allow us to analyze and be able to identify the gait transition change from Walking to Running and Running to Walking by observing a sudden jump or change in the relative phase, Fig. 15.

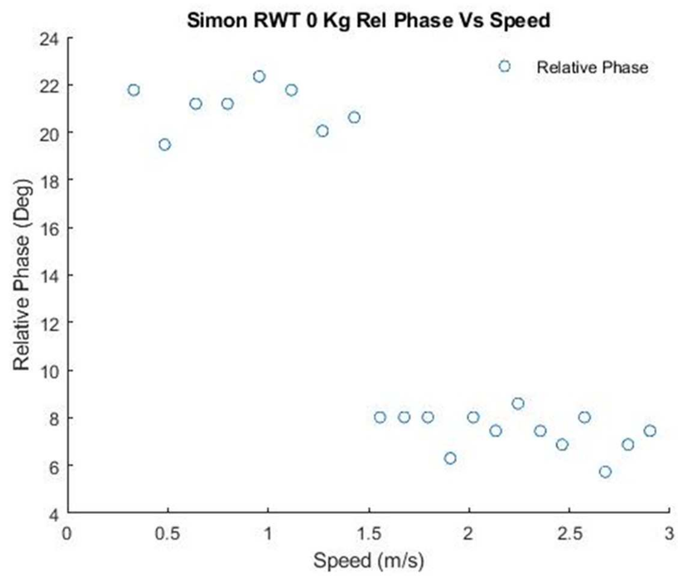

Fig. 15. Relative phase (deg) vs subject speed transition for subject 1 Simon on the RWT without weight added.

All calculations for Subject 1 Simon, Subject 2 Chuy and Subject 3 Salvador are presented on the appendix in Fig. 140 through Fig. 162.

CHAPTER V

CHANGING FREQUENCY RESULTS

5.1. Walking to running with different sampling frequency results

The objective of these experiments is to be able to identify if the capture speed (frequency) from the Vicon System affects the relative phase transition while speed is constantly increasing or decreasing.

The system setup was the standard 10 cameras configuration. The capture frequency was manually set on the Nexus Software of the VICON instrumentation. The chosen capture frequencies were 100 Hz (Standard capture frequency), 150 Hz, 250 Hz and 350 Hz.

The trials performed were WRT and RWT on the treadmill. The treadmill was horizontal and parallel to the ground. After recording the data, the data gaps were filled out in Nexus, and then the raw data was processed.

In order the eliminate the noise from the raw data, a cutoff frequency was calculated for each trial from the x coordinate of the right greater trochanter. A residual analysis was conducted to define the cutoff frequency. This cutoff frequency was used as cutoff frequency to filter all the markers of the trial.

Filtered data was processed to obtain the filtered knee and filtered ankle flexion angles, which were used to calculate the relative phase. In Fig. 16 is presented the filtered knee flexion angle plot used to calculate the relative phase, and on Fig. 17 is presented the ankle flexion angle plot used to calculate the relative phase.

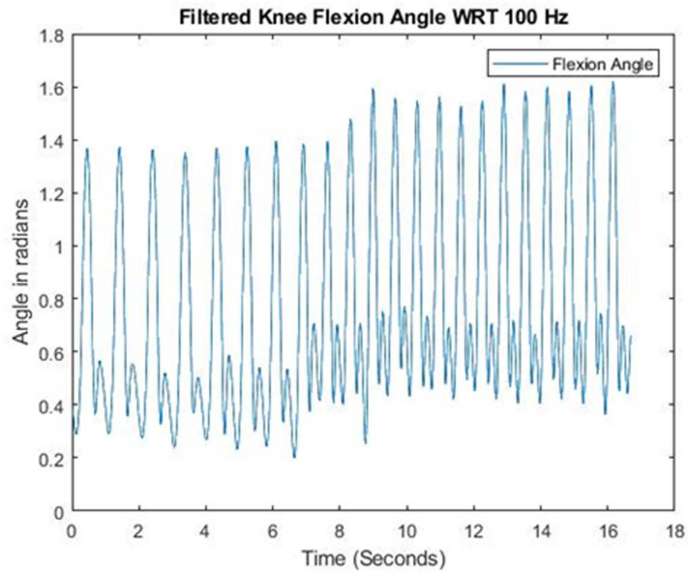

Fig. 16. Filtered knee flexion angle for WRT at 100 Hz

Once filtered the knee flexion angle and ankle flexion angle, the relative phase was calculated using Eq. (17).

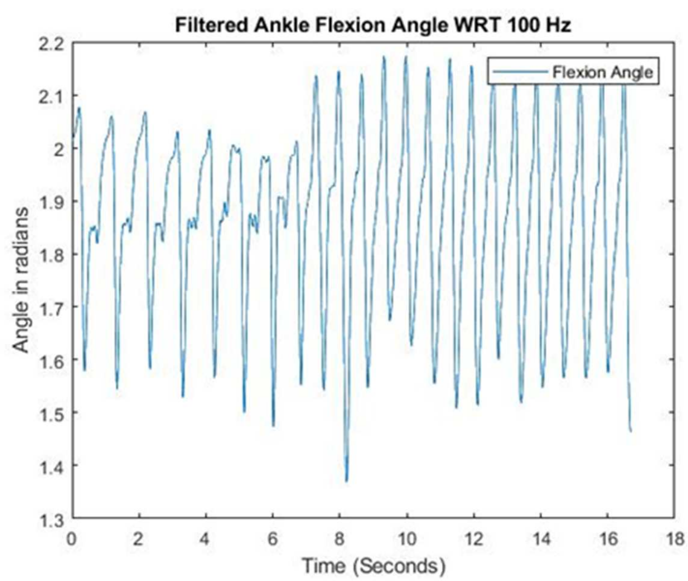

Fig. 17. Filtered ankle flexion angle calculation for WRT at 100 Hz.

The relative phase was calculated using three different methods: 1) hand calculations using Eq. (17) for each cycle of each trial. The result from this calculation was plotted in

Excel. 2) The second calculation method was using an excel template, which automatically created the relative phase plot, and 3) a Matlab code used to automatically calculate the relative phase and generate a plot.

Once the relative phase was calculated, the subject trial speed was calculated using a linear fitting on the constant acceleration zone for the trial, Fig. 18.

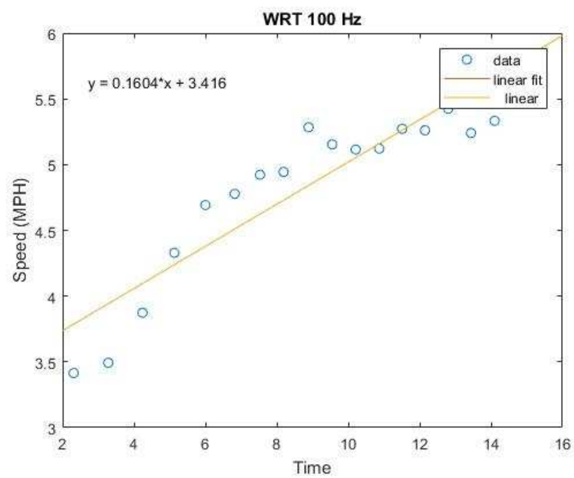

Fig. 18. Constant acceleration zone used to calculate the speed.

The equation from the linear fitting, Fig. (18), was used to generate the "Relative Phase Vs Speed" plots.

To calculate the speed, the trial time was multiplied by the slope of the linear fitting of the equation, in this case 0.1604 and the y intercept of the equation was added to the multiplication result. The relative phase vs speed plot could now be generated. To be able to check for the agreement of the three calculation methods, the relative phase of the three methods predictions were plotted. In Fig. 19 one can see the agreement between the predictions of the three methods.

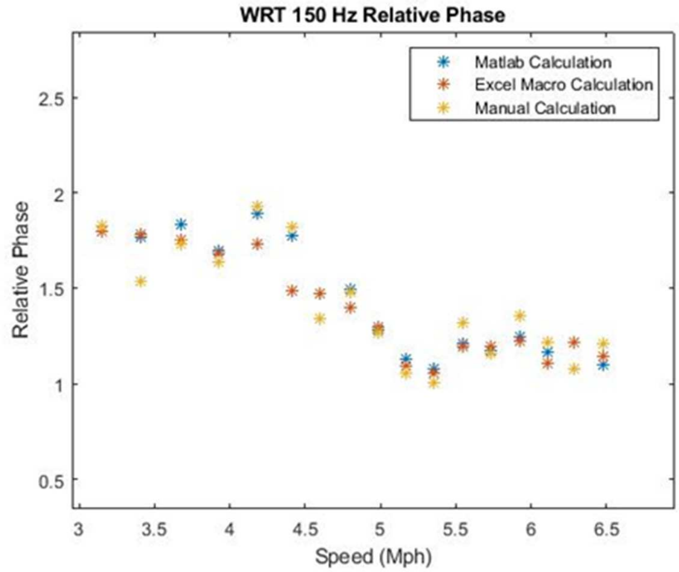

Fig. 19. Calculation methods convergence for the WRT at 150 Hz.

As the predictions agreed, the relative phase change with respect of capture frequency was analyzed. The relative phase transition speed predictions for each one of the 4 tested frequencies are shown in Table 2.

Table 2: Relative phase transition speed results by changing capture frequency

Trial	Relative Phase Transition Speed (mph)
WRT 100 Hz	4.3
WRT150 Hz	4.5
WRT 250 Hz	4.3
WRT 350 Hz	4.45
RWT 100 Hz	3.6
RWT 150 Hz	3.3
RWT 250 Hz	3.4
RWT 350 Hz	4

It can be seen that the transition speed had small variations with the capture frequency for WRT, with results that go from 4.3 to 4.5 mph. The increase in capture frequency does not show a significant increase in accuracy of the relative phase. As one can see in Fig. 20, the linear fitting line for the speed transition has a very small slope of 0.0002203, which indicates that the transition speed identification was almost constant. On the other hand, for the larger capture frequencies instead of being easier or more accurate to identify the transition speed, the amount of data needed to be handled was larger, thus, requiring more time to assign missing markers, fill gaps, calculate the cutoff frequency, filter the data, and calculate the relative phase and speed.

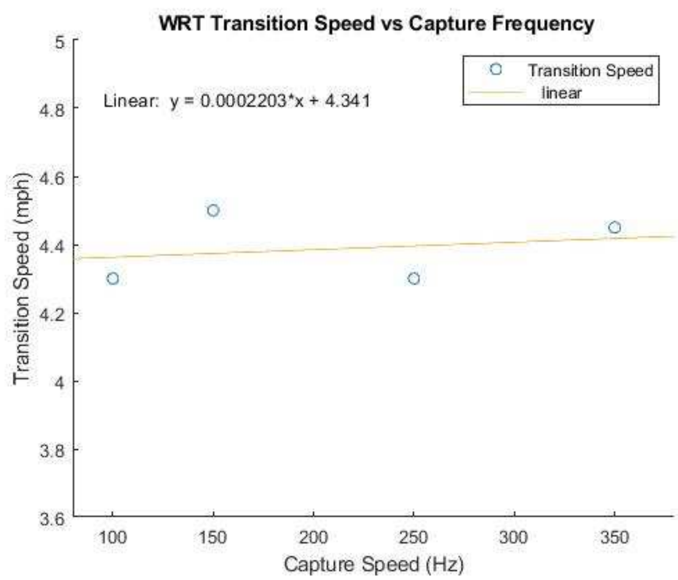

Fig. 20. Walking to running transition speed vs capture frequency linear fitting

In the case of Running to Walking exercises, the transition speed varied in the range of 3.3 to 4 mph, with the calculated linear fitting of slope of 0.001797 shown in Fig. 21. The transition speed does not show a consistent increase or decrease with the increase of the capture frequency. Also large capture frequency presents the inconvenience of large sets of data thar require significantly larger time of handling and processing.

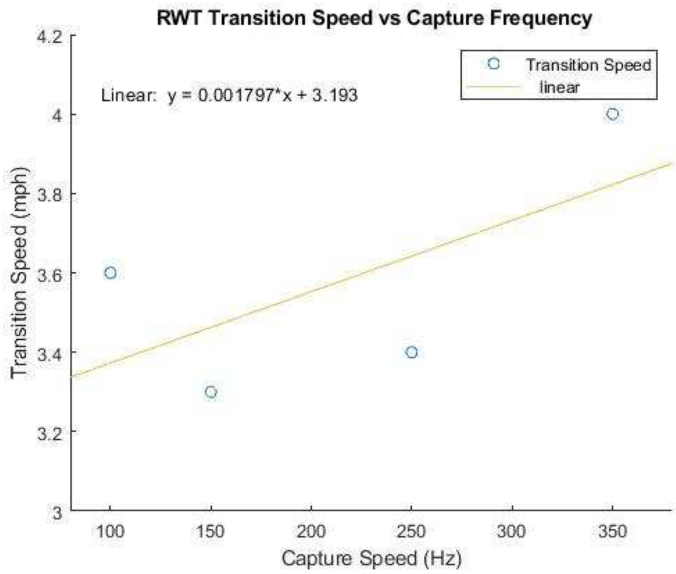

Fig. 21. Running to walking transition speed vs capture frequency linear fitting

From the results obtained on WRT and RWT, it would be recommended to keep the capture frequency at 100 Hz. This will help to avoid the amount of extra data that is not necessary and keep the data handling easier.

CHAPTER VI

EFFECT OF OBESITY ON THE TRANSITION GAIT

6.1. Running to walking results adding body weight.

From the results obtained on the second exercise, i.e. the effect of additional weight on the transition speed, it was demonstrated that added weight affected differently each subject. For Subject 1 Simon, the added weight increased the RWT speed, Table 3. This transition speed increase indicates that the higher the additional weight, the higher the speed where the transition occurs, in other words, the subject had to transition from running to walking at a higher speed.

Table 3: Subject 1 Simon Running to Walking transition speed per added weight.

Added Weight (Kg)	**Subject 1 Simon Transition Speed (m/s)**
0	1.48
5	1.47
10	1.83
15	1.79

Subject 2 Chuy, had a different behavior than Subject 1 Simon. Table 4 depicts the results from the Subject 2 Chuy, and a trend to increase speed can't be observed as in the Subject 1 Simon on Table 3. In this case, Subject 2 Chuy started without additional weight at 1.65 m/s and did increase the speed by 0.5 m/s when increased the weight to 10 Kg, as seen on Table 3, but then had a decrease in speed when the weight was increased to 15 Kg and had a speed reduction to 1.61 m/s, a lower speed than the recorded speed without weight added. So, when the weight was added, the subject kept running more time, and even at lower speeds than the Subject 1 Simon.

Table 4: Subject 2 Chuy running to walking transition speed per added weight

Added Weight (Kg)	**Subject 2 Chuy Transition Speed (m/s)**
0	1.65
5	2.01
10	1.69
15	1.51

For Subject 3 Salvador, the increase in additional weight increased the RWT speed, Table 5. Subject 3 Salvador had similar results to the ones obtained from Subject 1 Simon in Table 3, i.e. Subject 3 Salvador increased the transition speed as the added weight increased. The subject started with a transition speed of 1.73 m/s without added weight and increased the speed until the 15 Kg. added trial, where the transition speed resulted in 1.89 m/s.

Table 5: Subject 3 Salvador running to walking transition speed per added weight.

Added Weight (Kg)	**Subject 3 Salvador Transition Speed (m/s)**
0	1.73
5	1.77
10	1.91
15	1.89

In Fig. 22, are plotted the relative phase transition speeds vs. the added weight on each trial for Subject 1 Simon, Subject 2 Chuy, and Subject 3 Salvador. For each subject, a linear fitting line was calculated to see the impact of the added weight on the transition speed.

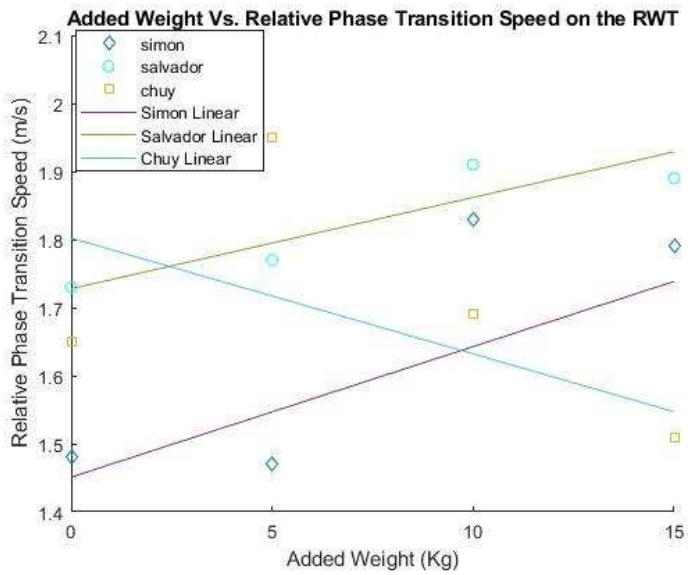

Fig. 22. Subject 1 Simon, subject 2 Chuy, and subject 3 Salvador relative phase transition speed vs added weight on the RWT trials.

For Subject 1 Simon and Subject 3 Salvador, the linear fitting lines have a positive slope, which indicates that the more weight that we add to the subject, the higher the relative phase transition speed, i.e. the subject prefers to change the transition speed at higher speeds than he does without the added weight.

For the Subject 2 Chuy, it is observed that the slope from the linear fitting line is negative, meaning that the more weight that is added, the lower the relative phase transition speed is. This is not consistent with the other two subjects analyzed (Subject 1 Simon and Subject 3 Salvador), which may be caused by several factors, such as subject bodyweight, physical condition, or a reported back injury from the subject.

Besides the added weight, the weight percent incremented for each subject was calculated, obtaining Table 6.

Table 6: Weight percent calculation for each subject.

	Added Weight	Weight Percent
Simon	0	0%
	5	7%
	10	13%
	15	20%
Chuy	0	0%
	5	4%
	10	8%
	15	12%
Salvador	0	0%
	5	5%
	10	10%
	15	14%

From Table 6, one can see the weight percent calculation for each subject, according to the measured bodyweight at the moment of the trials. With this calculation, the relative phase transition speed from RWT was also plotted, to see if there was an effect of the weight percentage from each subject and analyze if it caused a different effect on the transition speed.

A linear regression best fit line was calculated for each subject, as seen on Fig. 23, where can be observed that the Subject 3 Salvador and Subject 1 Simon kept the positive slope on the trials, which indicate that increasing the weight percentage of the subject also increased the relative phase transition speed, as shown in Fig. 22. Also, the transition speed for Subject 2 Chuy kept the negative slope, which means that as the weight percent increased, the subject preferred to decrease the transition speed.

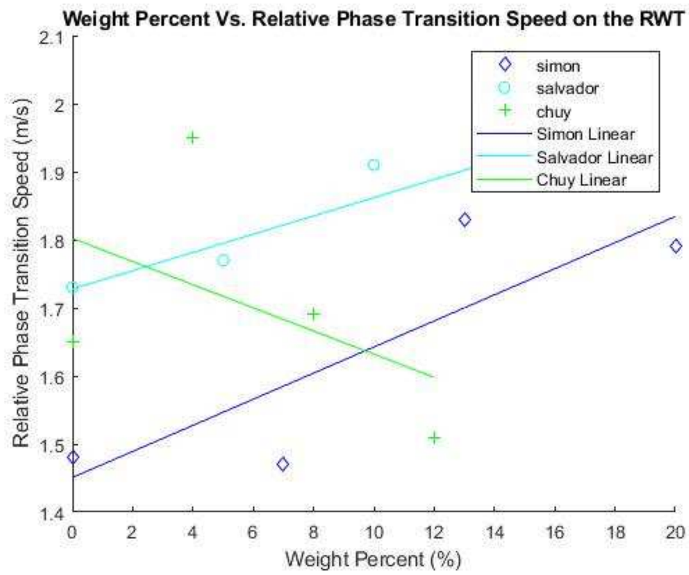

Fig. 23. Weight percent vs rel. phase transition speed on the RWT for each subject

A linear fitting for the three subjects was calculated as well, Fig. 24. This results in a positive slope linear fitting line, which indicates that as the additional weight increased, the relative phase transition speed also increased.

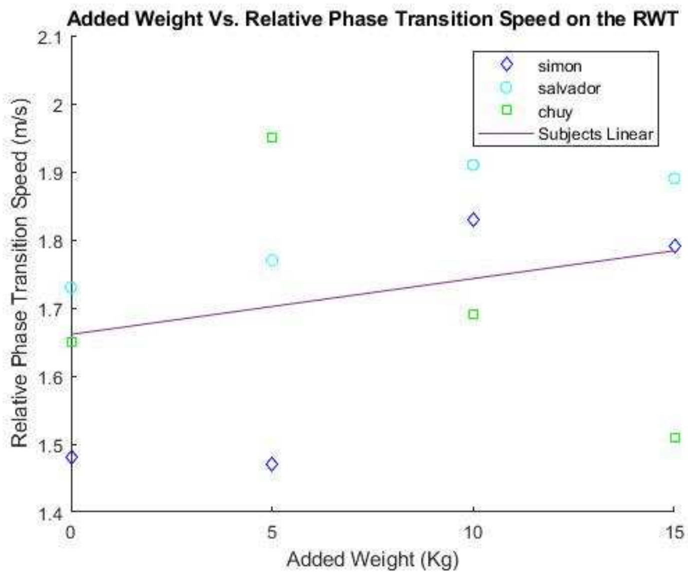

Fig. 24. Added weight vs relative phase transition speed for all subjects on the RWT.

On the weight percent vs, relative phase transition speed, was calculated a single linear fitting line to observe the effect from the three subjects, Fig. 25. From this linear regression line can be observed a positive slope, and conclude that as the weight percent is increased, the subjects stop running and transition to the walking pace at higher speeds.

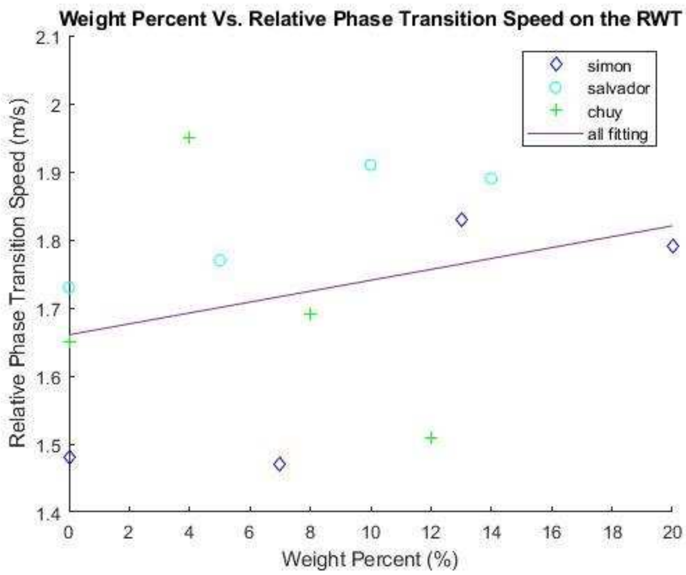

Fig. 25. Weight percent vs. rel. phase transition speed on the RWT

6.2. Running to walking results adding body weight.

In the case of walking to running exercise, the procedure was the same than the exercises performed on the running to walking trials presented on section 6.1 "running to walking results adding body weight". The results from Subject 1 Simon, are given in Table 7.

Table 7: Subject 1 Simon walking to running transition speed per added weight.

Added Weight (Kg)	**Subject 1 Simon Transition Speed (m/s)**
0	1.72
5	1.66
10	1.85
15	1.75

From this result, can be observed that the added weight affected the walking to running results from Subject 1 Simon. The transition speed without added weight is 1.72 m/s, and as the weight is increased, the transition speed changes to 1.75 m/s when 15 Kg were added. This means, that compared to the reference (no added weight) trial, increasing the subject body weight, kept Subject 1 Simon on the walking pace for slightly longer time.

The Running to Walking result from Subject 2 Chuy are presented on Table 8. It can be observed that the WRT speed for the Subject 2 Chuy, started with a reference speed of 1.64 m/s without added weight, and as the weight was added, the speed decreased to 1.49 m/s with 5 Kg added, and kept increasing until reaching the 1.65 m/s with 15 Kg added. The subject keep walking at lower then slightly higher speeds while increasing the weight.

Table 8: Subject 2 Chuy walking to running transition speed per added weight.

Added Weight (Kg)	**Subject 2 Chuy Transition Speed (m/s)**
0	1.64
5	1.49
10	1.53
15	1.65

For Subject 3 Salvador, the Walking to running transition speed results are depicted in

Table 9. It can be observed that Subject 3 Salvador had a transition speed without added weight of 1.84 m/s, and the speed increased as the weight increased, similar to the results obtained from the subjects Subject 1 Simon and Subject 2 Chuy. Subject 3 Salvador maximum weight was also 15 kg with a transition speed of 1.88 m/s.

Table 9: Subject 3 Salvador walking to running transition speed per added weight.

Added Weight (Kg)	**Subject 3 Salvador Transition Speed (m/s)**
0	1.84
5	1.92
10	2.03
15	1.88

To be able to better observe the WRT transition speed behavior, a linear fitting was calculated for each subject, Fig. 26.

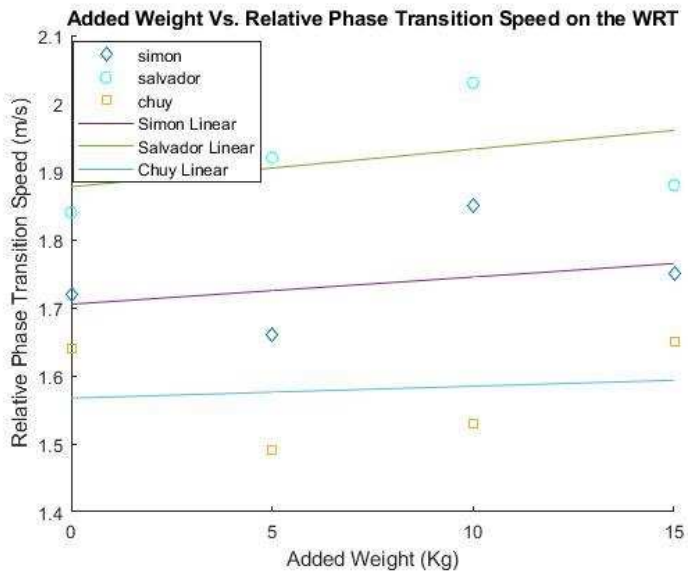

Fig. 26. Added weight vs relative phase transition speed on the walking to running transition.

On this figure, can be observed that Subject 1 Simon, Subject 3 Salvador and Subject 2 Chuy had a positive slope on the linear fitting lines, which indicates that as the weight was increased, the walking to running transition speed was increased, meaning that the subjects kept the walking pace at higher speeds.

Also, the Relative Phase Transition Speed was plotted vs Weight percent, to observe the effect on the transition speed, using the same calculations shown on Table 6. From the weight percent vs relative phase plot, Fig. 27, it can be identified a similar behavior to the added weight results from Fig. 26. For the three subjects, a positive slope is identified, confirming that the relative phase transition speed increased as the weight percent increased on each subject.

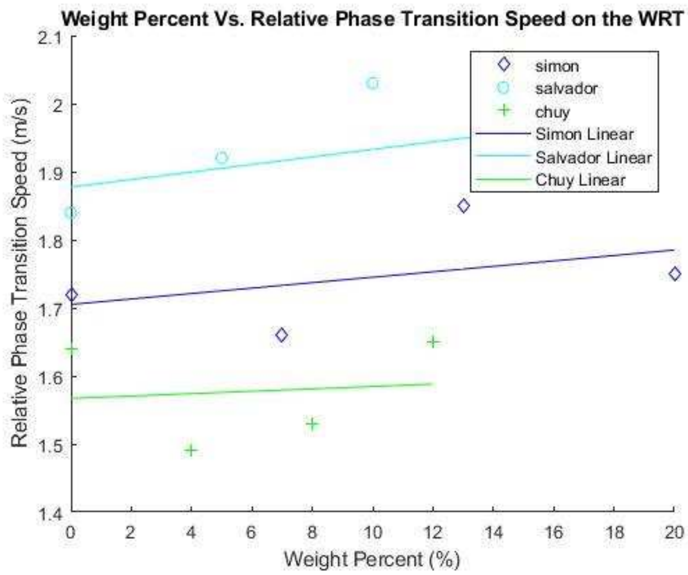

Fig. 27. Relative phase transition speed vs weight percent of WRT.

A linear fitting plot was calculated for the three subjects and presented in Fig. 28, where it can be observed that for the three subjects the fitting line presents a positive slope on the plot, which means that as the weight is increased, the relative phase transition speed is higher, thus, the subject walks at a higher speed before transitioning to running.

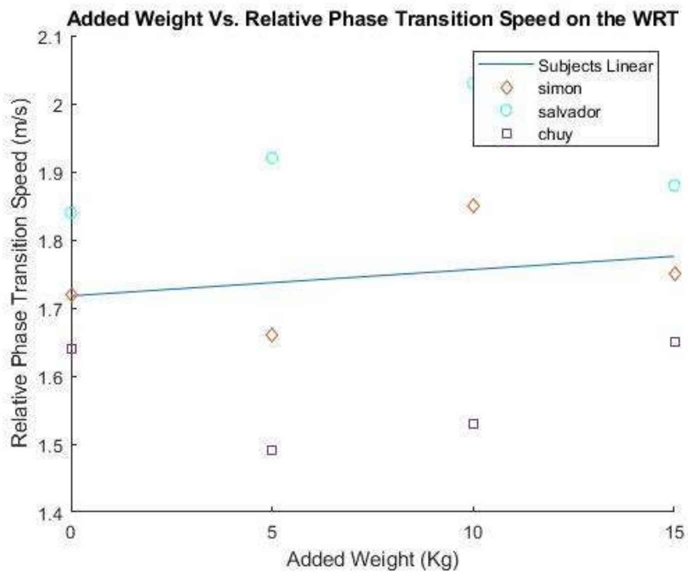

Fig. 28. Added weight vs relative phase transition speed on the WRT.

Also, a linear fitting line was created to analyze the impact of the weight percent added on all subjects, Fig. 29.

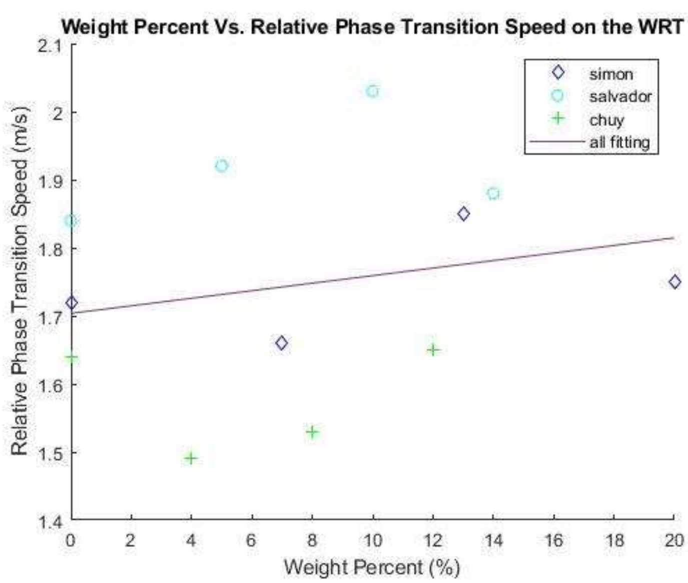

Fig. 29. Relative phase transition speed vs weight percent of WRT exercise.

The linear fitting presented on Fig. 29 confirms the analysis from Fig. 28, by observing a positive slope on the graph, and which concludes that by increasing the percentage of bodyweight also increases the relative phase transition speed on the walking to running by making the subject walk at higher speeds.

6.3 Limitations.

The exercise presented as capture speed change, reflects the analysis of the gait transition in only one subject (Salvador). Thus, the results are limited. Also, the lack of ground reaction force measurements doesn't allow us to compare to other results where these forces are analyzed.

On the added weight exercise, the analysis was limited to 3 subjects. The result is limited to a small population and would be necessary to increase the number of subjects analyzed with the same method and be able to obtain a correct statistical model for the effect of obesity on the walking to running and running to walking transition.

REFERENCES

[1] W. W. Lu, "Gait Patterns," University of Hong Kong, Hong Kong.

[2] Y. Shih, Y.-C. Chen, Y.-S. Lee, M.-S. Chan and T.-Y. Shiang, "Walking beyond preferred transition speed increases muscle," *Gait and Posture,* vol. 46, pp. 5-10, 2016.

[3] V. Segers, K. De Smet, I. V. Caekenberghe, P. Aerts and D. De Clerq, "Biomechanics of spontaneous overground walk-to-run transition," *The Journal of Experimental Biology,* vol. 216, pp. 3047-3054, 2013.

[4] K. Sasaki and R. R. Neptune, "Differences in muscle function during walking and running at the same speed," *Journal of Biomechanics,* pp. 2005-2013, 2006.

[5] V. Segers, M. Lenoir, P. Aerts and D. De clerq, "Kinematics of the transition between walking and running when," *Gait & Posture,* vol. 26, p. 13, 2006.

[6] C. T. Farley and D. P. Ferris, "Biomechanics of Walking and Running: Center of mass movements to muscle action".

[7] A. Hreljac, "Preferred and energetically optimal gait transition speeds in human locomotion," *Medicine and Science in Sports And Exercise,* vol. 25, pp. 1158-1162, 1993.

[8] D. A. Winter, "Processing of raw Kinematic data," in *Biomechanics and Motor Control of Human Movement*, Waterloo, Ontario, Canada, Wiley, 2005, p. 44.

[9] F. J. Diedricj and W. H. Warren, "Why change gaits? Dynamics of the walk-run transition," *Journal of experimental psychology: Human perception and performance,* vol. 21, no. 1, pp. 183-202, 1995.

[10] K. Sasaki and R. R. Neptune, "Muscle mechanical work and elastic energy utilization during walking and running near the preferred gait transition speed," *Gait & Posture,* vol. 23, pp. 383-390, 2006.

[11] A. Rotstein, O. Inbar, T. Berginsky and Y. Meckel, "Preferred Transition Speed between Walking and Running: Effects of Training Status," *Medicine & Science in Sports & Exercise,* pp. 1864-1870, 2005.

[12] T. F. Novacheck, "The Biomechanics of running," Gait and Posture, St. Paul, MN, 1198.

[13] A. E. Minetti, L. P. Ardigo and F. Saibene, "The transition between walking and running in humans: metabolic and mechanical aspects at different gradients.," *Acta Physiol Scand,* pp. 315-323, 1994.

[14] S. Hagio, M. Fukuda and M. Kouzaki, "Identification of muscle synergies associated with gait transition in humans," Froniters in Human Neuroscience, Tokyo, Japan, 2015.

[15] S. Hagio, M. Fukuda and M. Kouzaki, "Identification of muscle synergies associated with gait," *Frontiers in Human Neuroscience,* p. 12, 2015.

[16] A. J. Raynor, C. J. Yi, B. Abernethy and Q. J. Jong, "Are transitions in human gait determined by mechanical, kinetic or energy factors?," *Human Movement Science,* vol. 21, pp. 785-805, 2002.

[17] I. Ranisavljev, V. Ilic, I. Soldatovic and D. Stefanovic, "The relationship between allometry and preferred transition speed in human locomotion," *Human Movement Science,* vol. 34, pp. 196-204, 2014.

[18] A. Ruina, J. E. Bertram and M. Srinivasan, "A collisional model of the energetic cost of support work qualitatively explains leg sequencing in walking and galloping, pseudo-elastic leg behavior in running and the walk-to-run transition," *Journal of Theoretical Biology,* vol. 237, pp. 170-192, 2005.

APPENDIX

APPENDIX

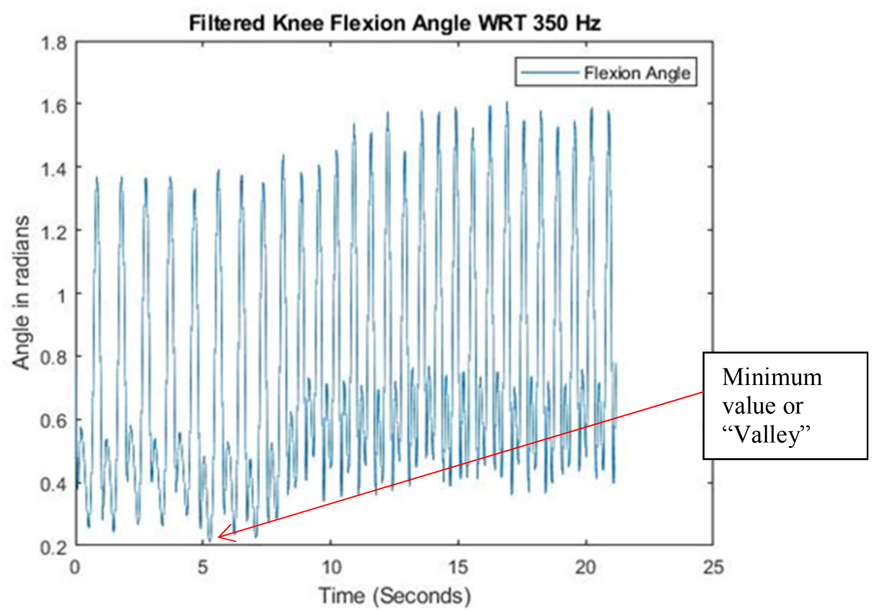

Fig. 30. Minimum value or "Valley" example

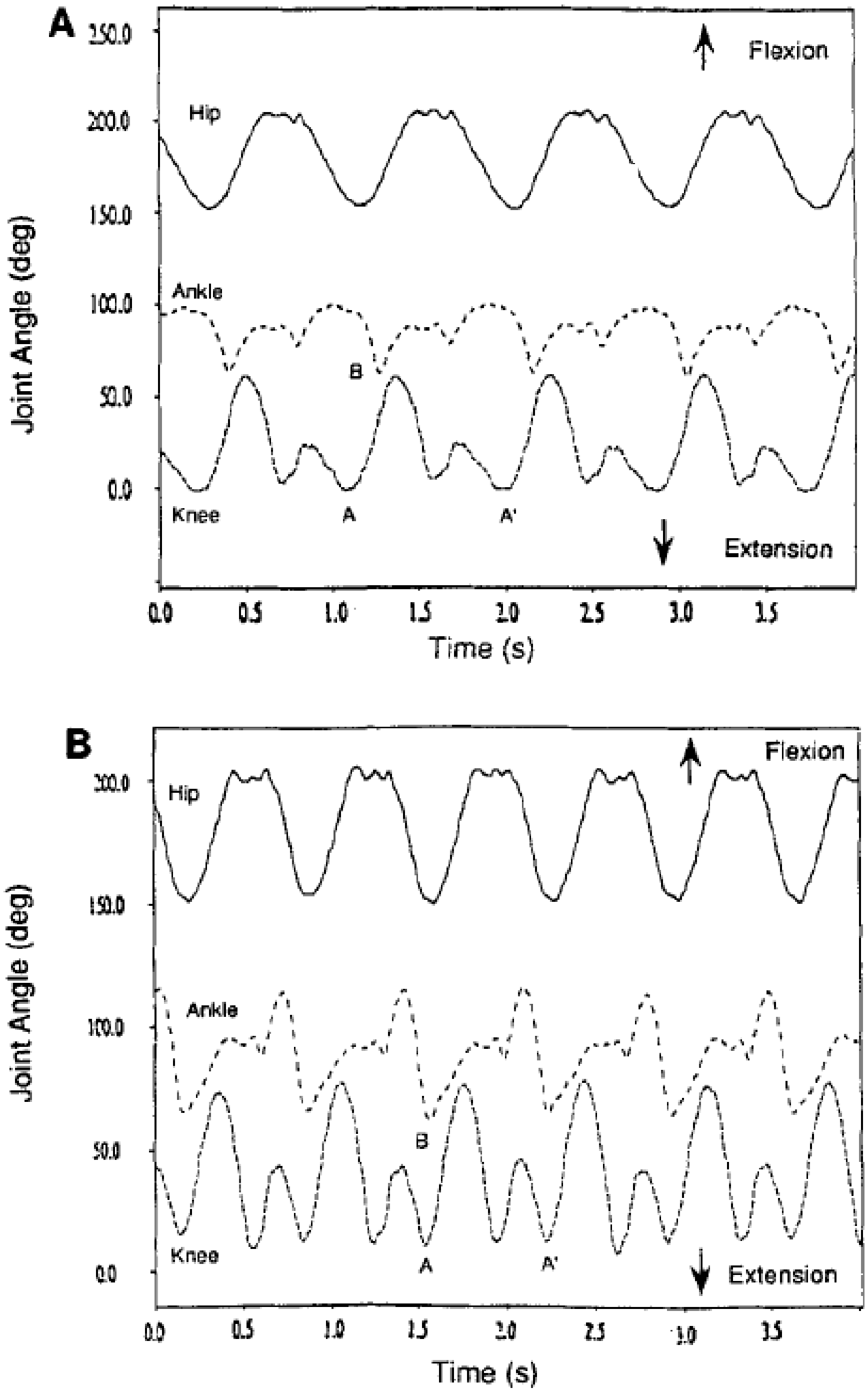

Figure 4. Sample trials from Participant 8 showing joint angles as a function of time during (A) walking and (B) running. Relative phase is calculated by defining A to A′ as the 360° reference cycle, and defining Event B as a proportion of this cycle.

Fig. 31 Relative phase calculation method used by Diedricj [9].

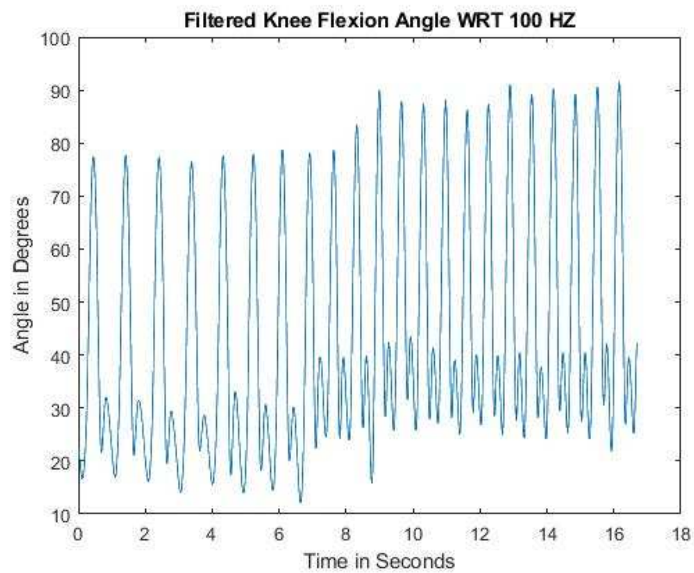

Fig. 32. Filtered knee flexion angle in the WRT transition with capture speed of 100 Hz.

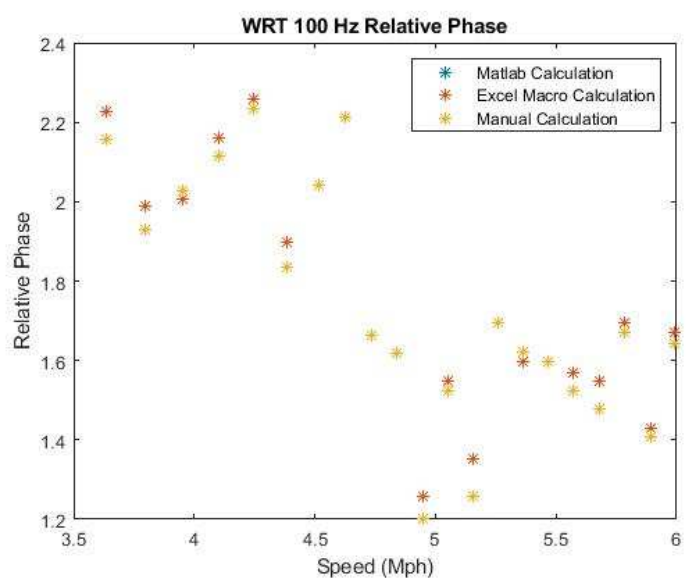

Fig. 33. Relative phase vs speed on the WRT transition, with capture speed of 100 Hz.

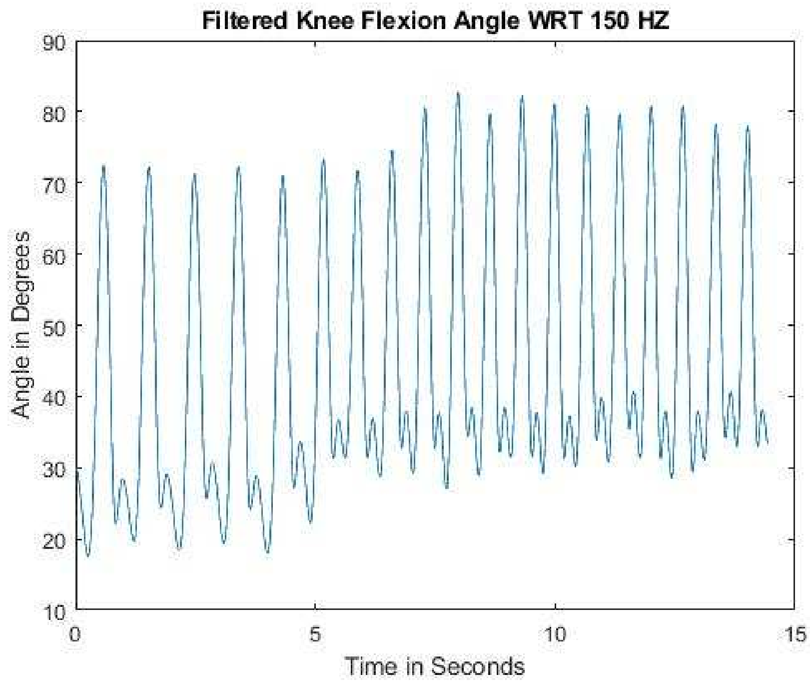

Fig. 34. Filtered knee flexion angle in the WRT transition with capture speed of 150 Hz.

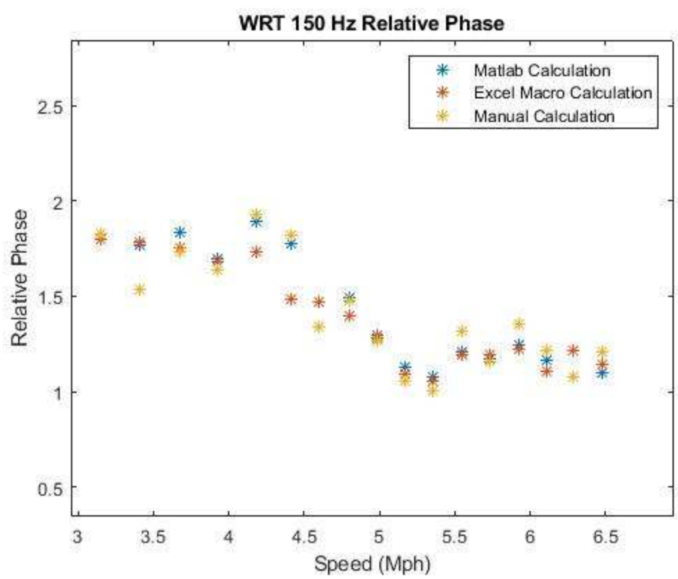

Fig. 35. Relative phase vs speed on the WRT transition, with capture speed of 150 Hz.

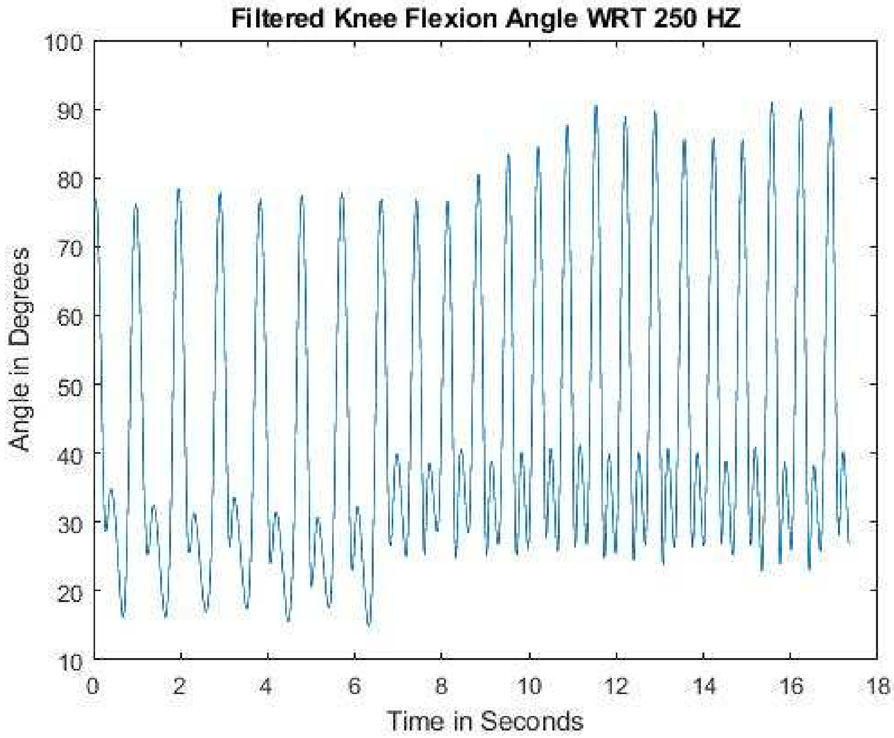

Fig. 36. Filtered knee flexion angle in the WRT transition with capture speed of 250 Hz.

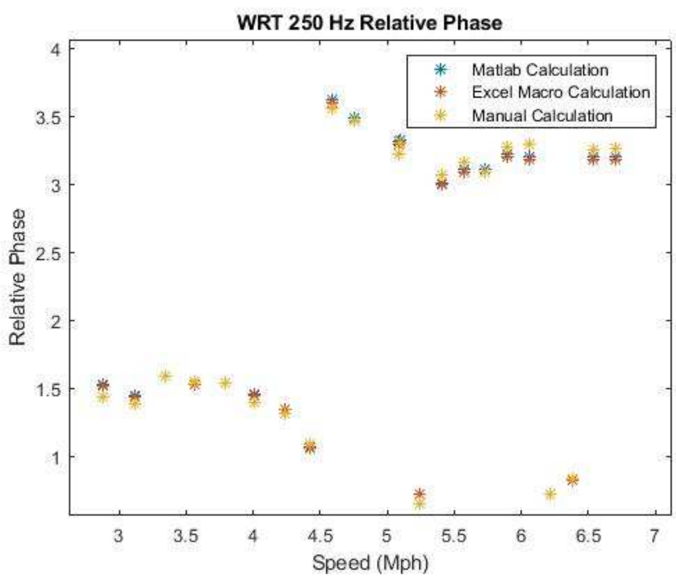

Fig. 37. Relative phase vs speed on the WRT transition, with capture speed of 250 Hz.

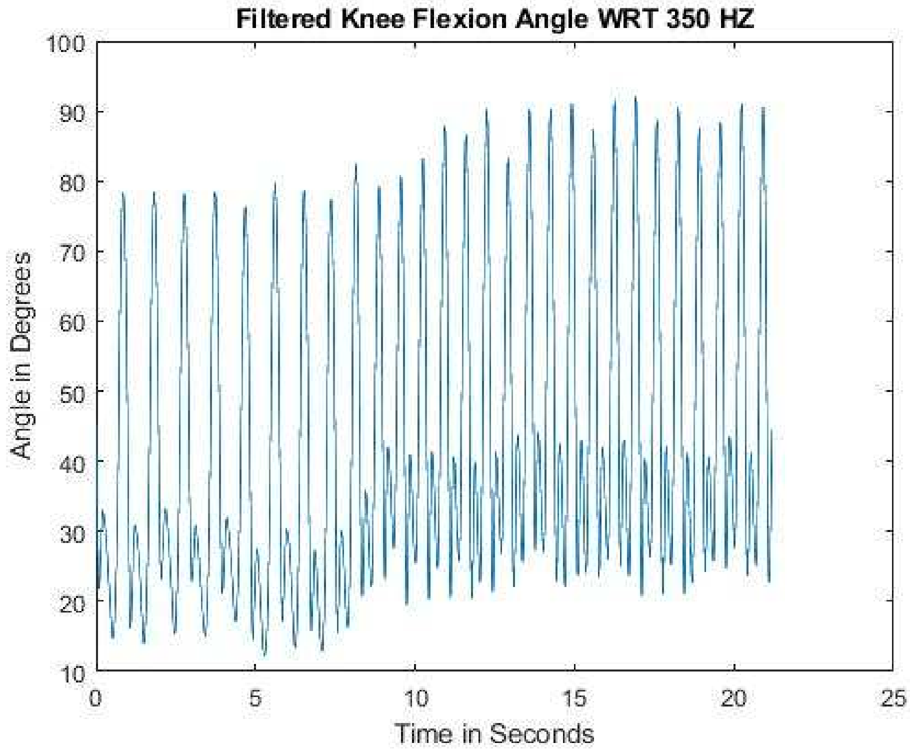

Fig. 38 .Filtered knee flexion angle in the WRT transition with capture speed of 350 Hz.

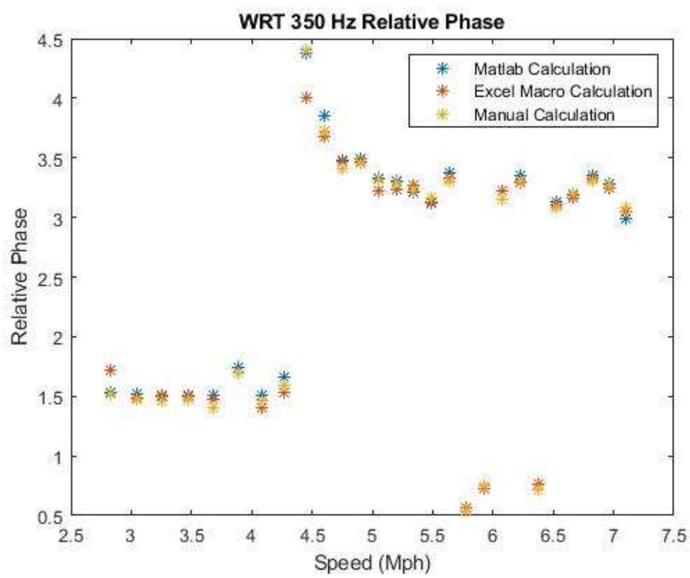

Fig. 39. Relative phase vs speed on the WRT transition, with capture speed of 350 Hz.

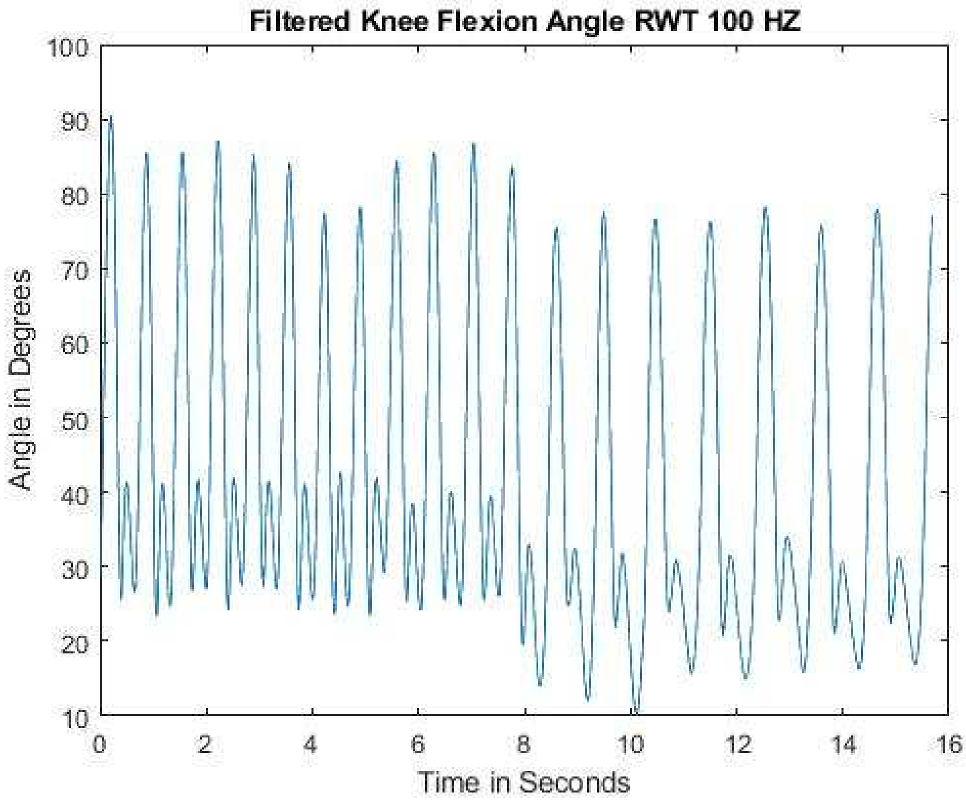

Fig. 40. Filtered knee flexion angle in the RWT transition with capture speed of 100 Hz.

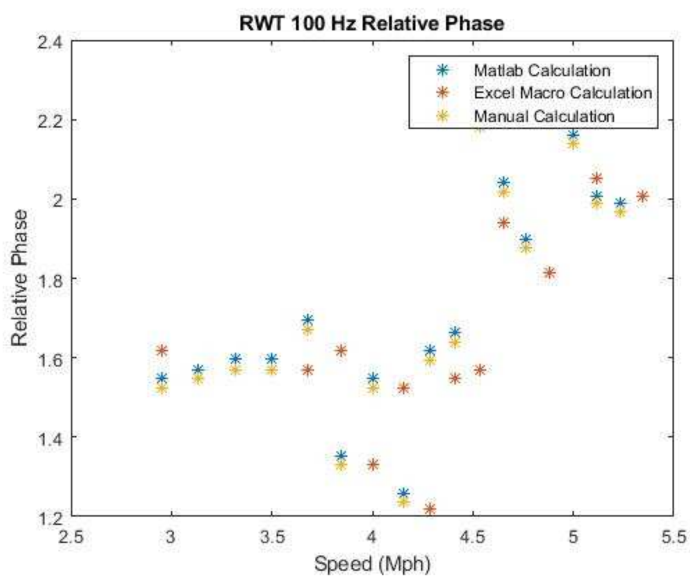

Fig. 41. Relative phase vs speed on the RWT transition, with capture speed of 100 Hz.

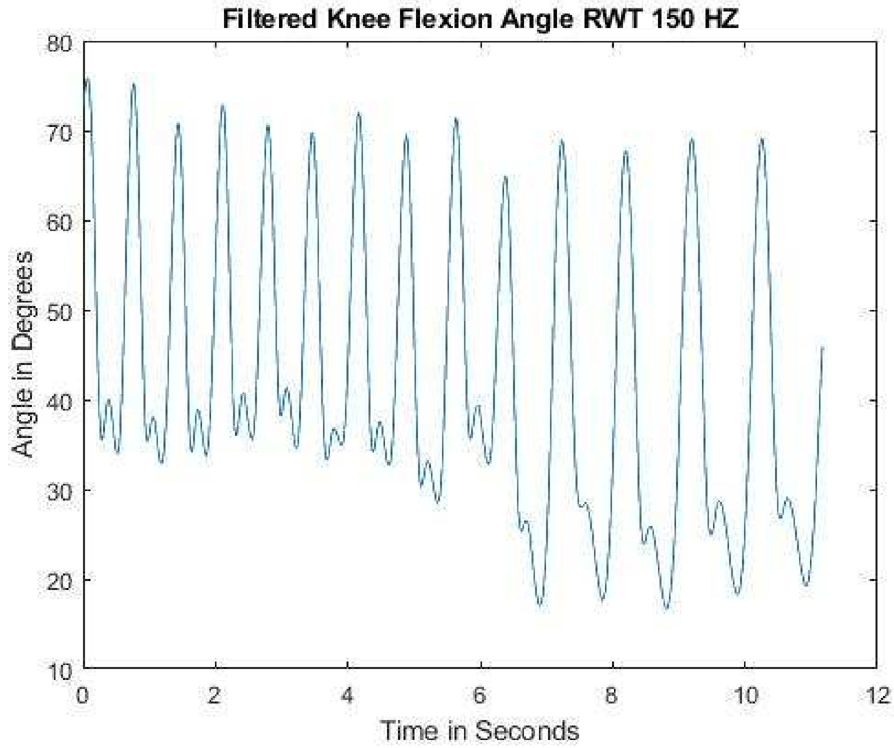

Fig. 42. Filtered knee flexion angle in the RWT transition with capture speed of 150 Hz.

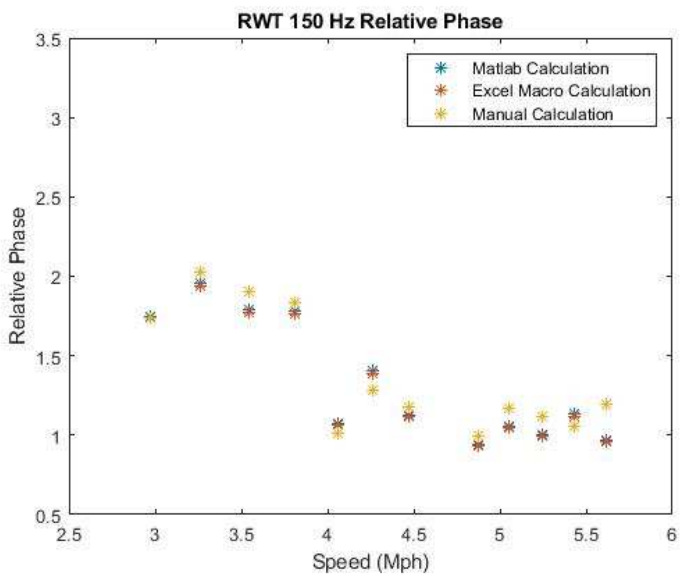

Fig. 43. Relative phase vs speed on the RWT transition, with capture speed of 150 Hz.

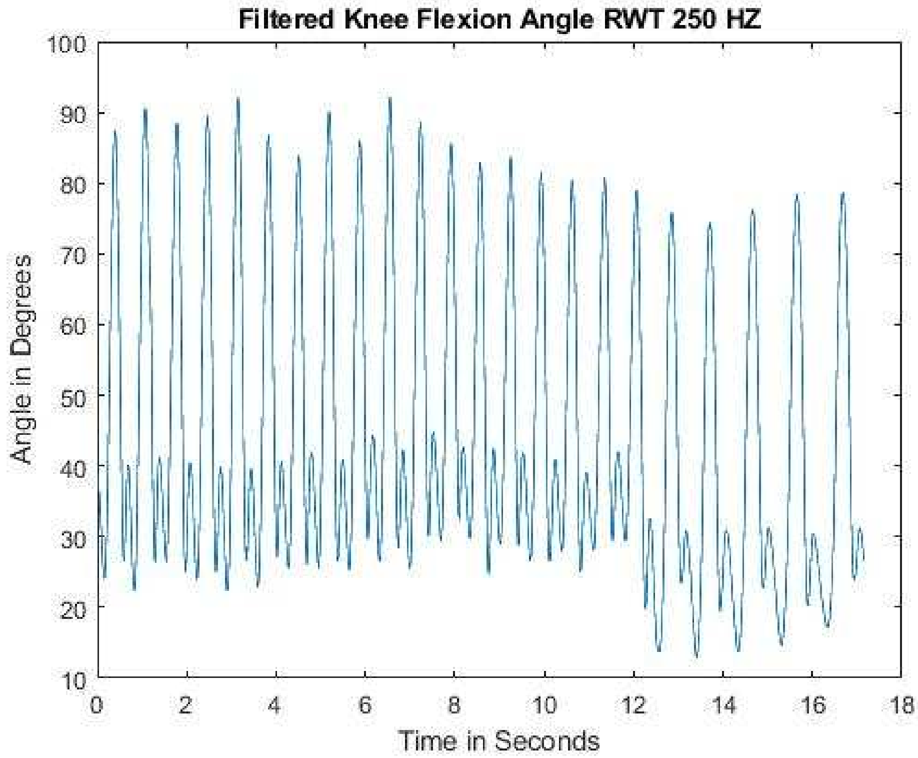

Fig. 44. Filtered knee flexion angle in the RWT transition with capture speed of 250 Hz.

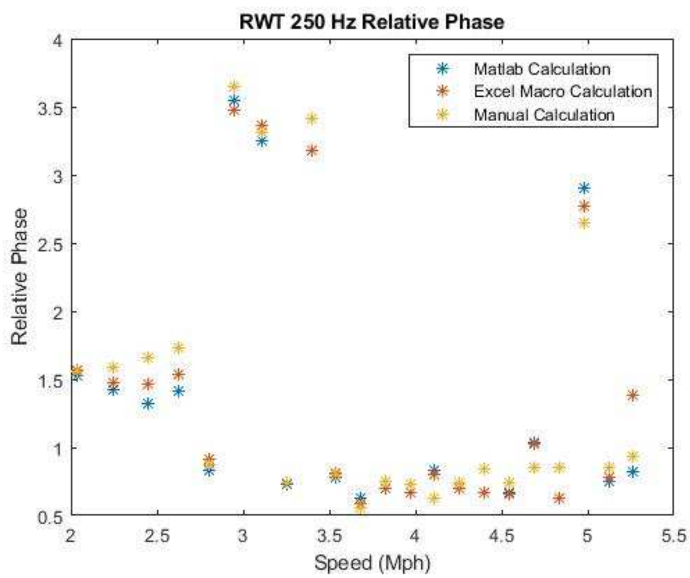

Fig. 45. Relative phase vs speed on the RWT transition, with capture speed of 250 Hz.

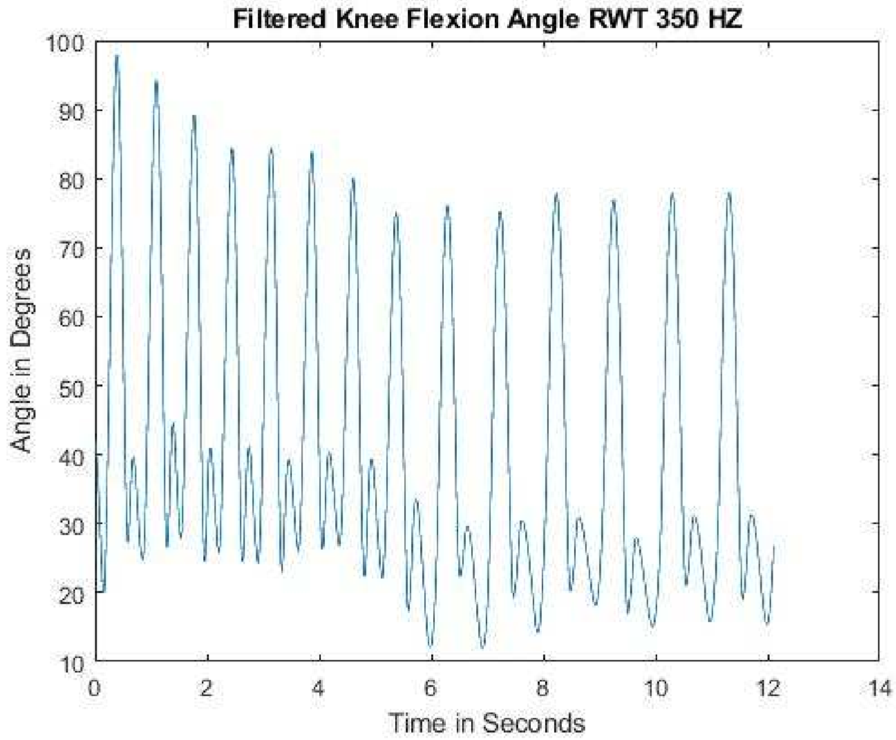

Fig. 46. Filtered knee flexion angle in the RWT transition with capture speed of 350 Hz.

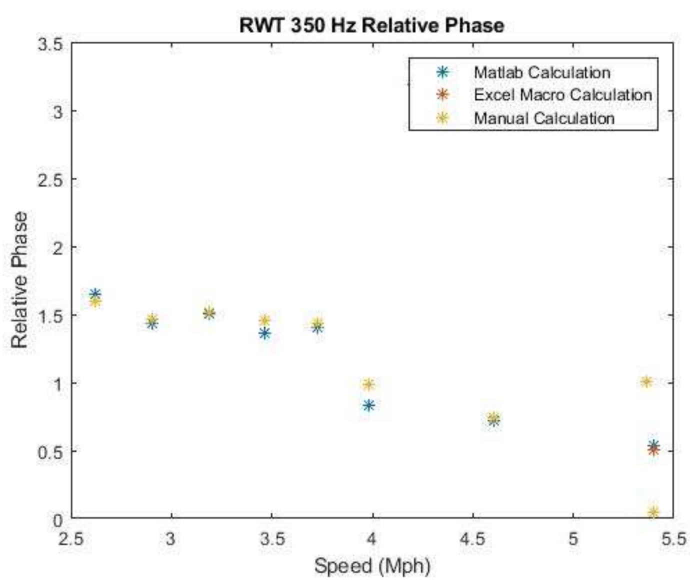

Fig. 47. Relative phase vs speed on the RWT transition, with capture speed of 350 Hz.

Changing body weight Fig.s

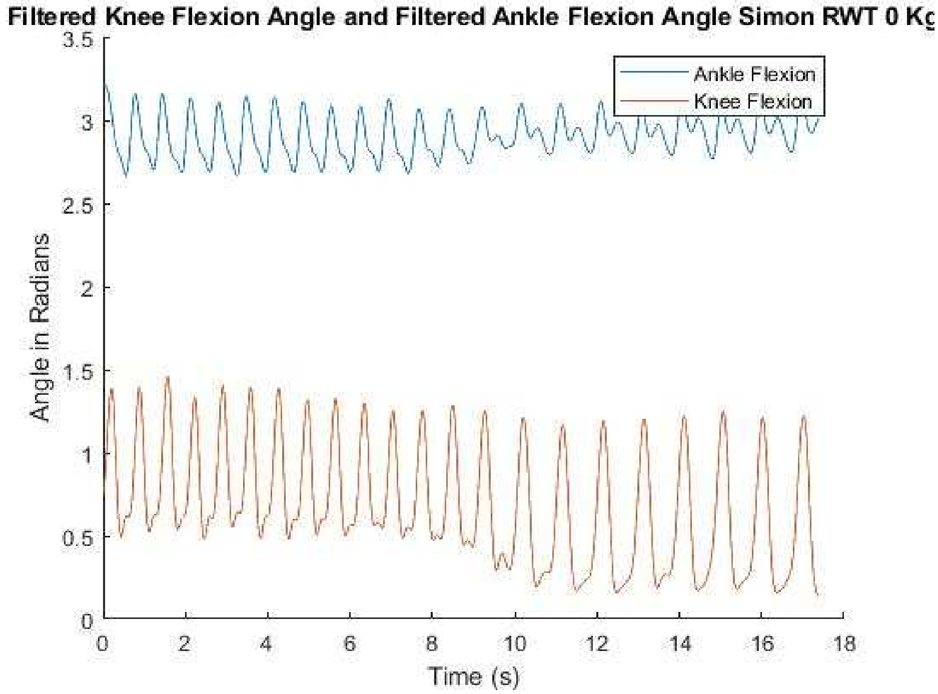

Fig. 48. Filtered knee flexion angle and filtered ankle flexion angle for subject 1 Simon RWT 0 Kg

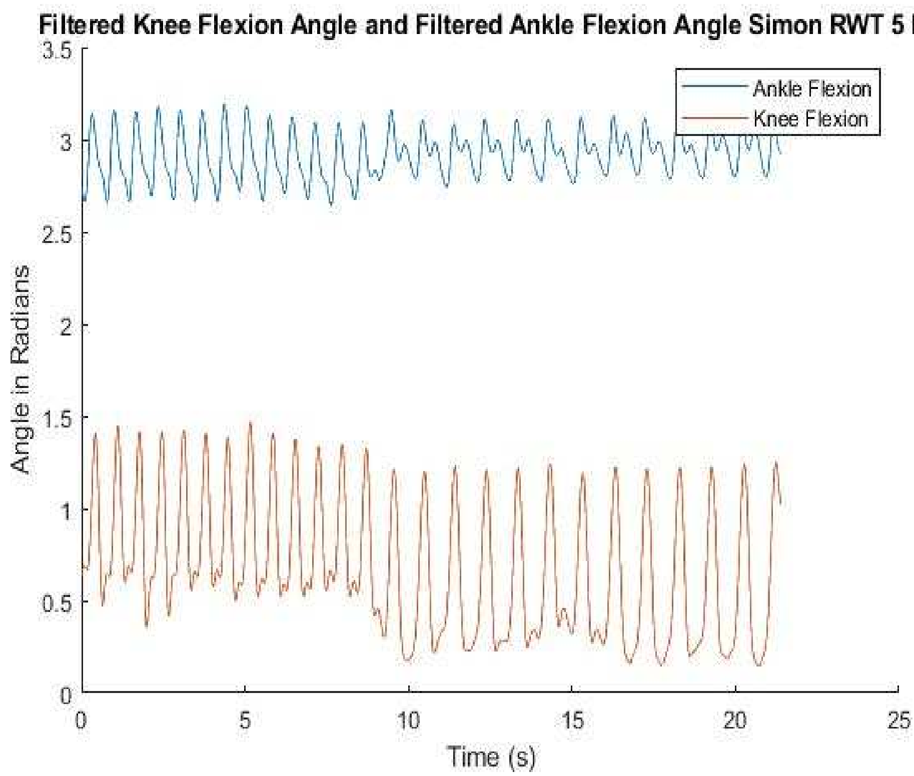

Fig. 49. filtered knee flexion angle and filtered ankle flexion angle for subject 1 Simon RWT 5 Kg

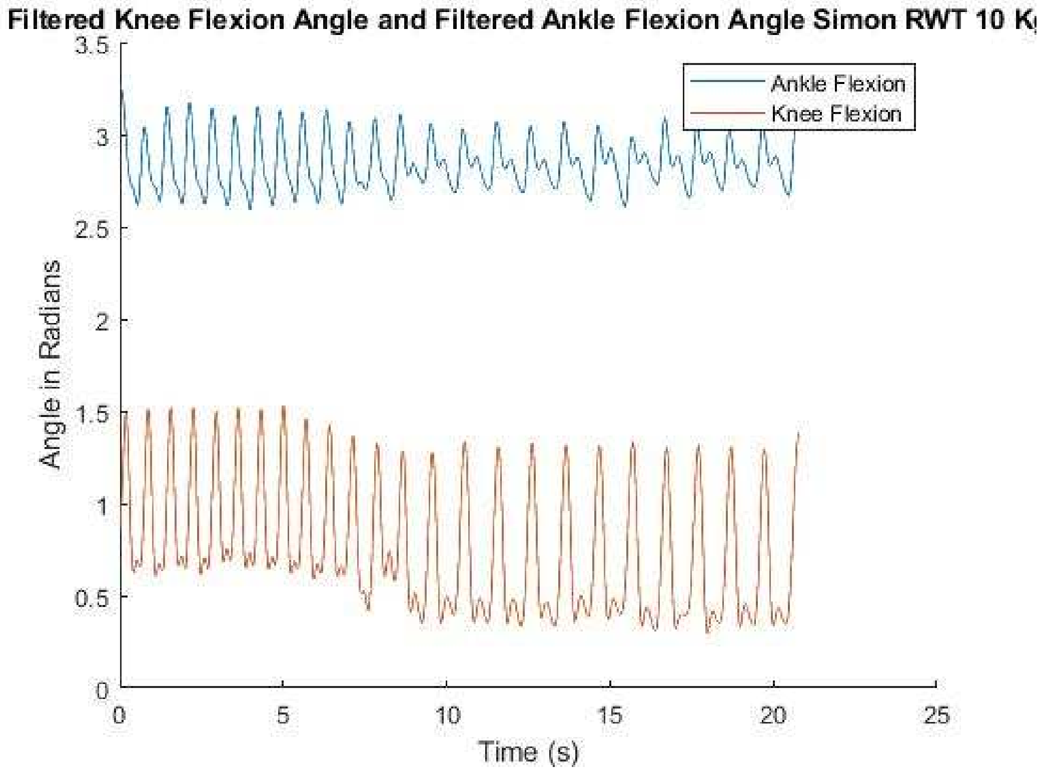

Fig. 50. Filtered knee flexion angle and filtered ankle flexion angle for subject 1 Simon RWT 10 Kg

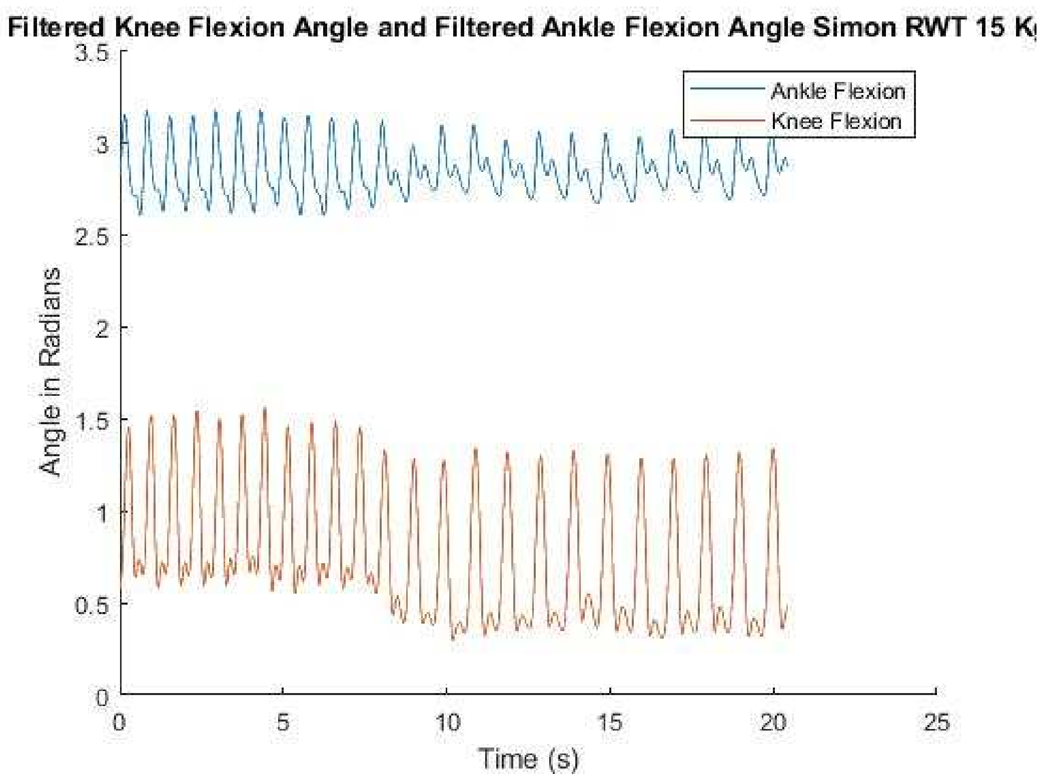

Fig. 51. Filtered knee flexion angle and filtered ankle flexion angle for subject 1 Simon RWT 15 Kg

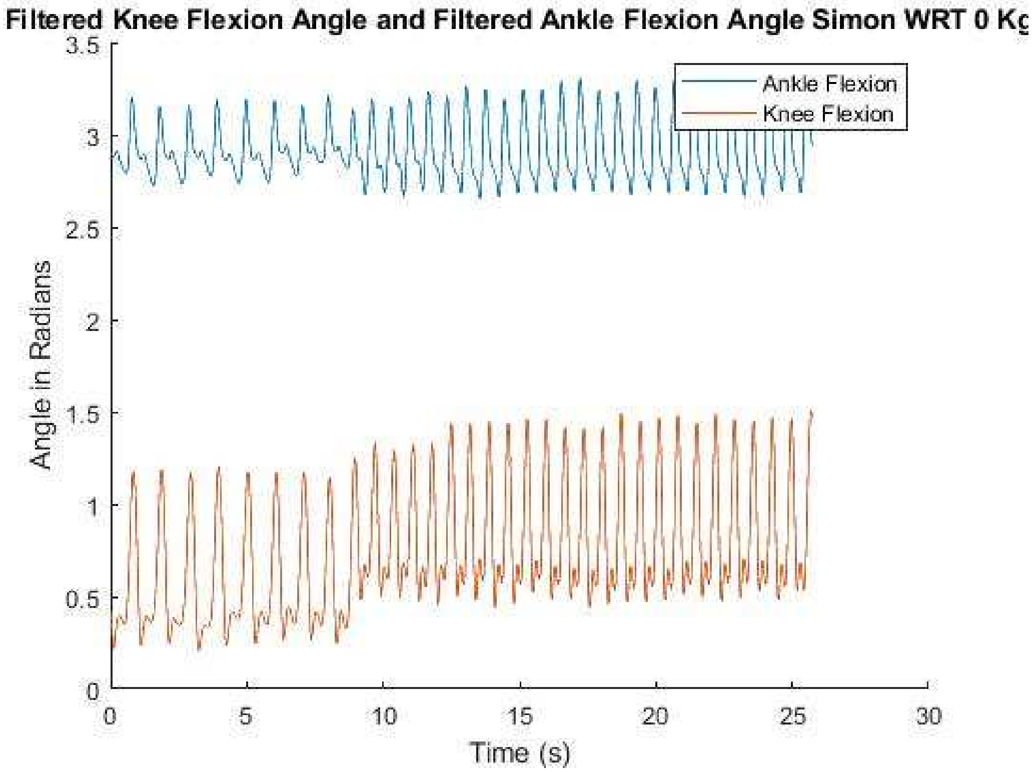

Fig. 52. Filtered knee flexion angle and filtered ankle flexion angle for subject 1 Simon WRT 0 Kg.

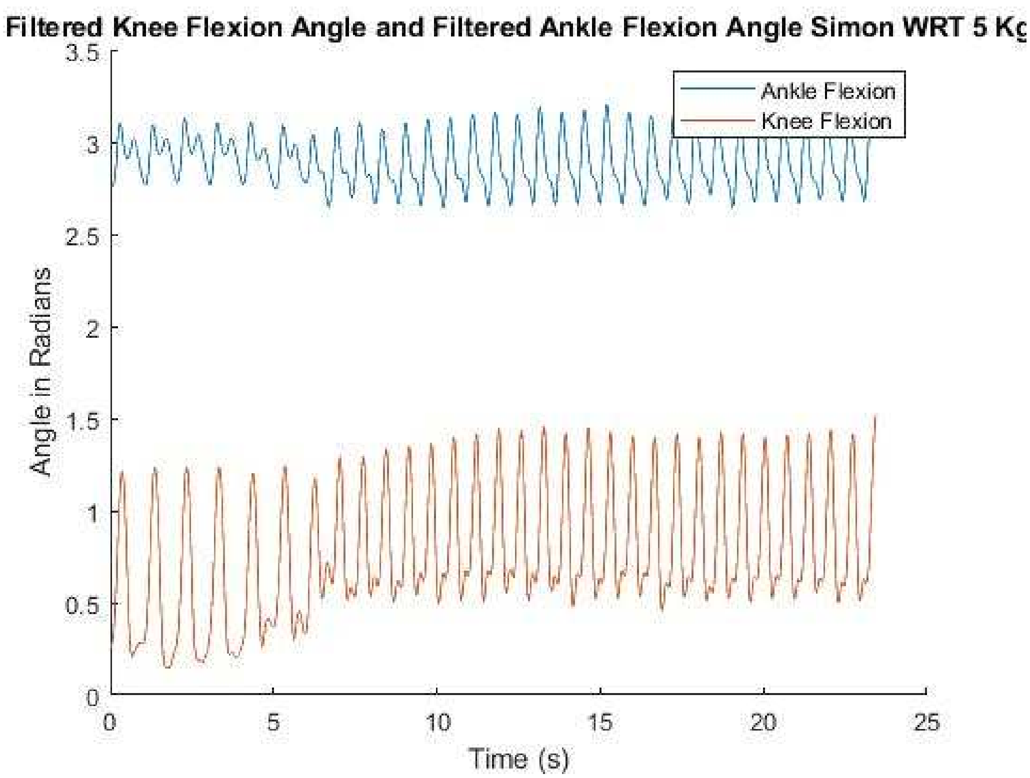

Fig. 53. Filtered knee flexion angle and filtered ankle flexion angle for subject 1 Simon WRT 5 Kg.

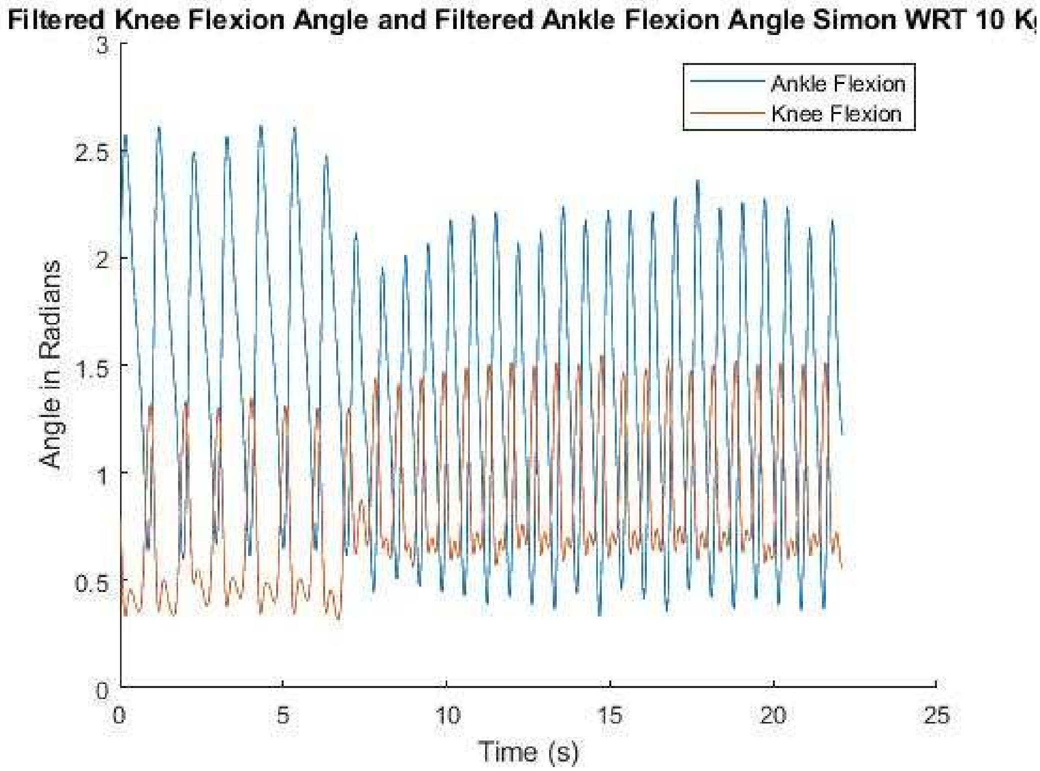

Fig. 54. Filtered knee flexion angle and filtered ankle flexion angle for subject 1 Simon WRT 10 Kg

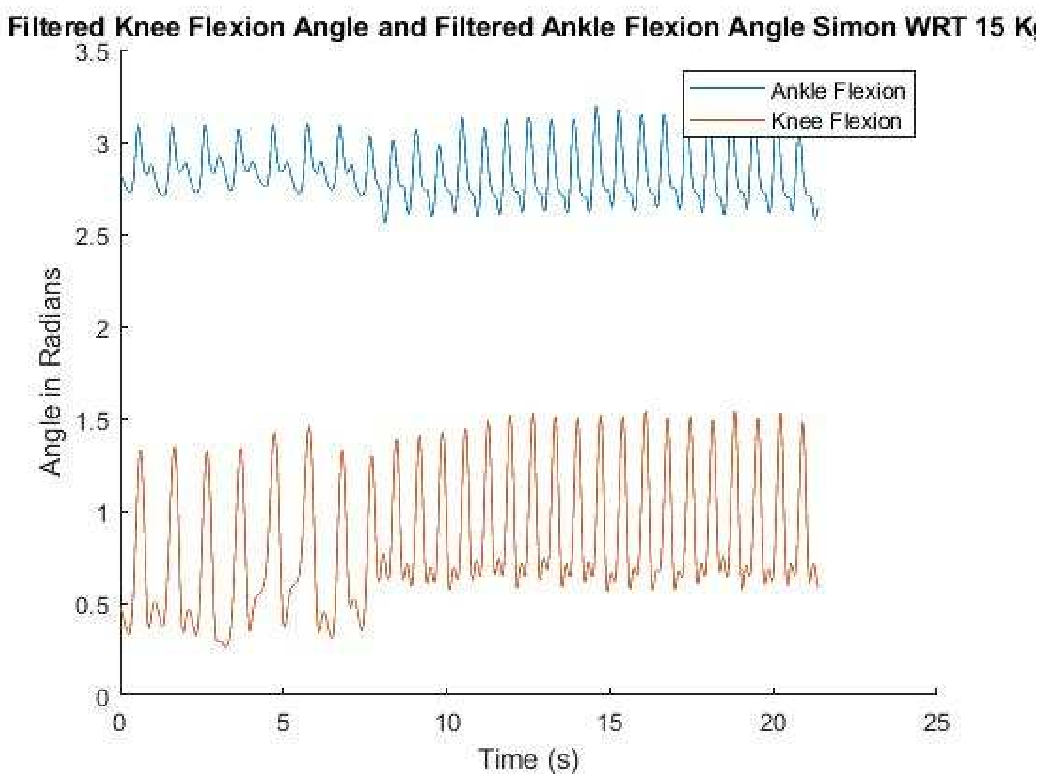

Fig. 55. Filtered knee flexion angle and filtered ankle flexion angle for subject 1 Simon WRT 15 Kg

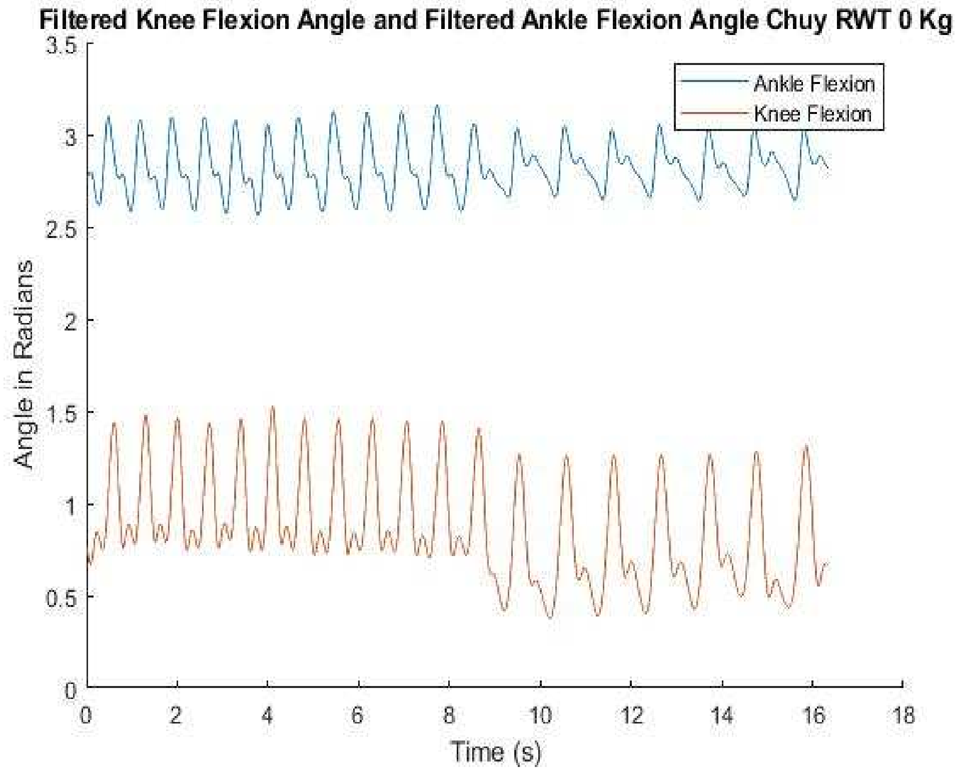

Fig. 56. Filtered knee flexion angle and filtered ankle flexion angle for subject 2 Chuy RWT 0 Kg

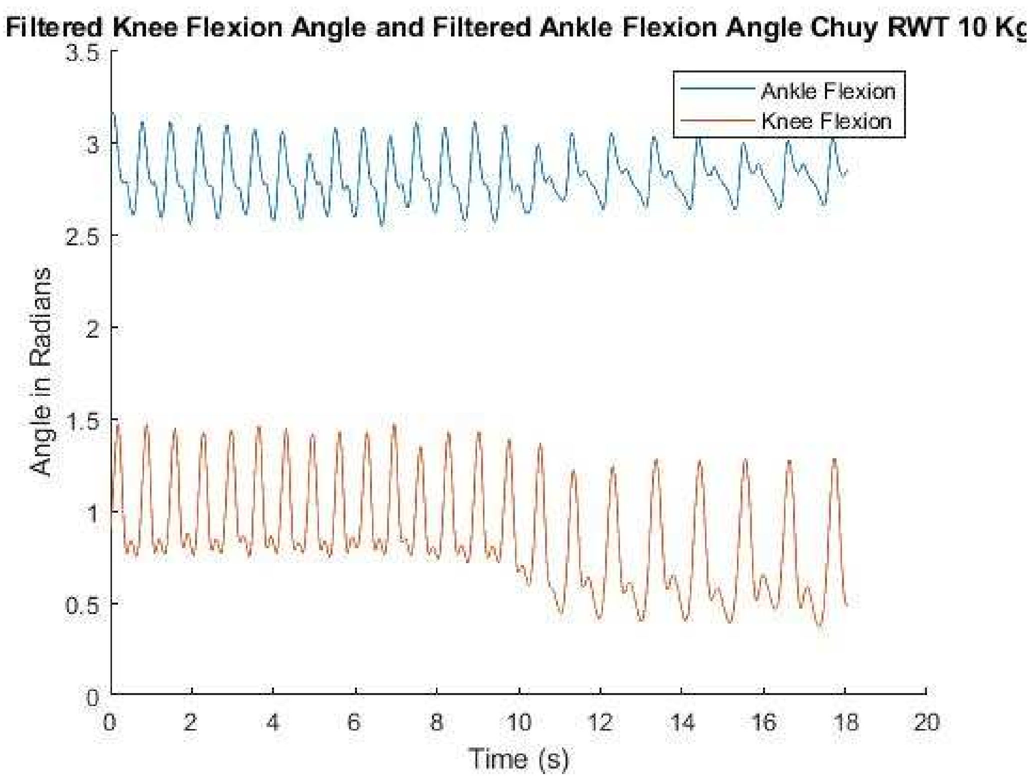

Fig. 57. Filtered knee flexion angle and filtered ankle flexion angle for subject 2 Chuy RWT 10 Kg

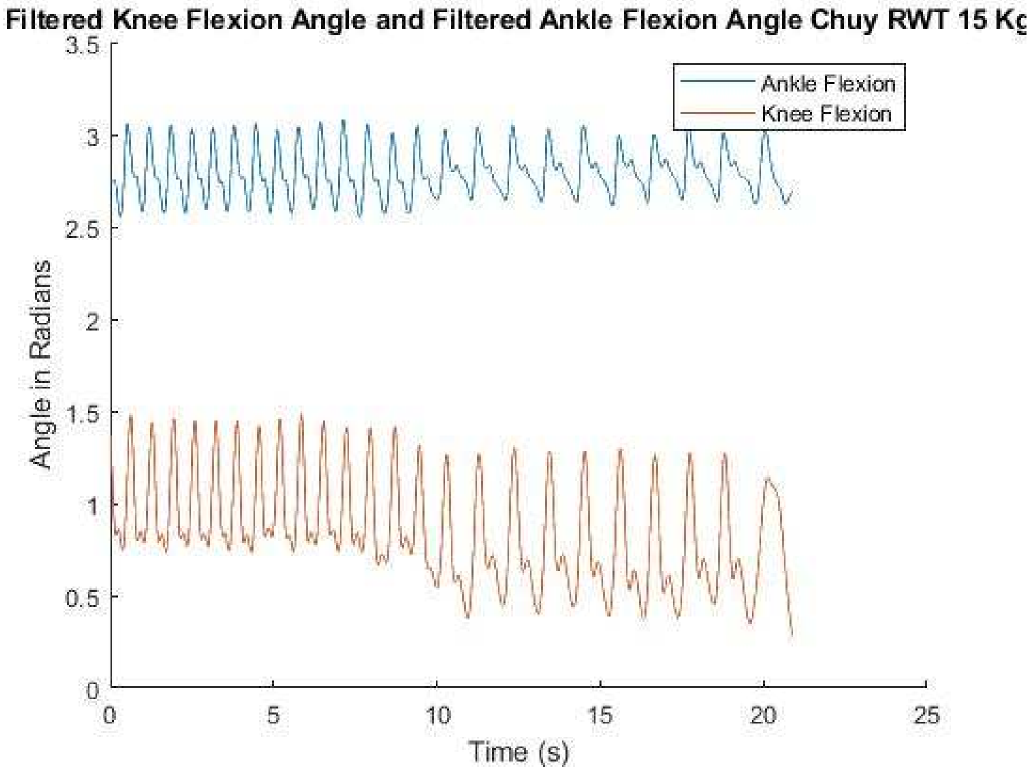

Fig. 58. Filtered knee flexion angle and filtered ankle flexion angle for subject 2 Chuy RWT 15 Kg

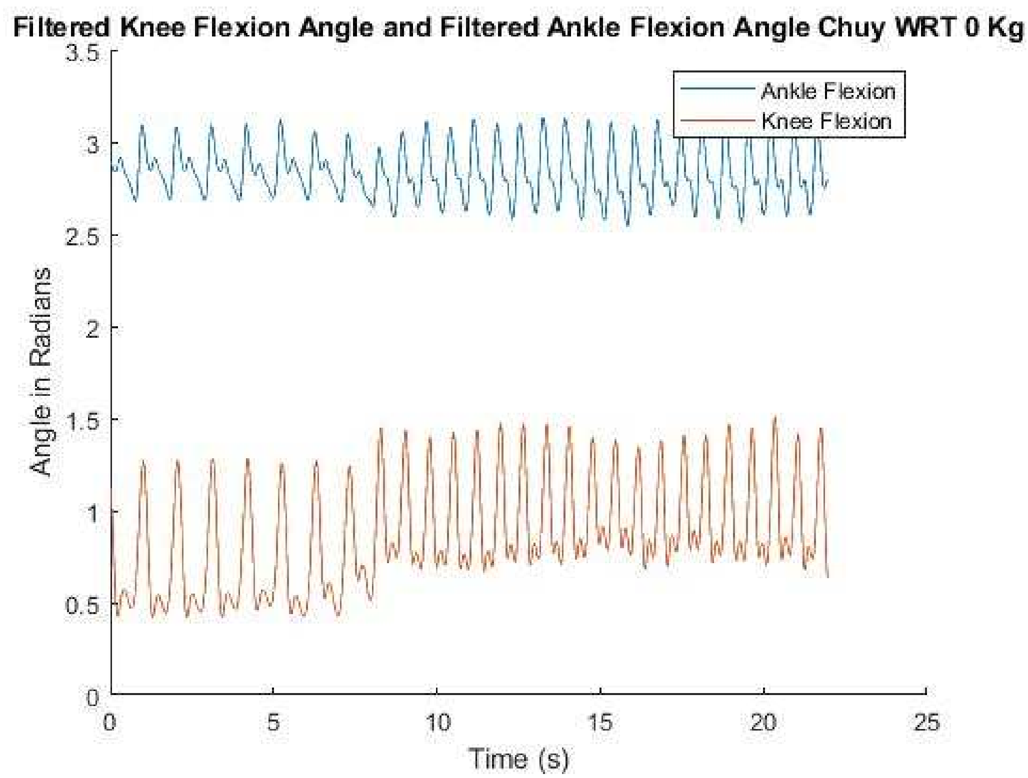

Fig. 59. Filtered knee flexion angle and filtered ankle flexion angle for subject 2 Chuy WRT 0 Kg

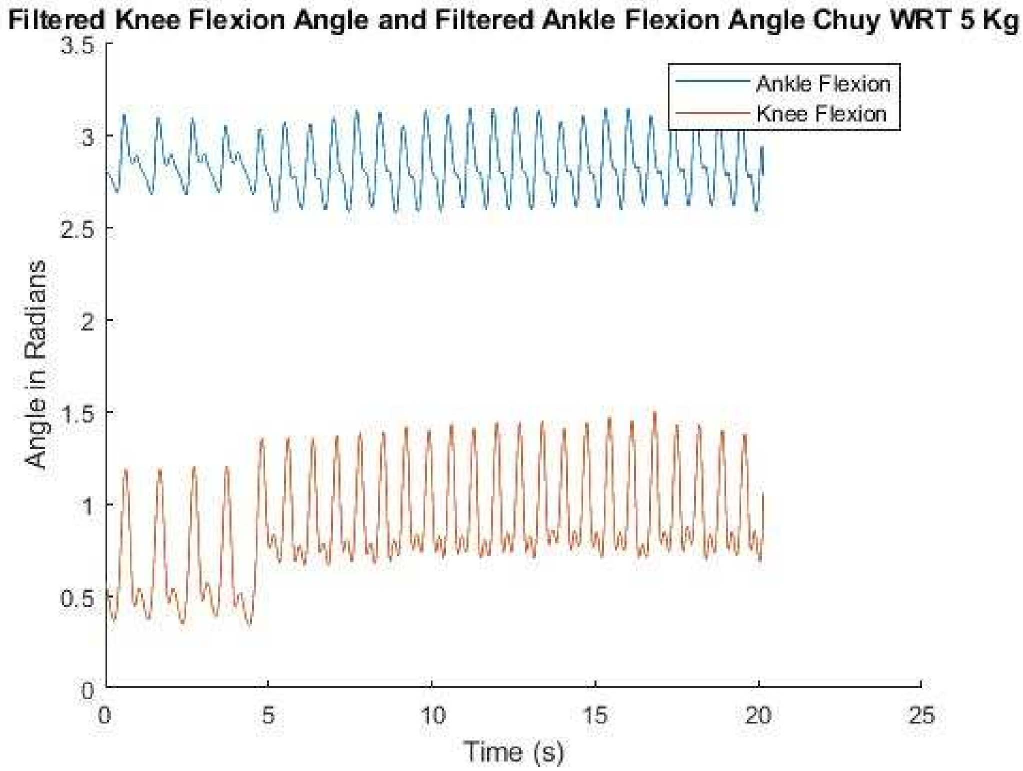

Fig. 60. Filtered knee flexion angle and filtered ankle flexion angle for subject 2 Chuy WRT 5 Kg

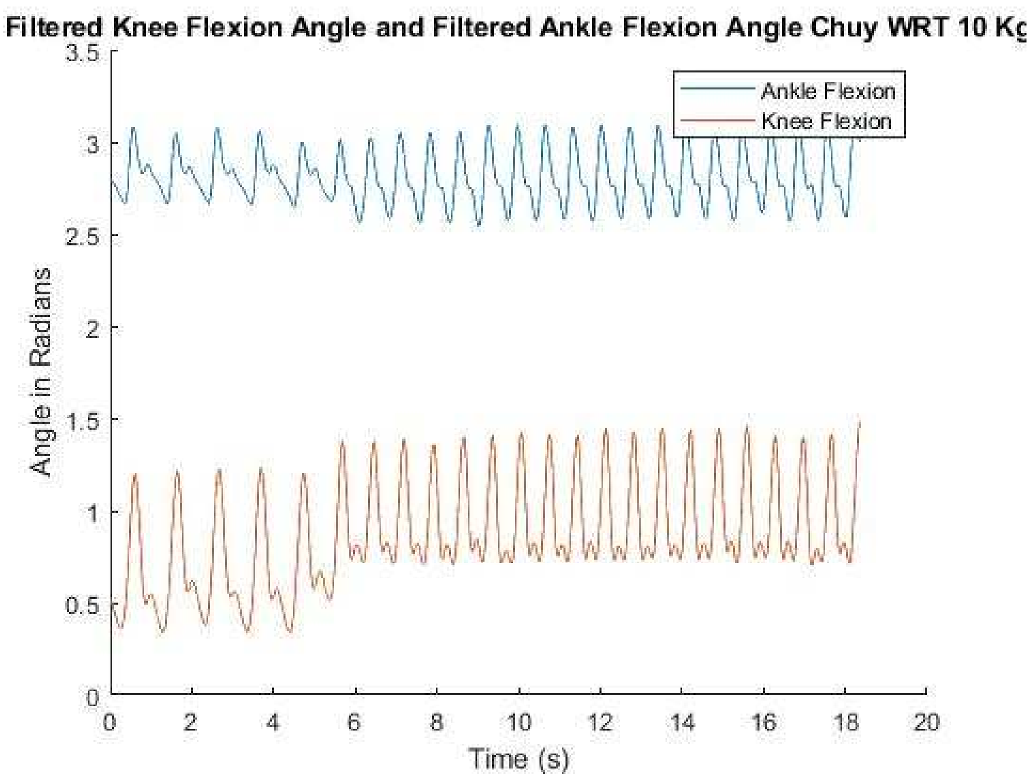

Fig. 61. Filtered knee flexion angle and filtered ankle flexion angle for subject 2 Chuy WRT 10 Kg

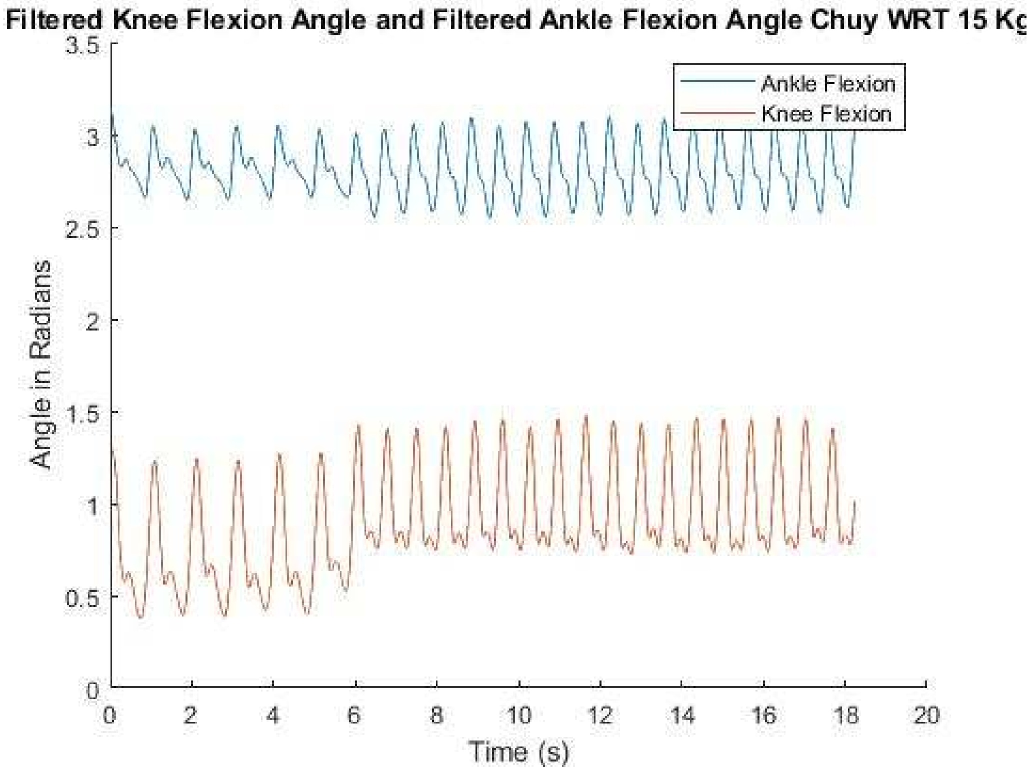

Fig. 62. Filtered knee flexion angle and filtered ankle flexion angle for subject 2 Chuy WRT 15 Kg.

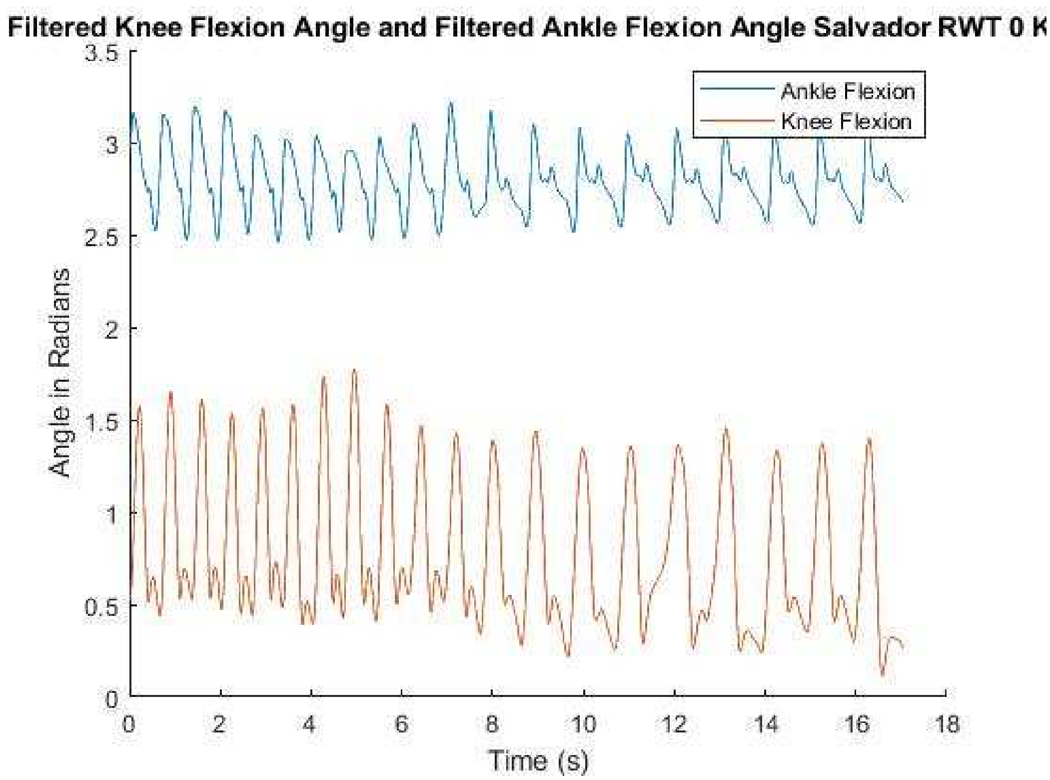

Fig. 63. Filtered knee flexion angle and filtered ankle flexion angle for subject 3 Salvador RWT 0 Kg.

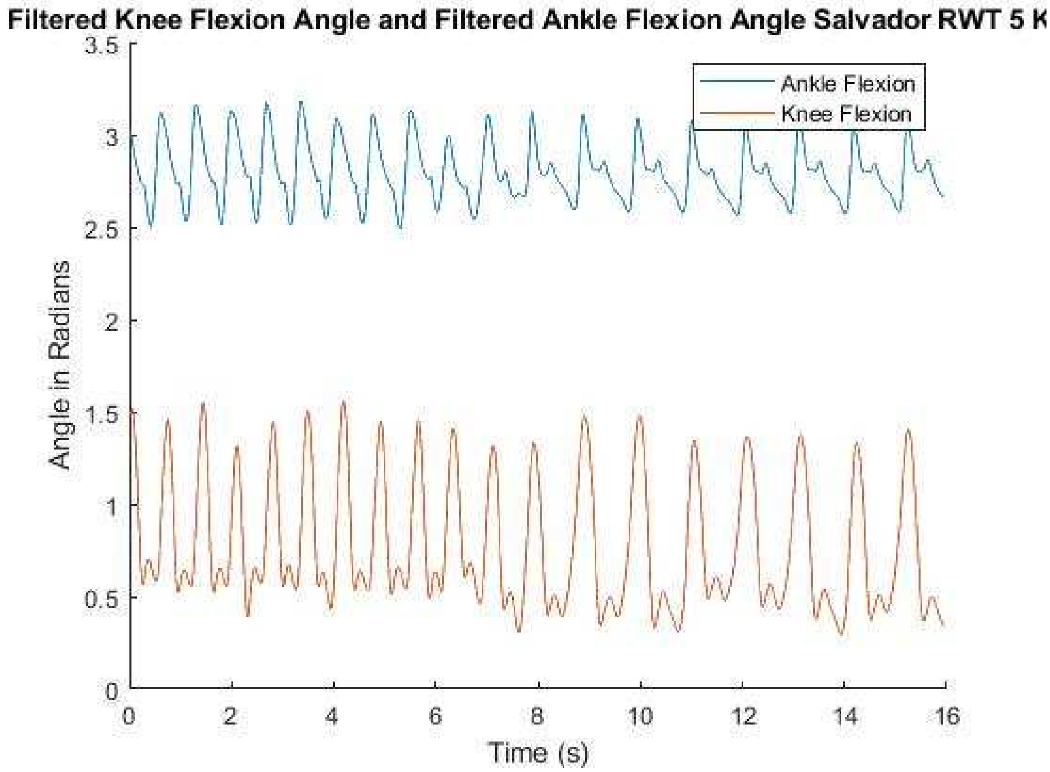

Fig. 64. Filtered knee flexion angle and filtered ankle flexion angle for subject 3 Salvador RWT 5 Kg.

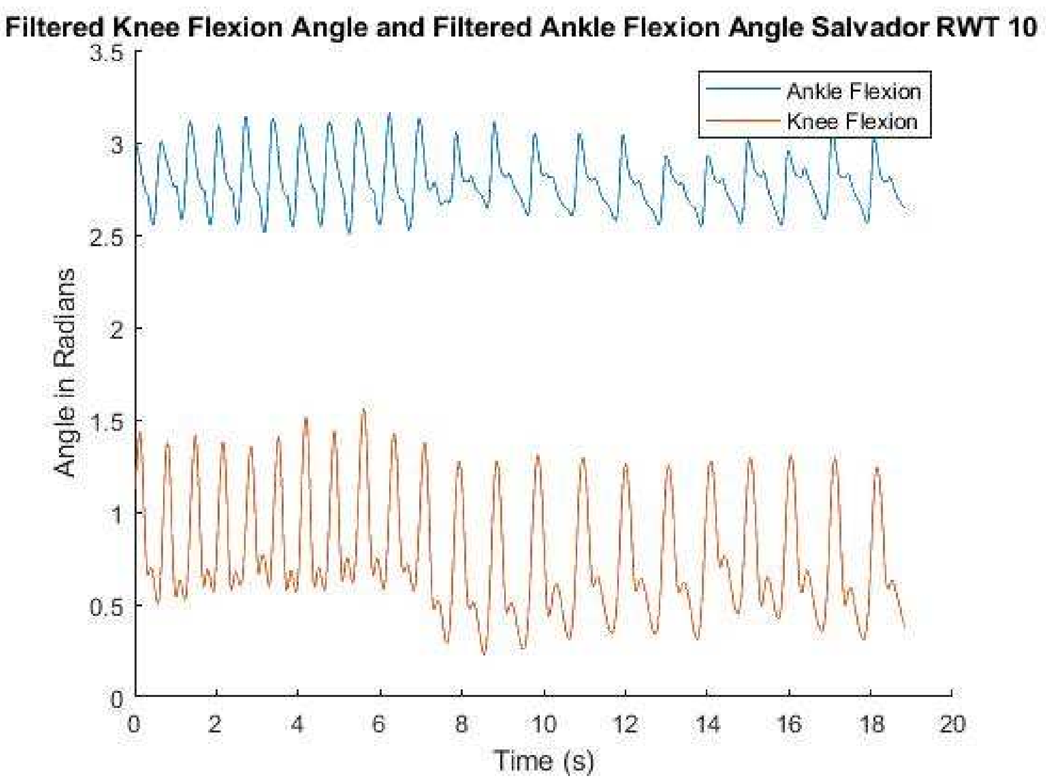

Fig. 65. Filtered knee flexion angle and filtered ankle flexion angle for subject 3 Salvador RWT 10 Kg.

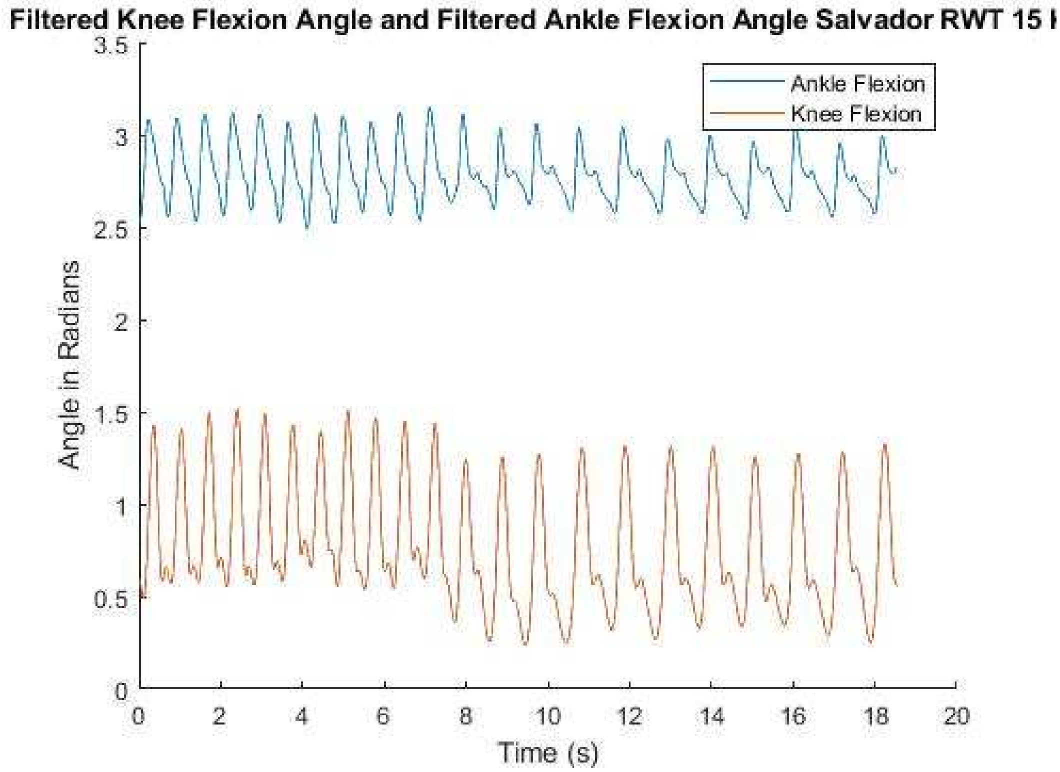

Fig. 66. Filtered knee flexion angle and filtered ankle flexion angle for subject 3 Salvador RWT 15 Kg.

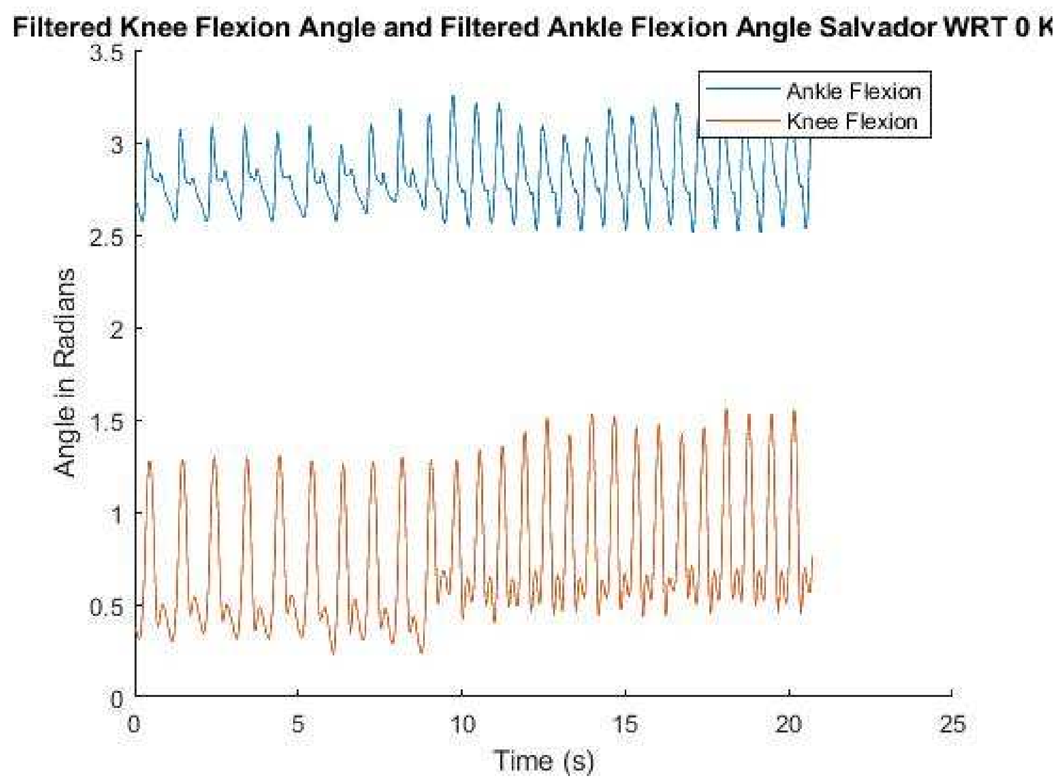

Fig. 67. Filtered knee flexion angle and filtered ankle flexion angle for subject 3 Salvador WRT 0 Kg.

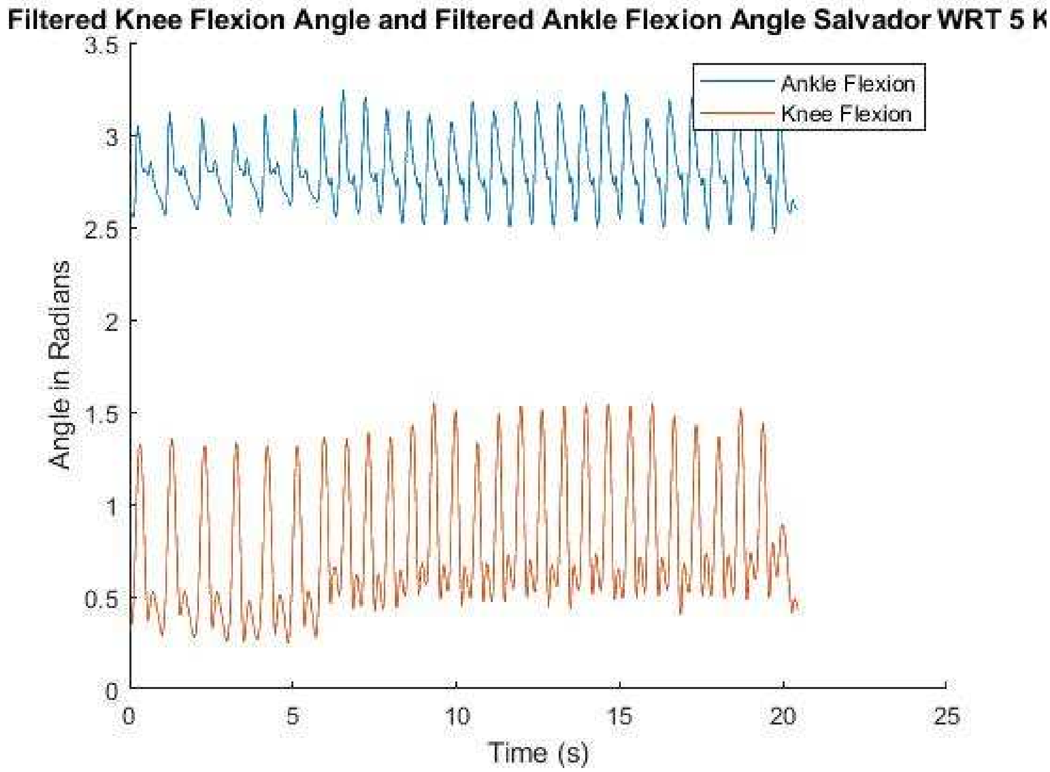

Fig. 68. Filtered knee flexion angle and filtered ankle flexion angle for subject 3 Salvador WRT 5 Kg.

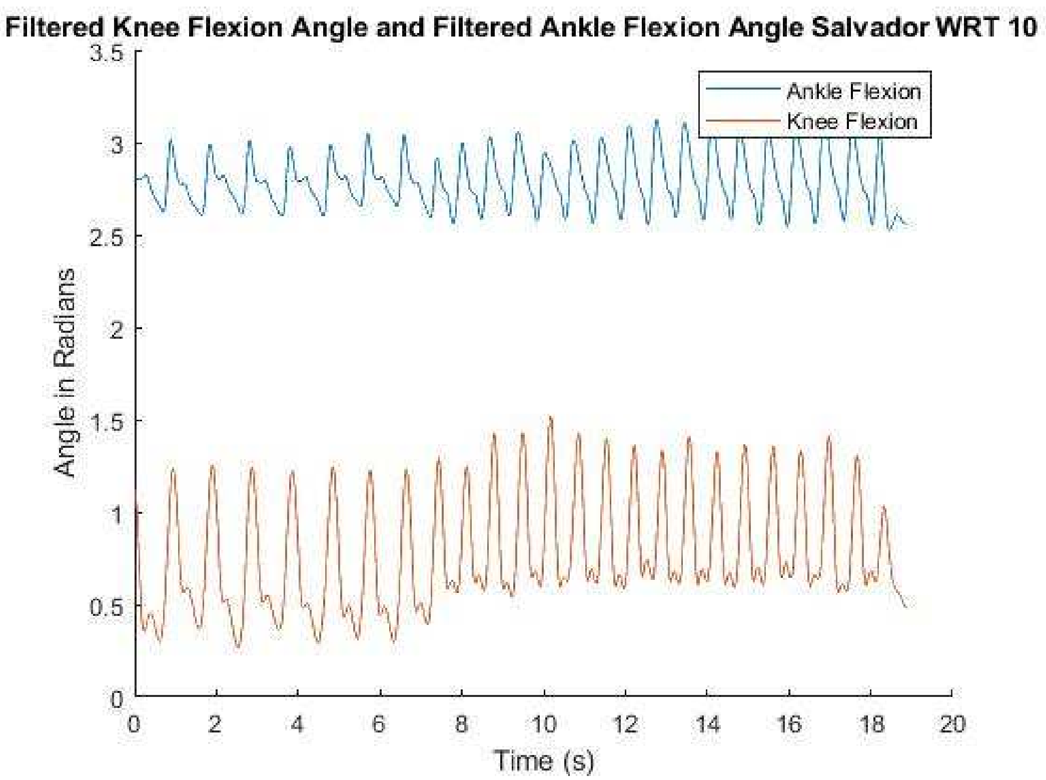

Fig. 69. Filtered knee flexion angle and filtered ankle flexion angle for subject 3 Salvador WRT 10 Kg.

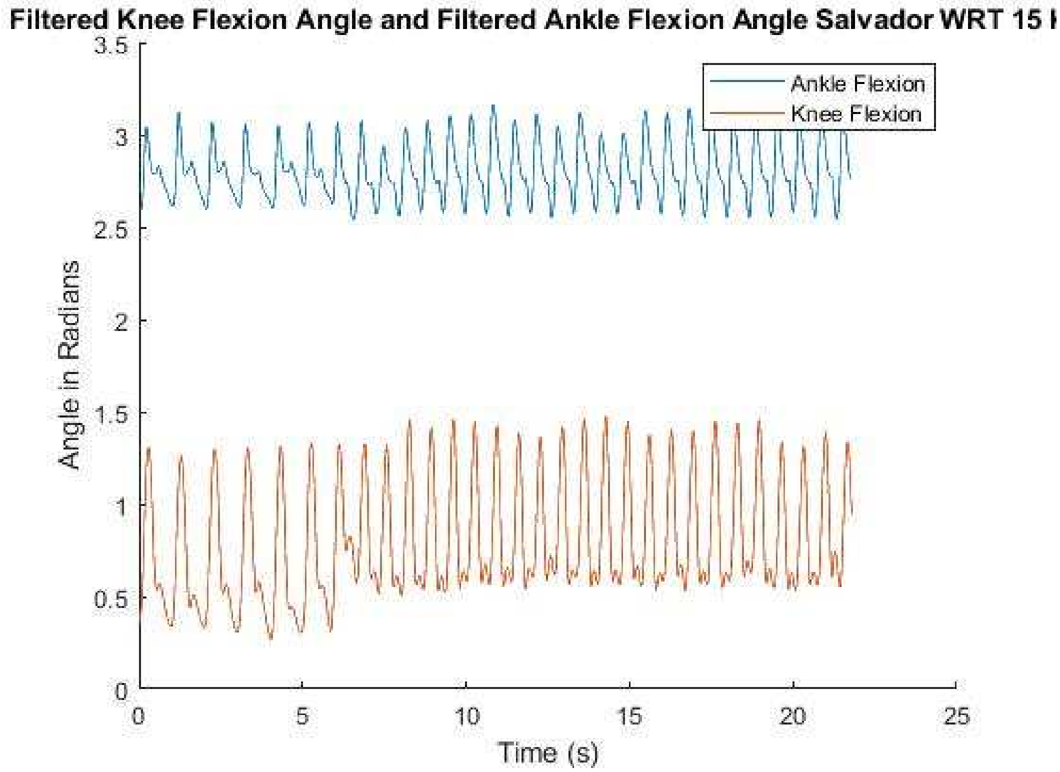

Fig. 70. Filtered knee flexion angle and filtered ankle flexion angle for subject 3 Salvador WRT 15 Kg.

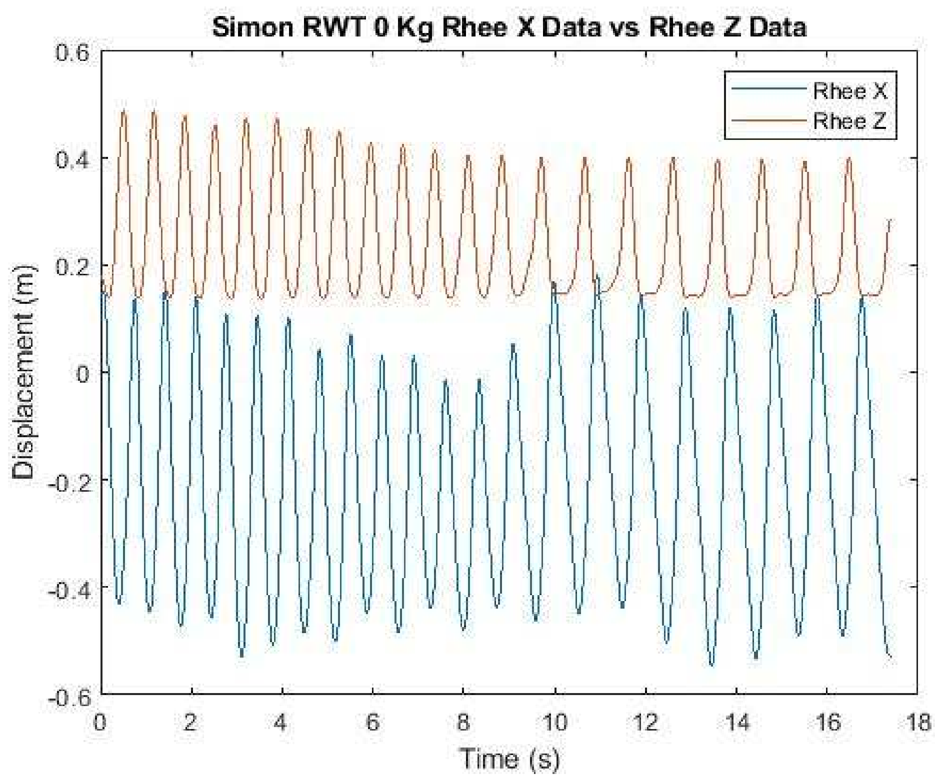

Fig. 71. Subject 1 Simon x vs z heel data vs time plot, without added wight on the RWT trial, used to calculate speed.

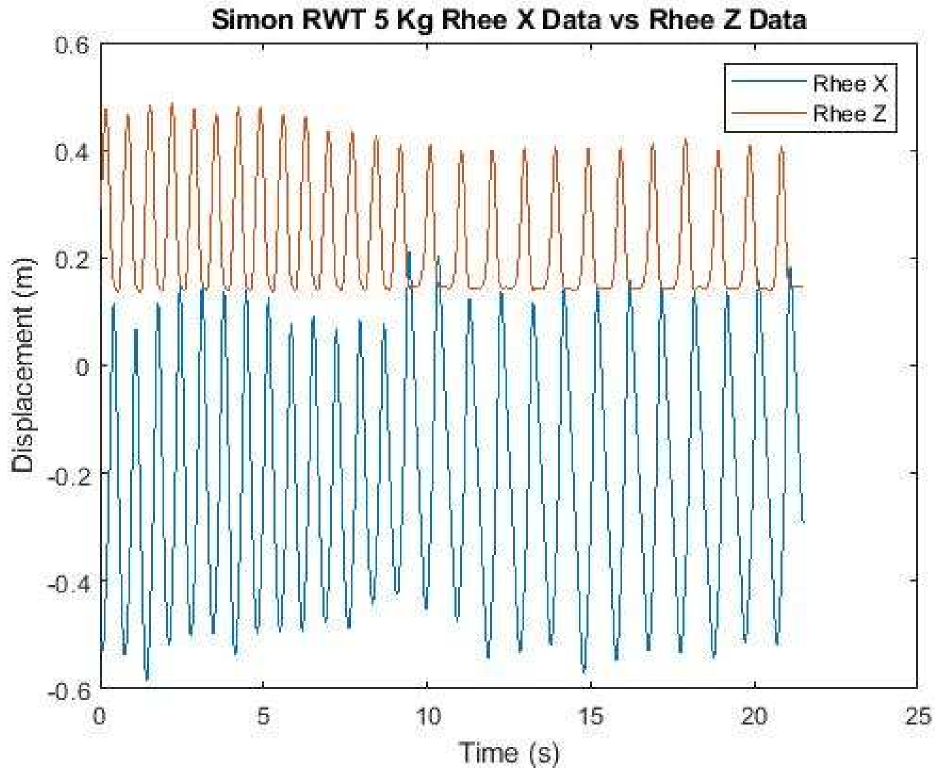

Fig. 72. Subject 1 Simon x vs z heel data vs time plot, with 5kg added wight on the RWT trial, used to calculate speed.

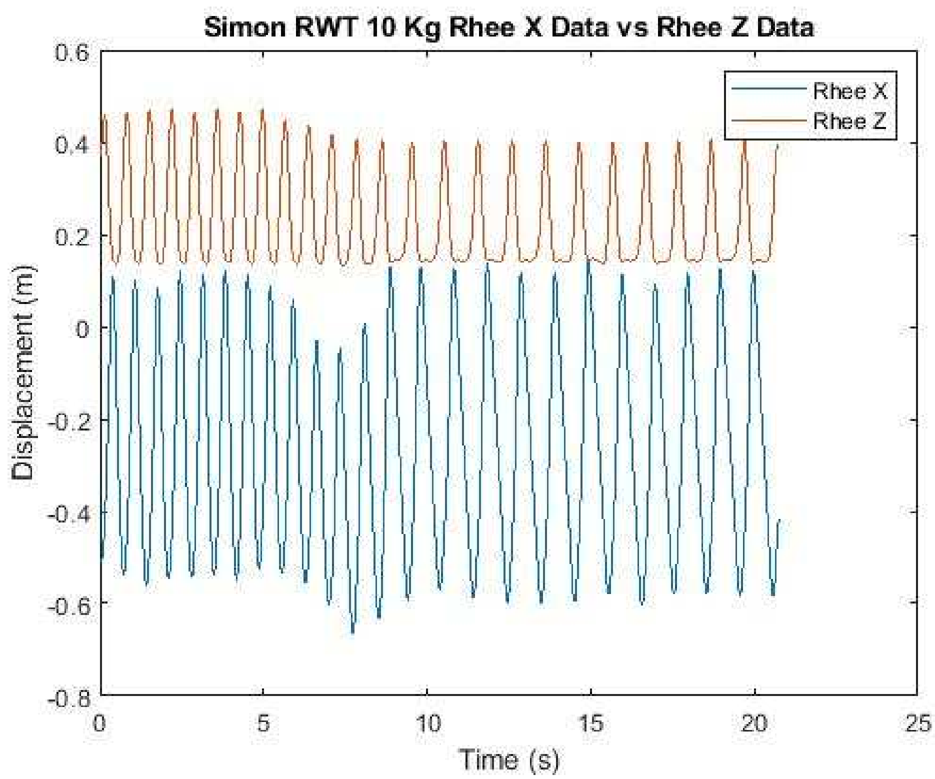

Fig. 73. Subject 1 Simon x vs z heel data vs time plot, with 10 Kg added wight on the RWT trial, used to calculate speed.

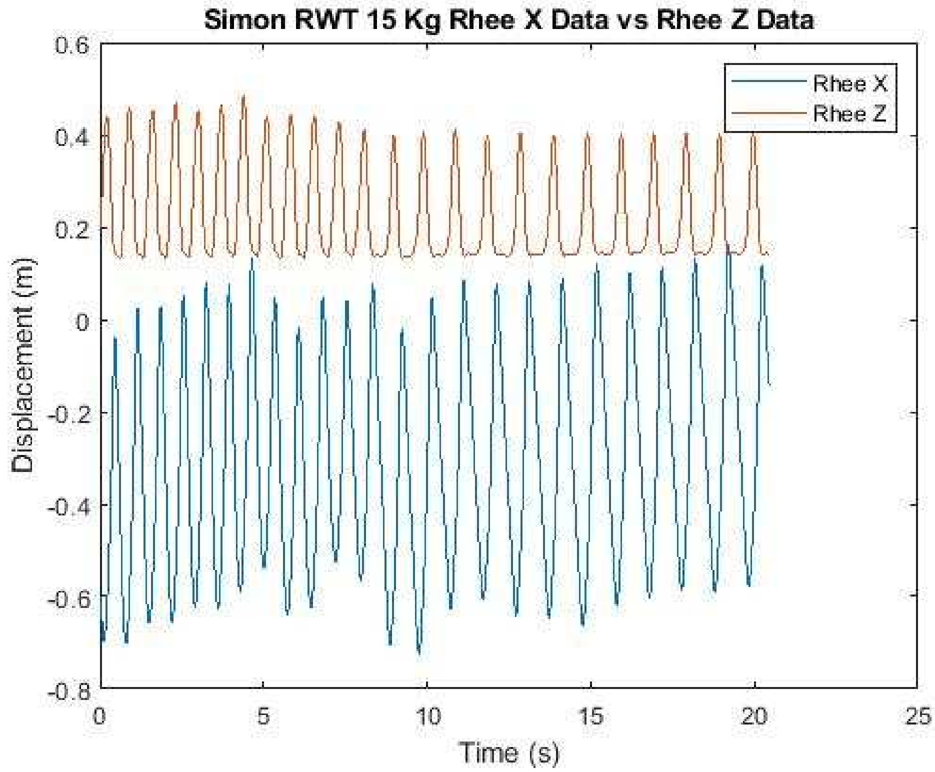

Fig. 74. Subject 1 Simon x vs z heel data vs time plot, with 15 Kg added wight on the RWT trial, used to calculate speed.

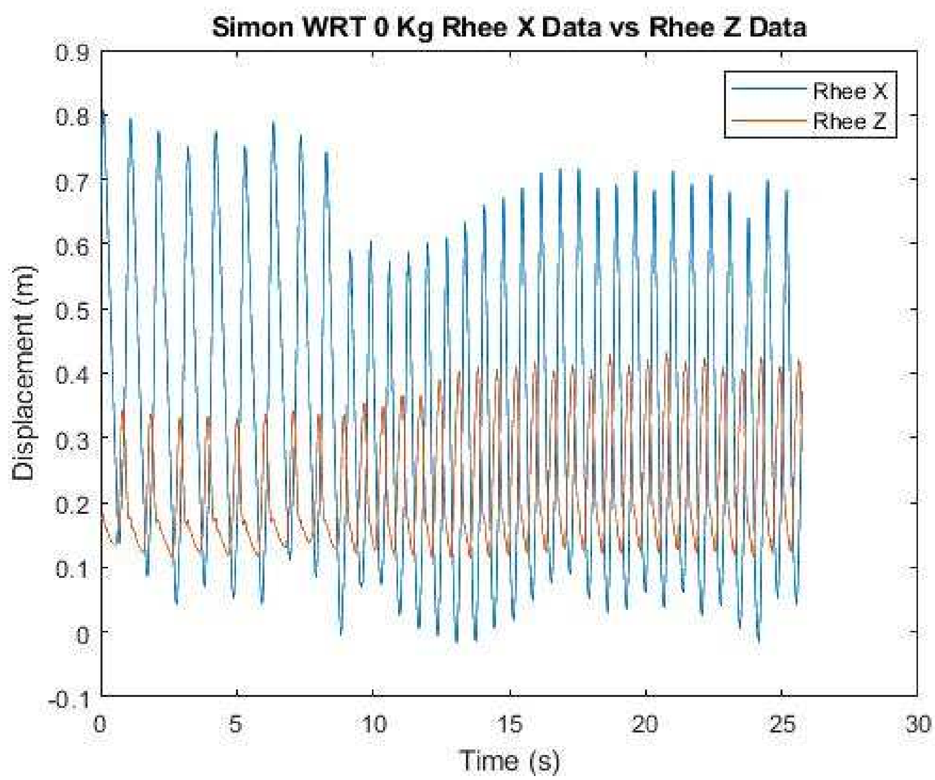

Fig. 75. Subject 1 Simon x vs z heel data vs time plot, with 0 Kg added wight on the WRT trial, used to calculate speed.

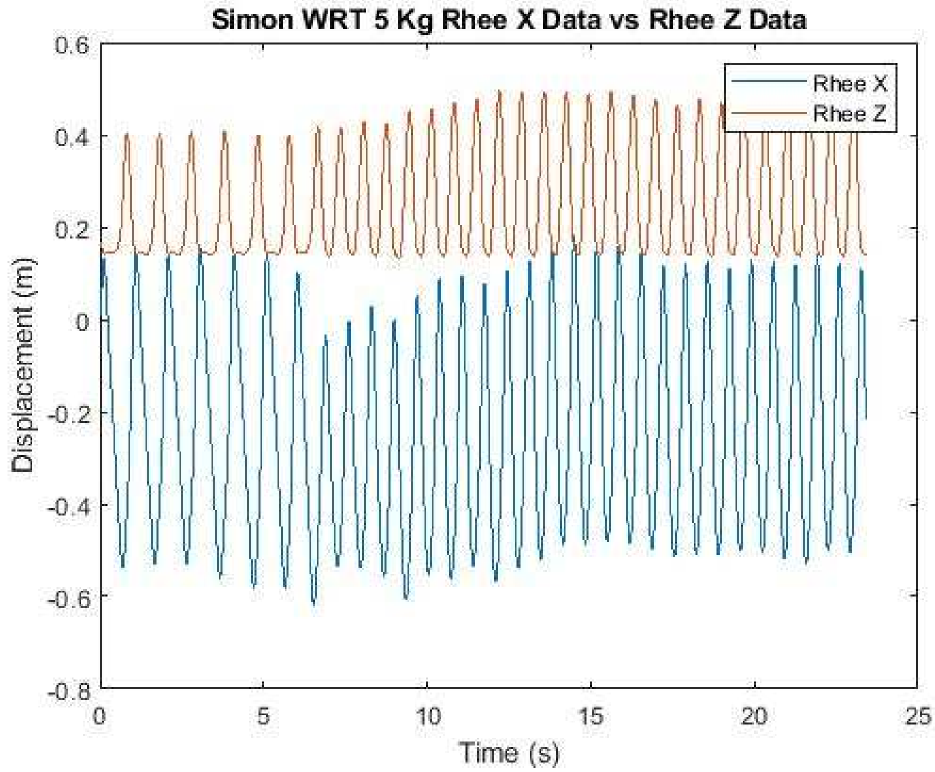

Fig. 76. Subject 1 Simon x vs z heel data vs time plot, with 5 Kg added wight on the WRT trial, used to calculate speed.

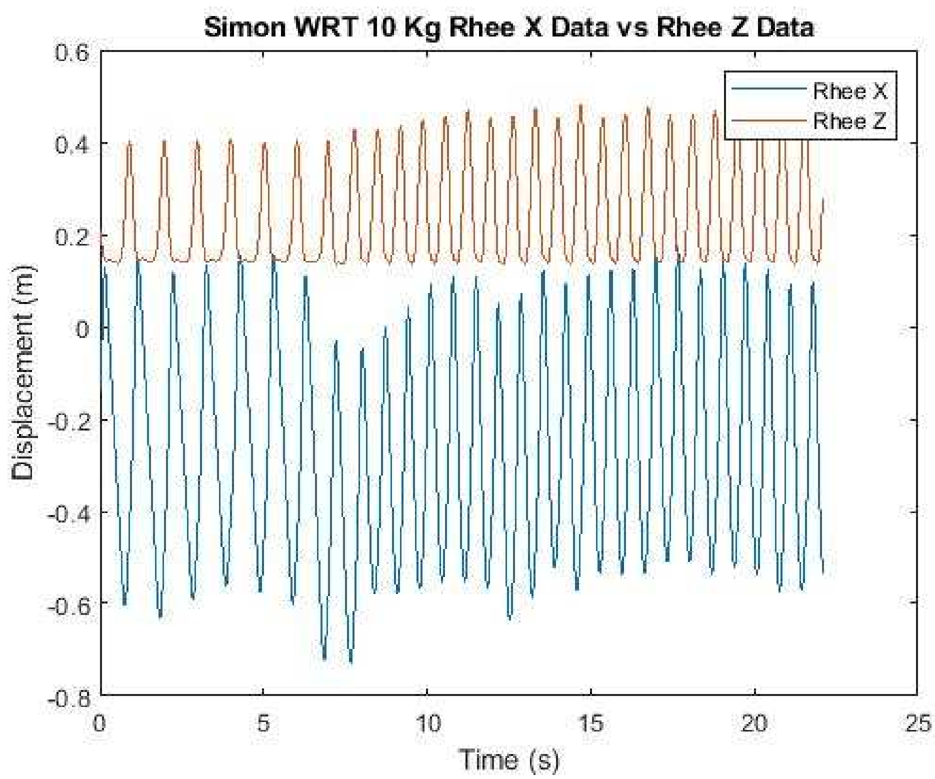

Fig. 77. Subject 1 Simon x vs z heel data vs time plot, with 10 Kg added wight on the WRT trial, used to calculate speed.

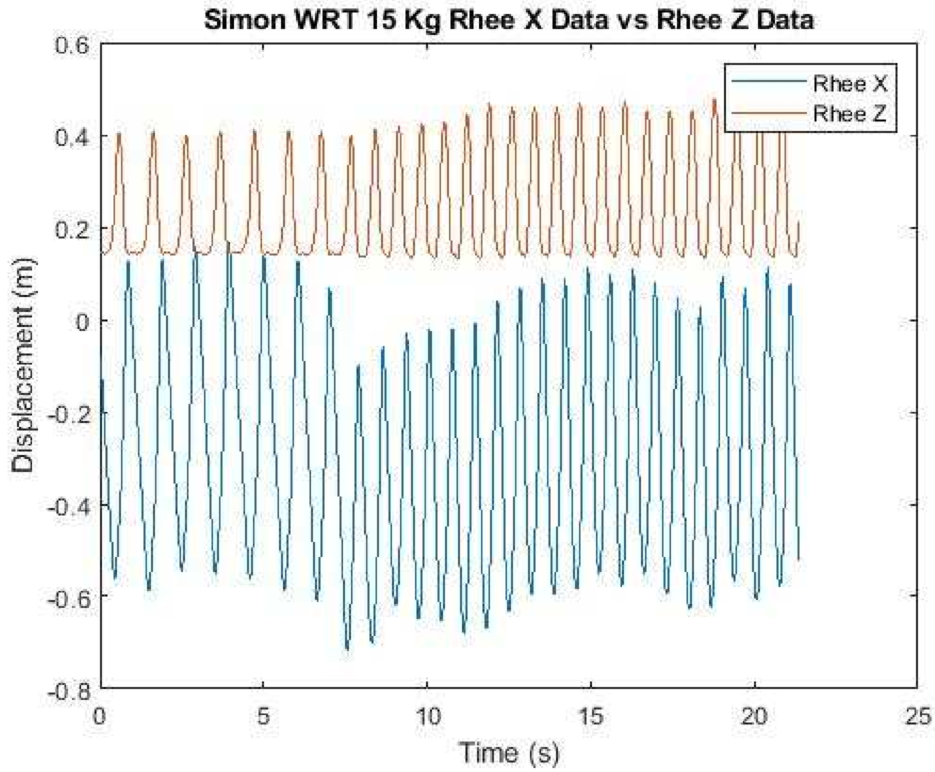

Fig. 78. Subject 1 Simon x vs z heel data vs time plot, with 15 Kg added wight on the WRT trial, used to calculate speed.

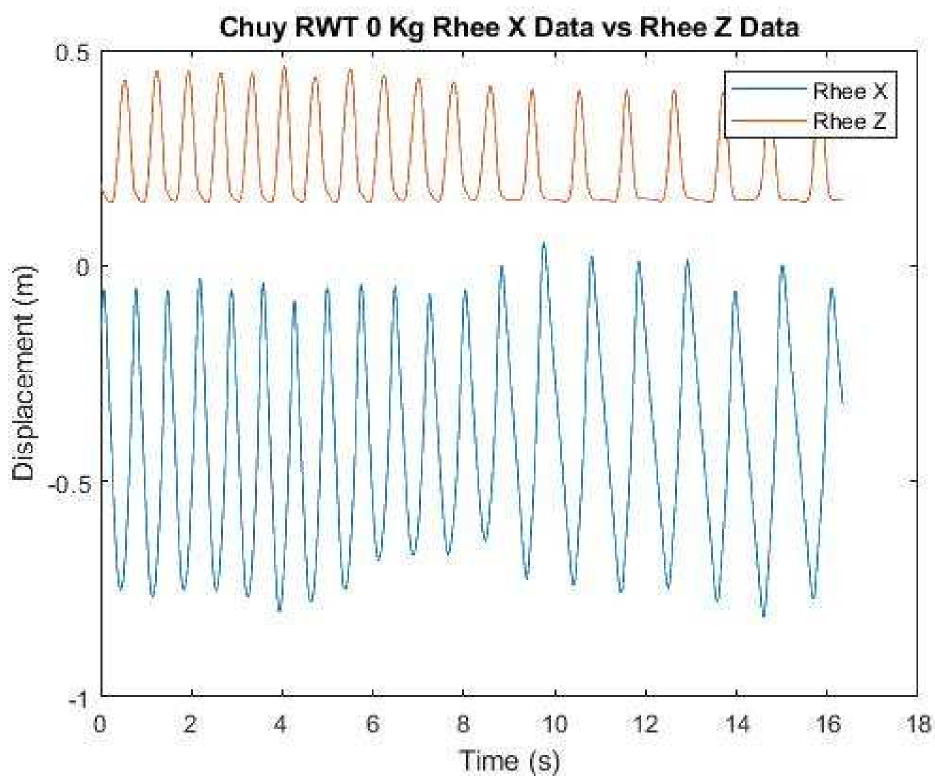

Fig. 79. Subject 2 Chuy x vs z heel data vs time plot, without added wight on the RWT trial, used to calculate speed.

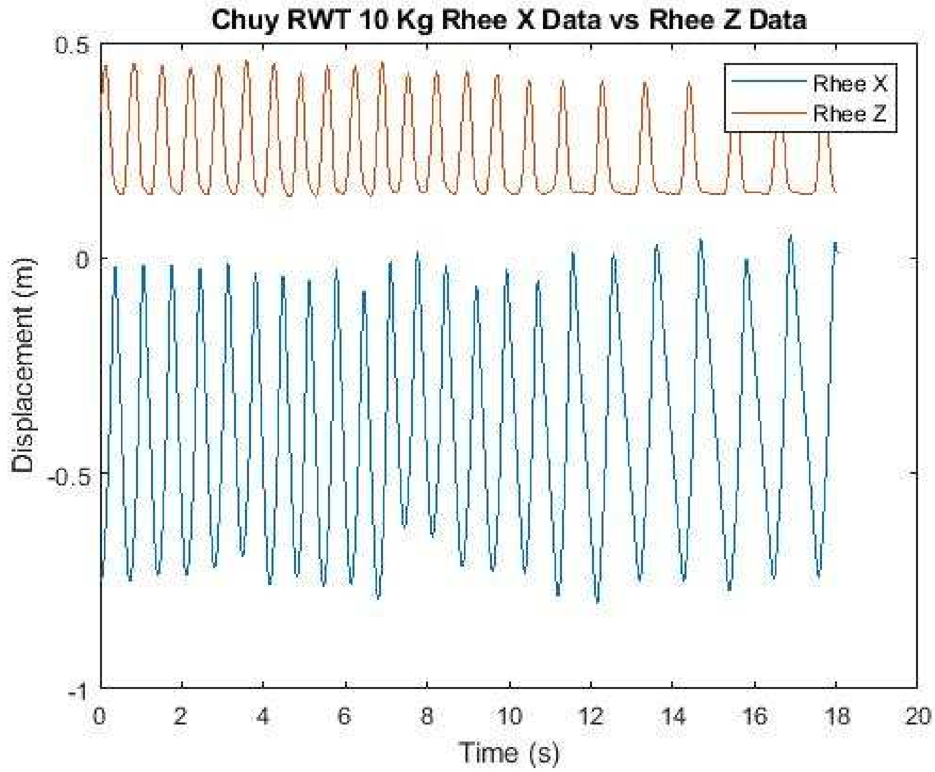

Fig. 80. Subject 2 Chuy x vs z heel data vs time plot, with 10 Kg added wight on the RWT trial, used to calculate speed.

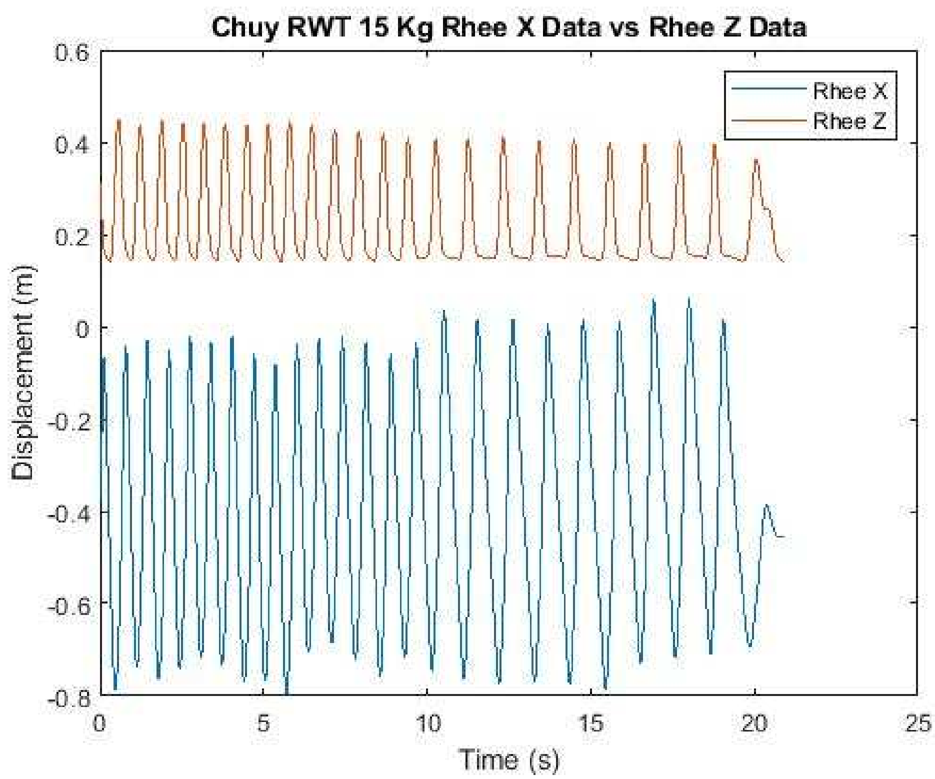

Fig. 81. Subject 2 Chuy x vs z heel data vs time plot, with 15 Kg added wight on the RWT trial, used to calculate speed.

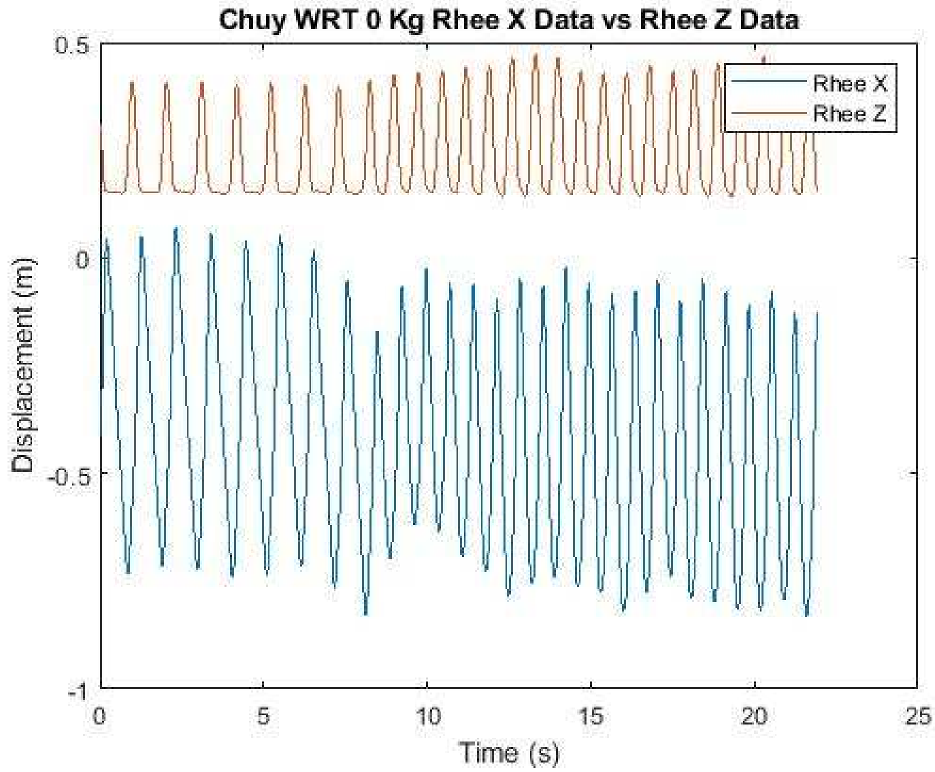

Fig. 82. Subject 2 Chuy x vs z heel data vs time plot, without added wight on the WRT trial, used to calculate speed.

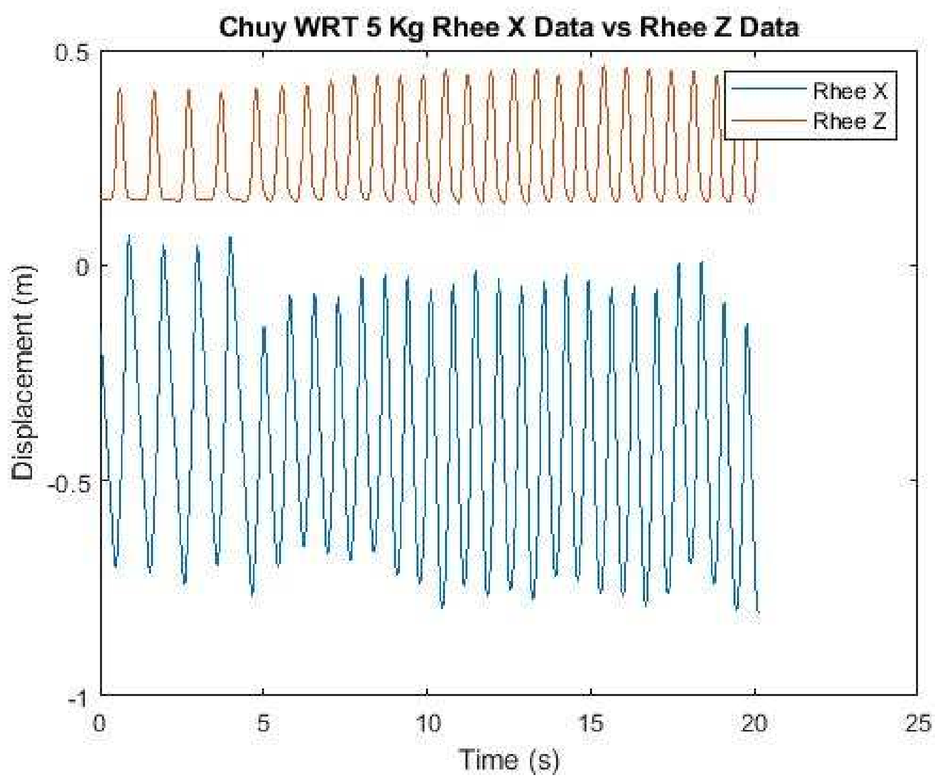

Fig. 83. Subject 2 Chuy x vs z heel data vs time plot, with 5 Kg added wight on the WRT trial, used to calculate speed.

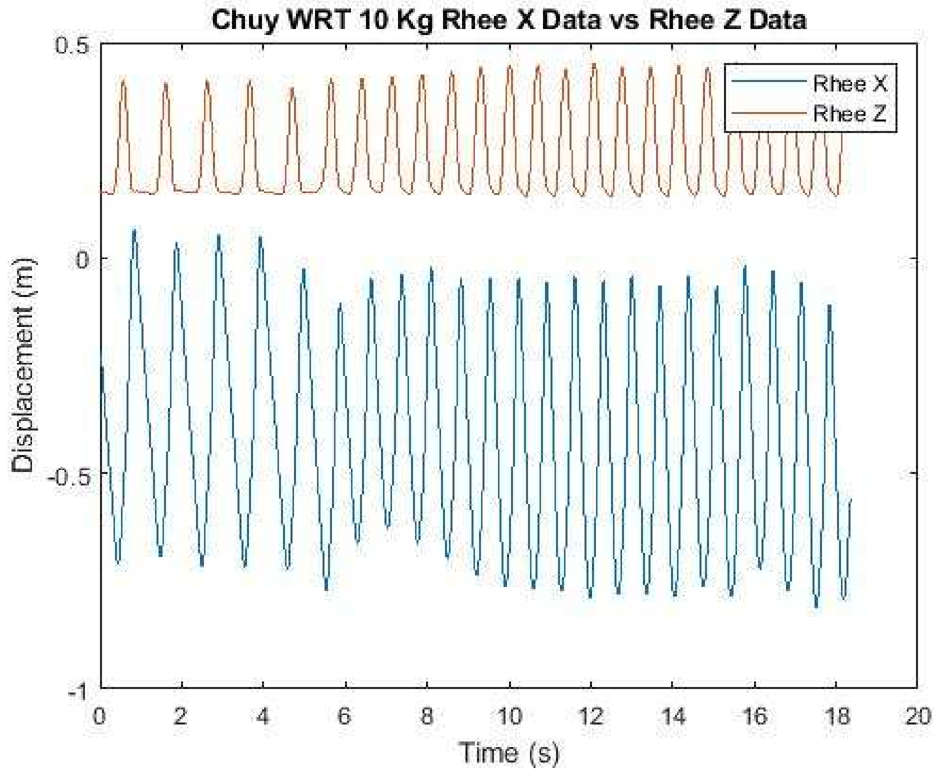

Fig. 84. Subject 2 Chuy x vs z heel data vs time plot, with 10 Kg added wight on the WRT trial, used to calculate speed.

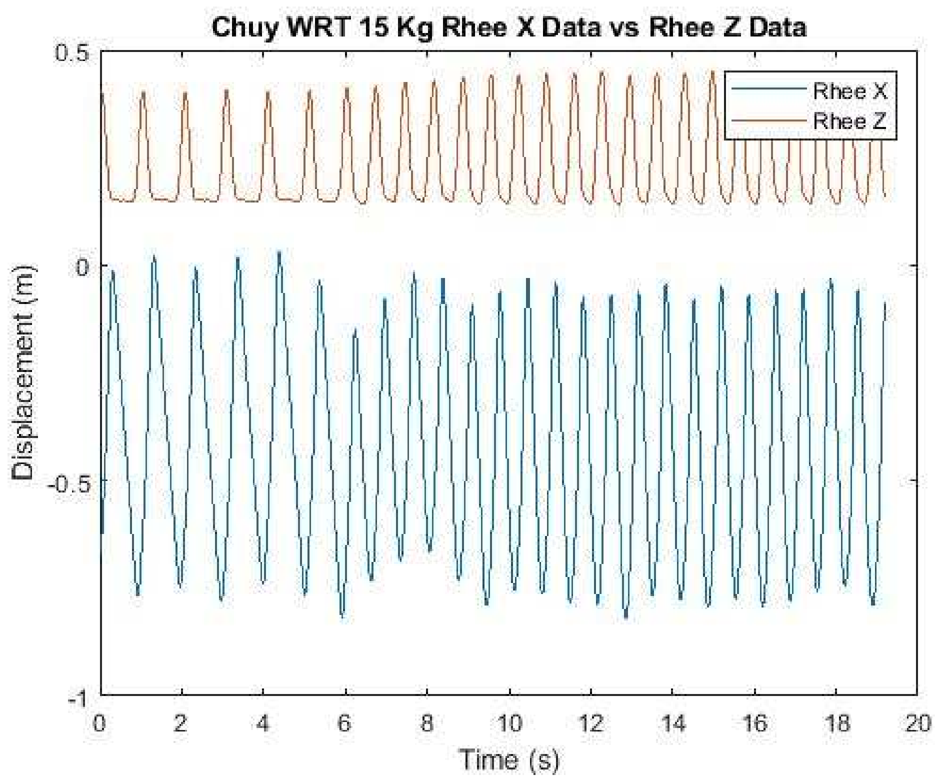

Fig. 85. Subject 2 Chuy x vs z heel data vs time plot, with 15 Kg added wight on the WRT trial, used to calculate speed.

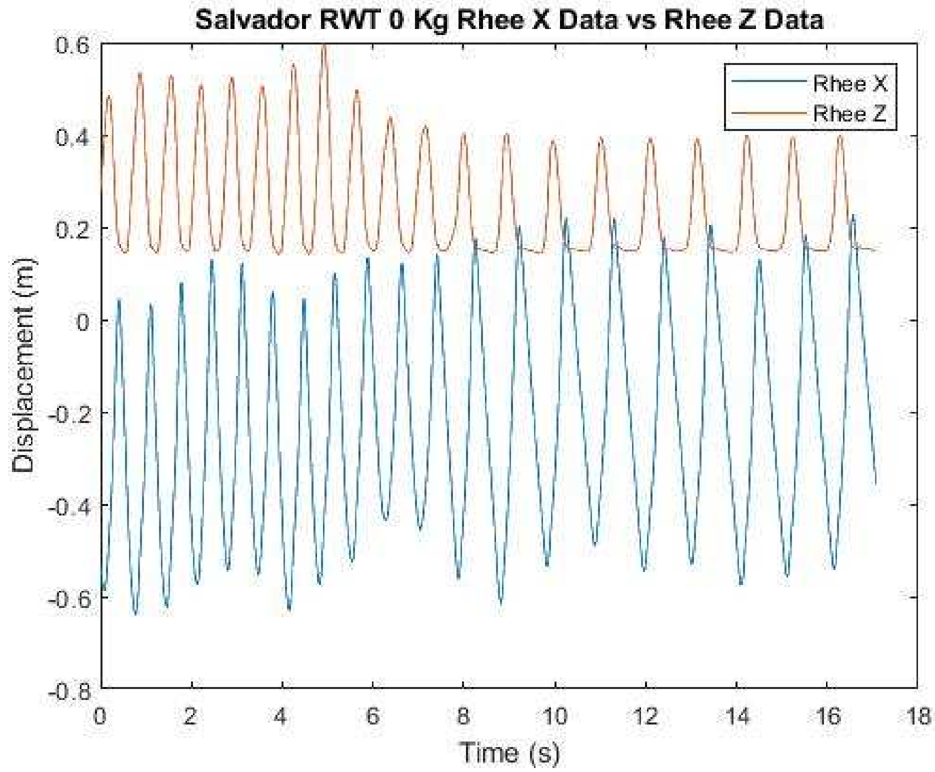

Fig. 86. Subject 3 Salvador x vs z heel data vs time plot, with 0 Kg added wight on the RWT trial, used to calculate speed.

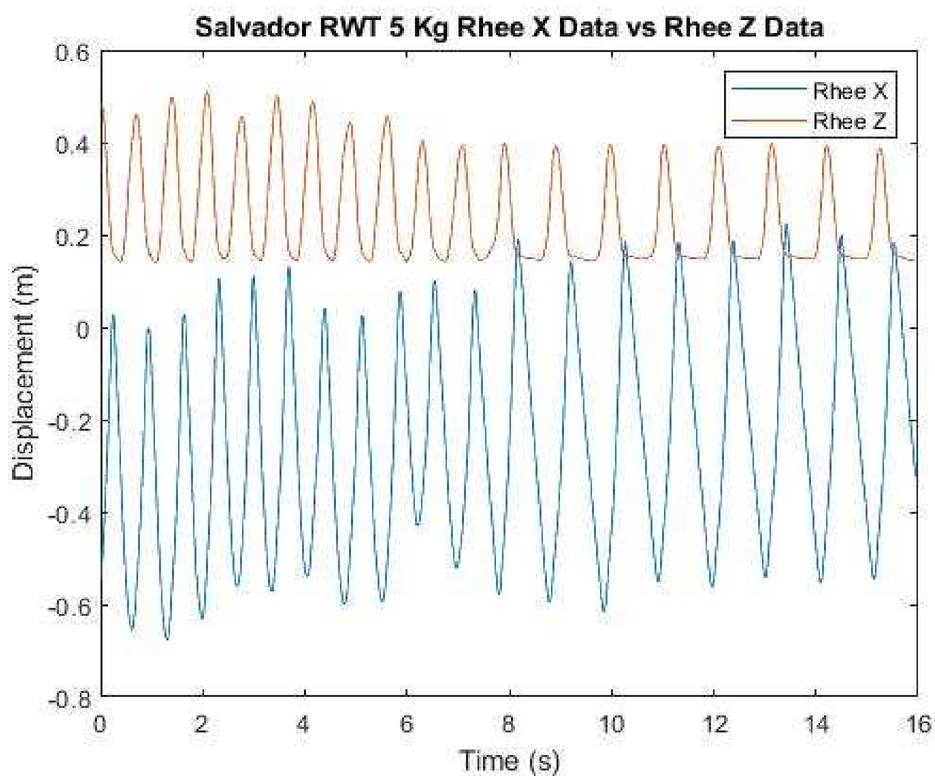

Fig. 87. Subject 3 Salvador x vs z heel data vs time plot, with 5 Kg added wight on the RWT trial, used to calculate speed.

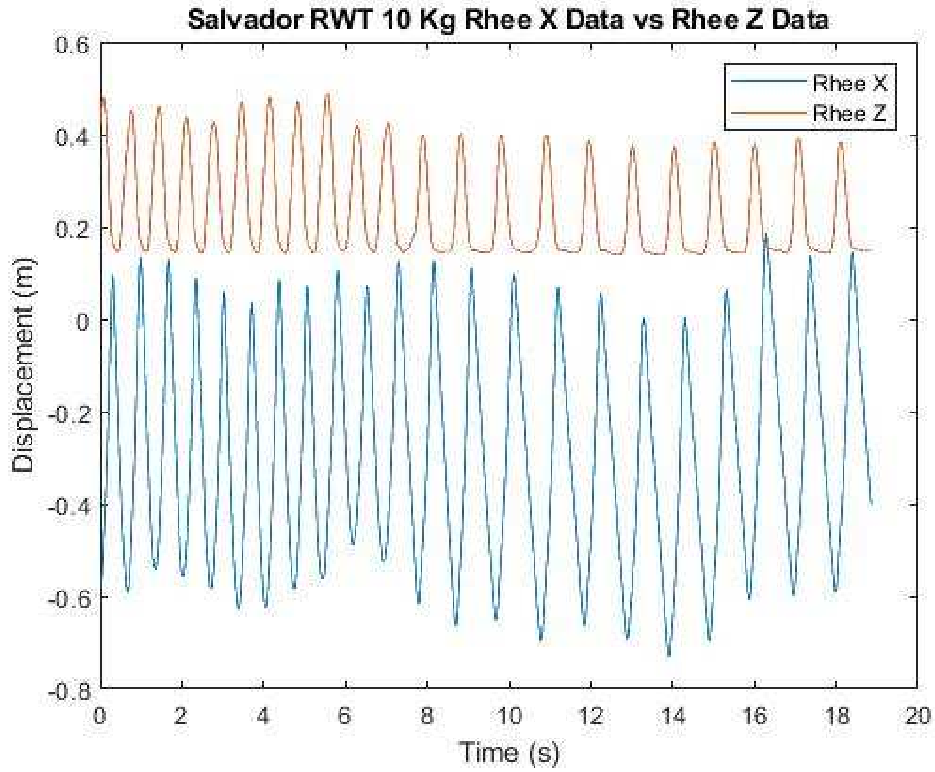

Fig. 88. Subject 3 Salvador x vs z heel data vs time plot, with 10 Kg added wight on the RWT trial, used to calculate speed.

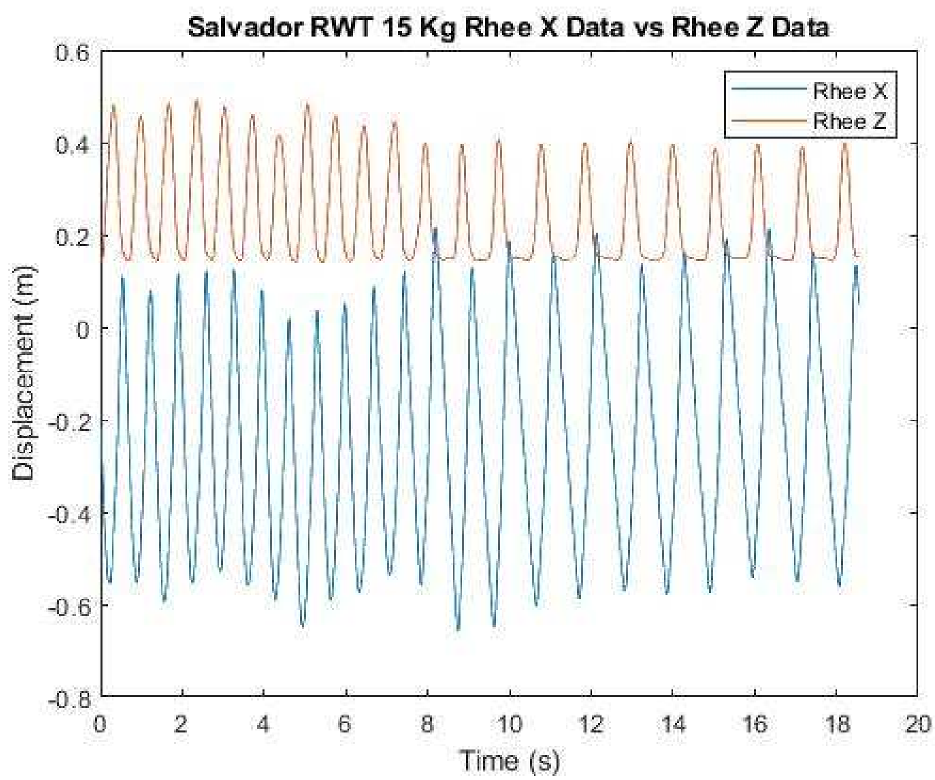

Fig. 89. Subject 3 Salvador x vs z heel data vs time plot, with 15 Kg added wight on the RWT trial, used to calculate speed.

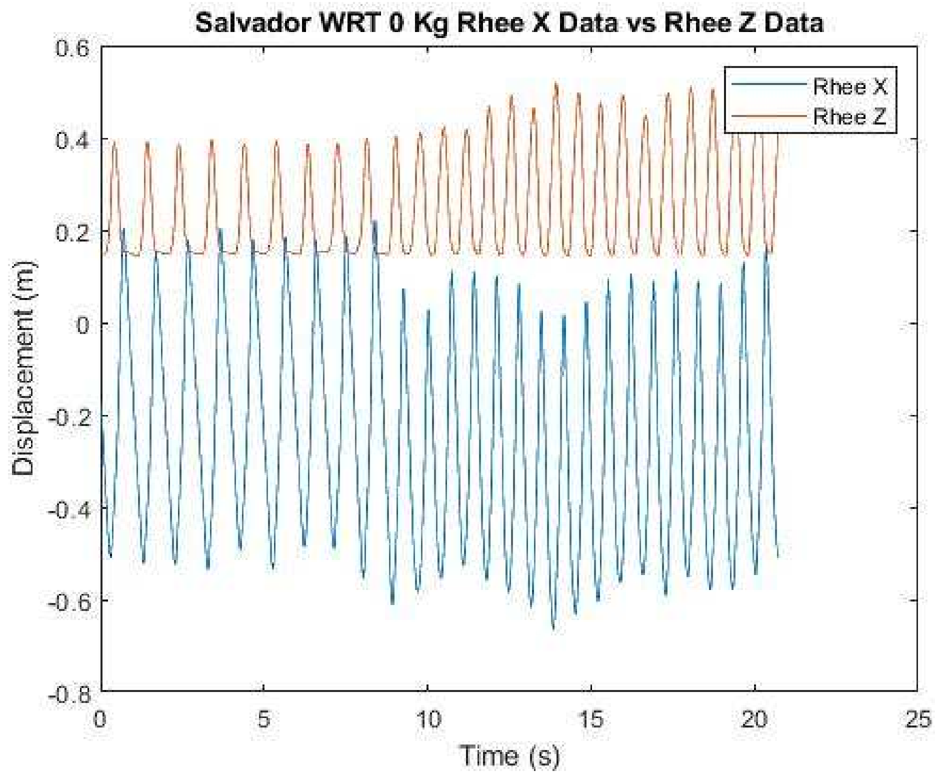

Fig. 90. Subject 3 Salvador x vs z heel data vs time plot, with 0 Kg added wight on the WRT trial, used to calculate speed.

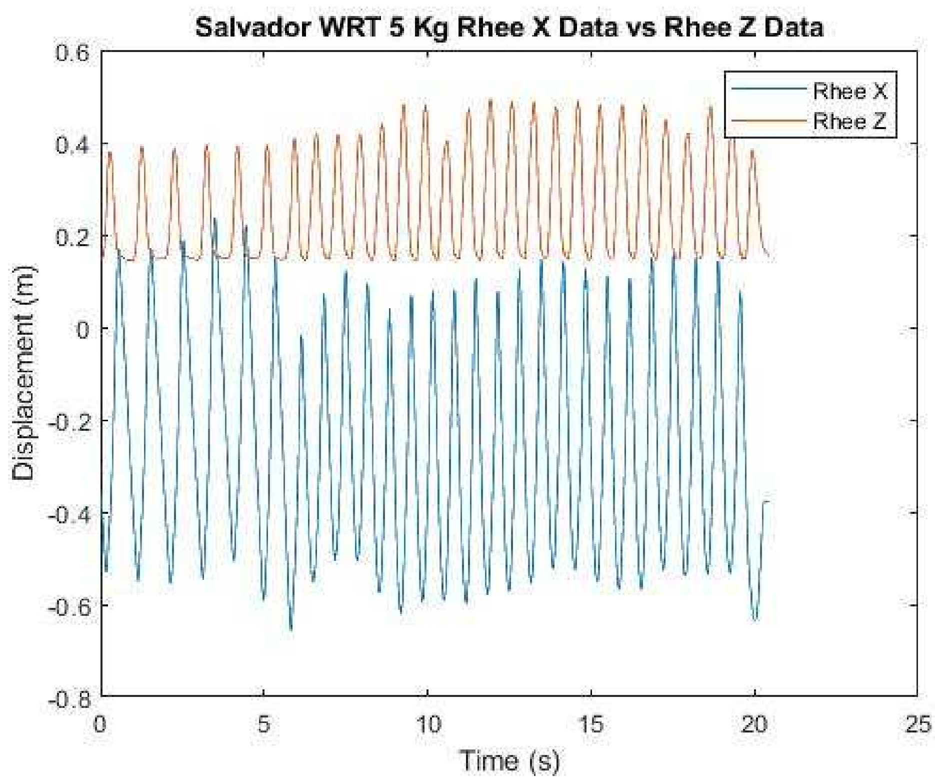

Fig. 91. Subject 3 Salvador x vs z heel data vs time plot, with 5 Kg added wight on the WRT trial, used to calculate speed.

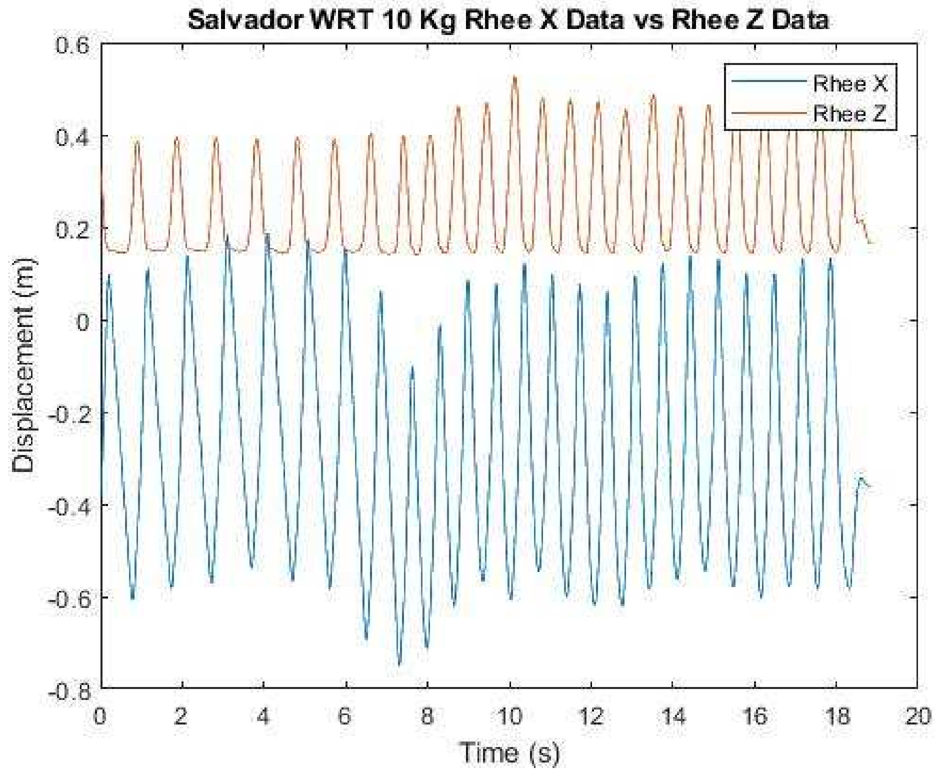

Fig. 92. Subject 3 Salvador x vs z heel data vs time plot, with 10 Kg added wight on the WRT trial, used to calculate speed.

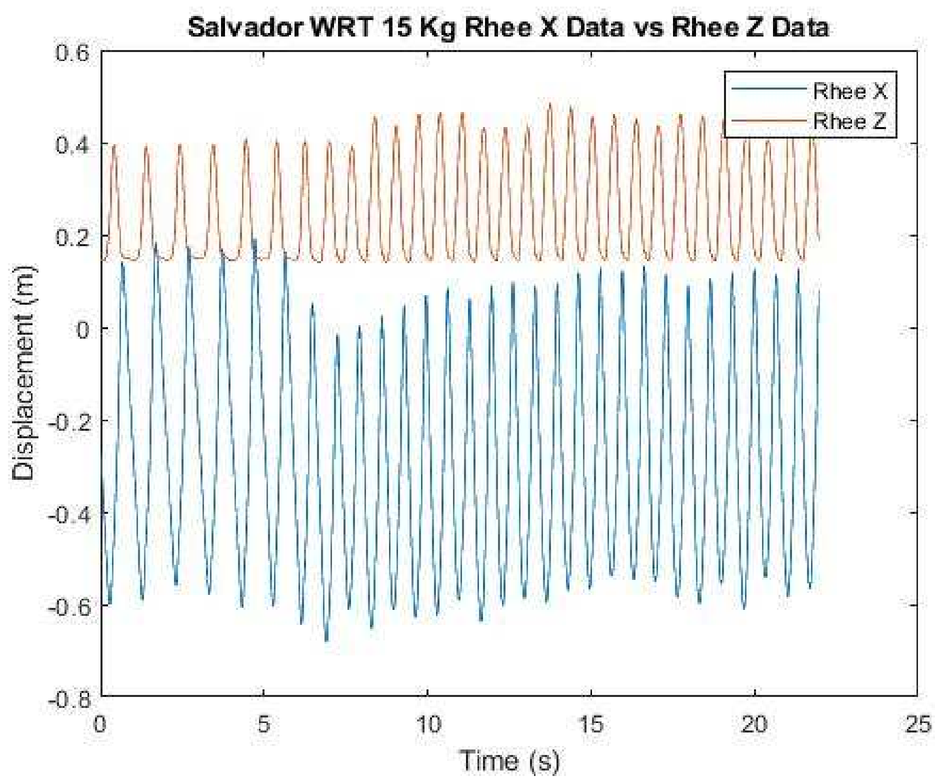

Fig. 93. Subject 3 Salvador x vs z heel data vs time plot, with 15 Kg added wight on the WRT trial, used to calculate speed.

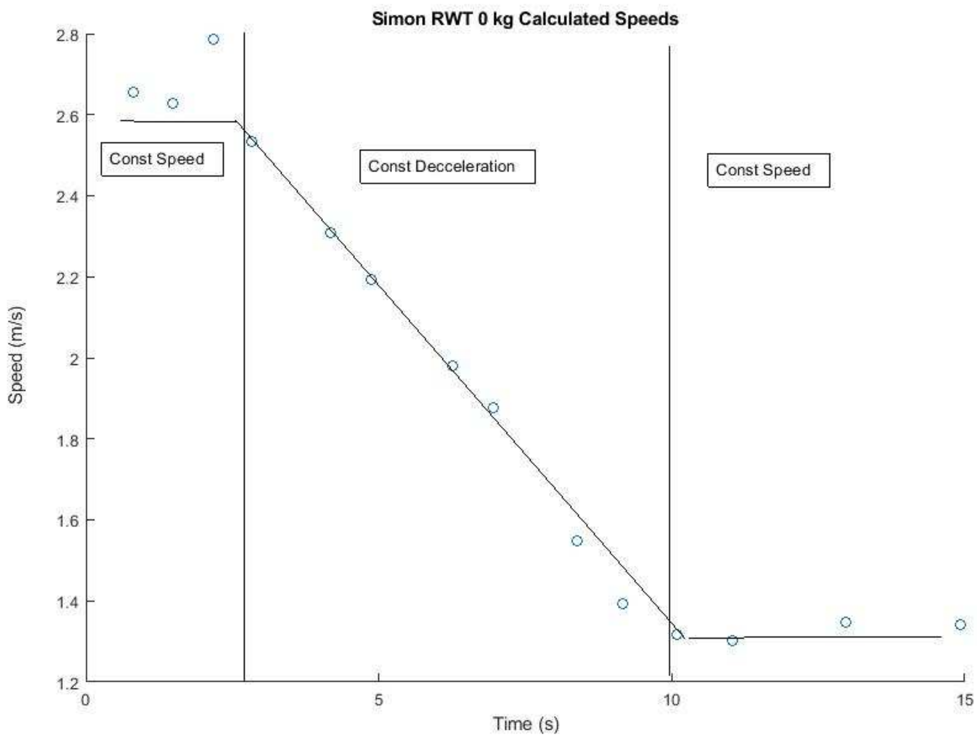

Fig. 94. Calculated speed from Subject 1 Simon's RWT trial without added weight.

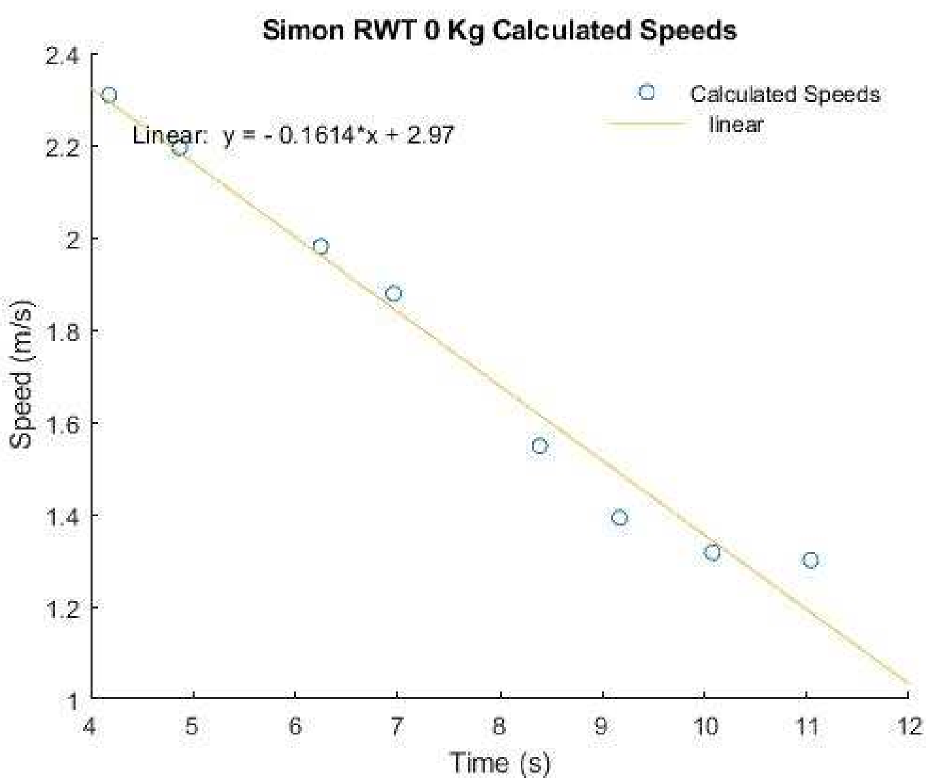

Fig. 95. Zoom from Fig. 94 and linear fitting from constant acceleration zone.

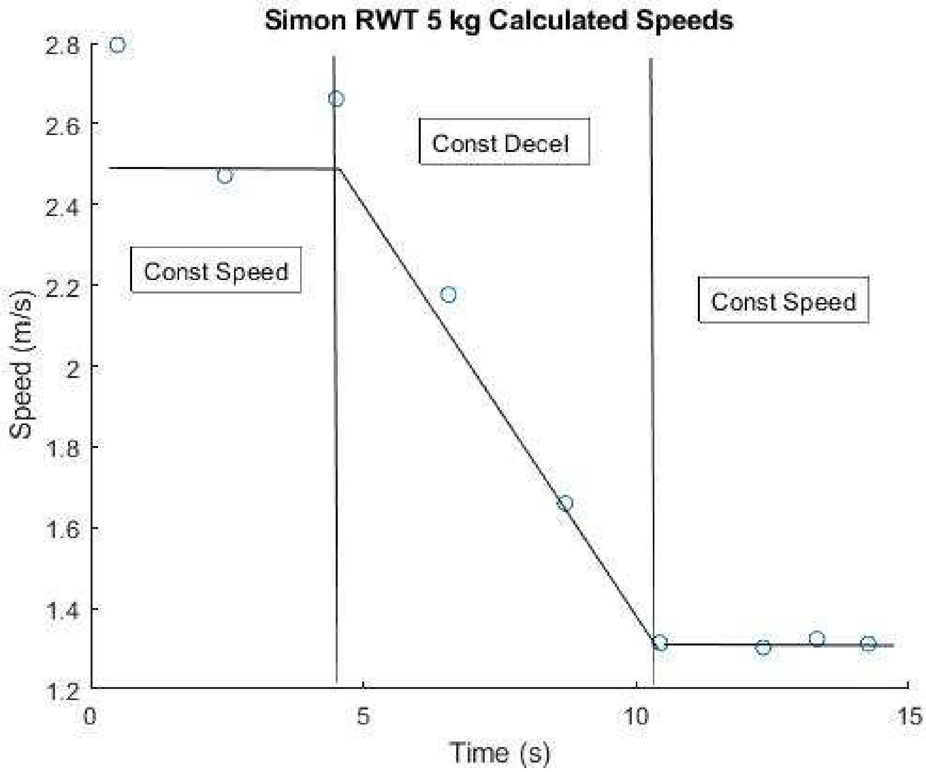

Fig. 96. Calculated speed from Subject 1 Simon's RWT trial with 5 Kg added weight.

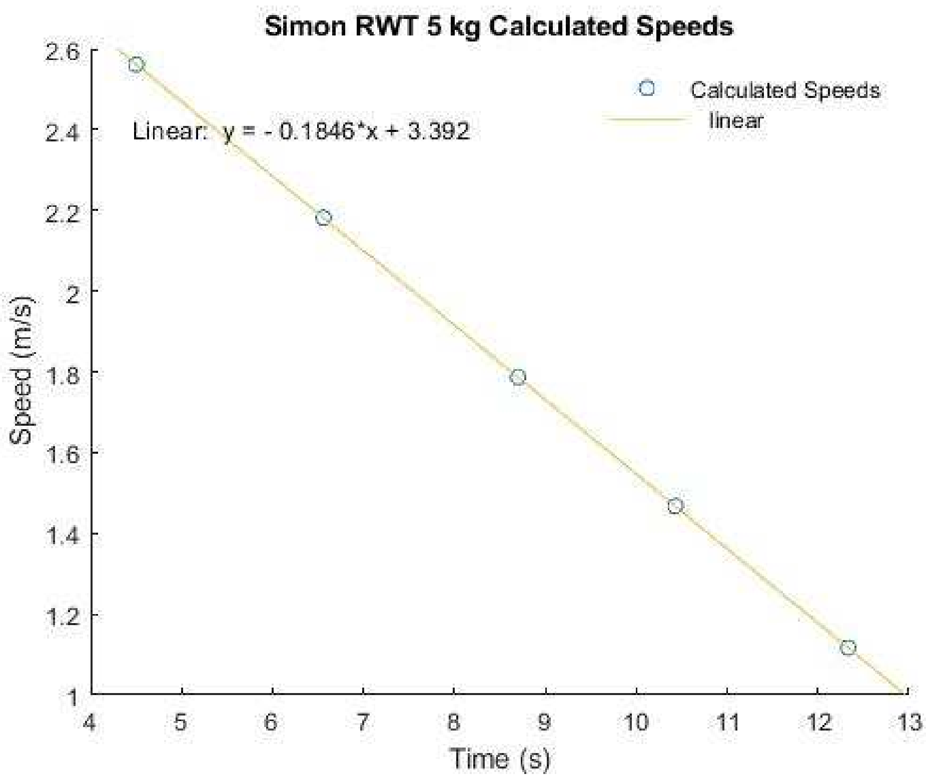

Fig. 97. Zoom from Fig. 96 and linear fitting from constant acceleration zone.

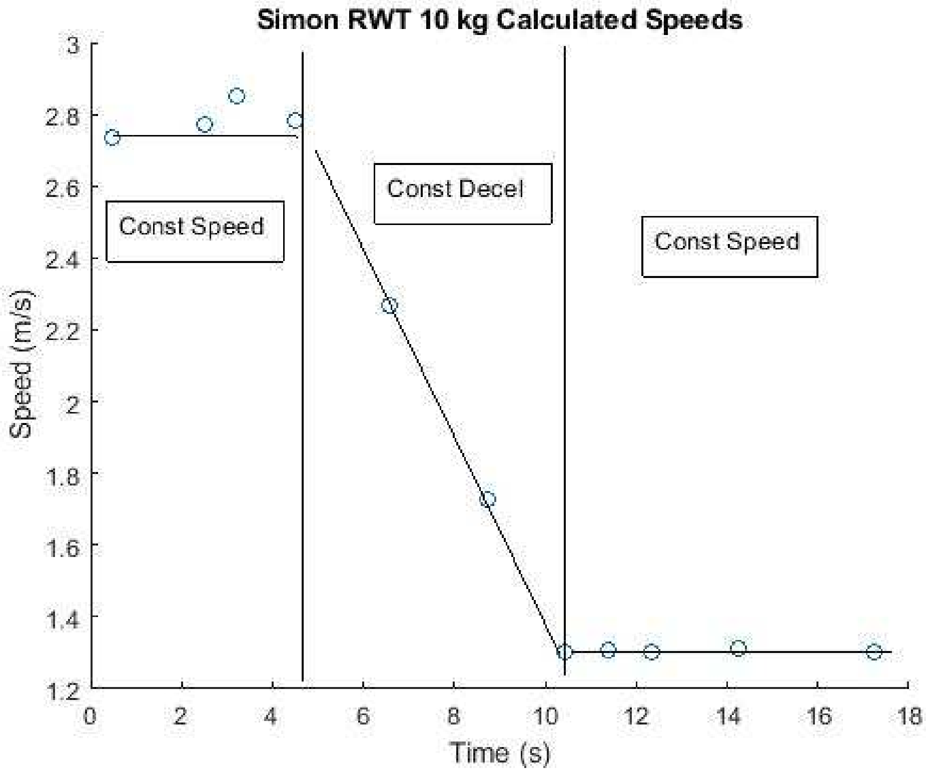

Fig. 98. Calculated speed from Subject 1 Simon's RWT trial with 10 Kg added weight.

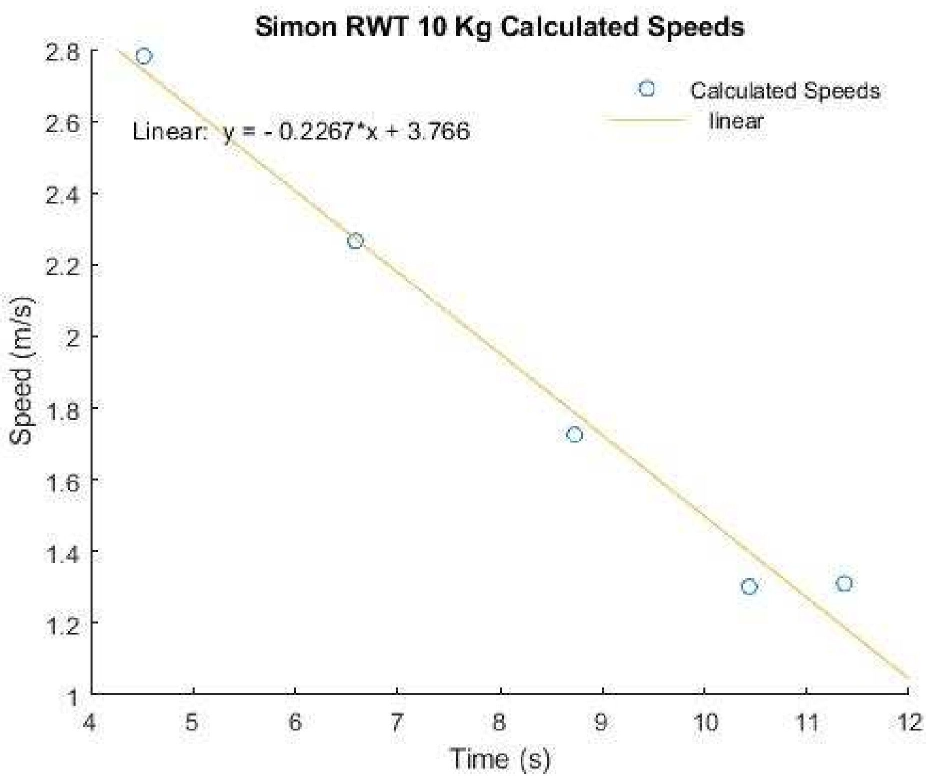

Fig. 99. Zoom from Fig. 98 and linear fitting from constant acceleration zone.

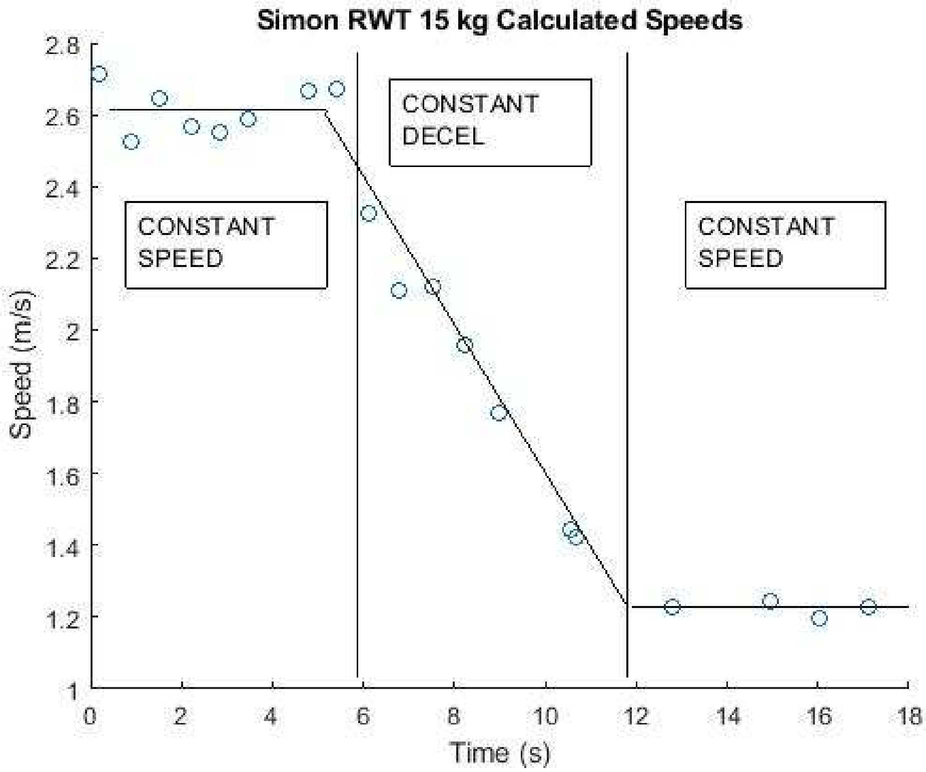

Fig. 100. Calculated speed from Subject 1 Simon's RWT trial with 15 Kg added weight.

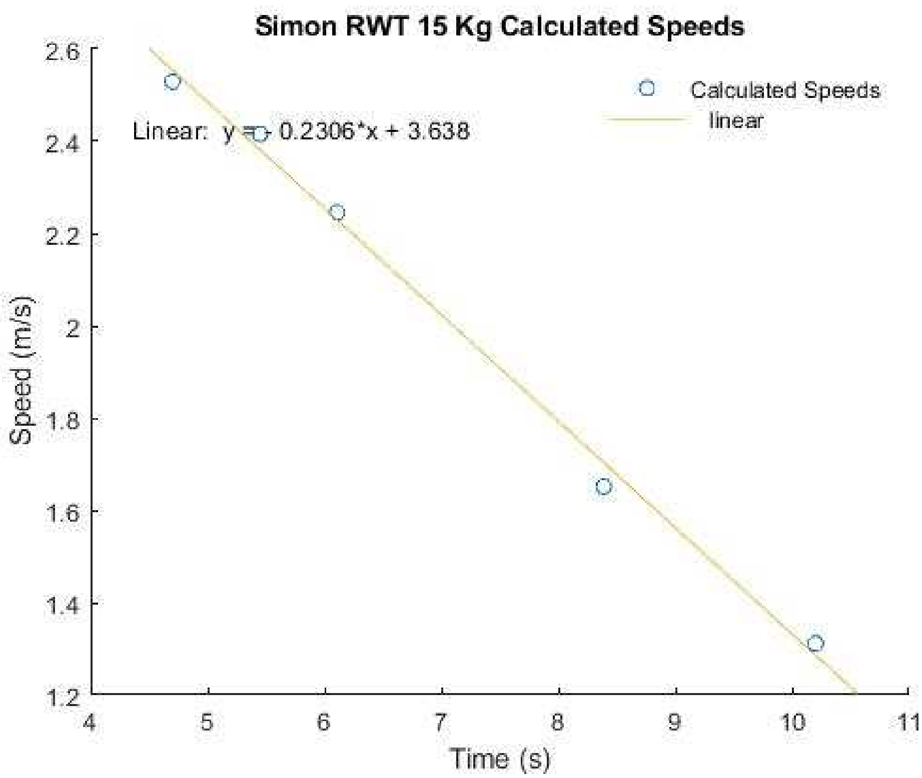

Fig. 101. Zoom from Fig. 100 and linear fitting from constant acceleration zone.

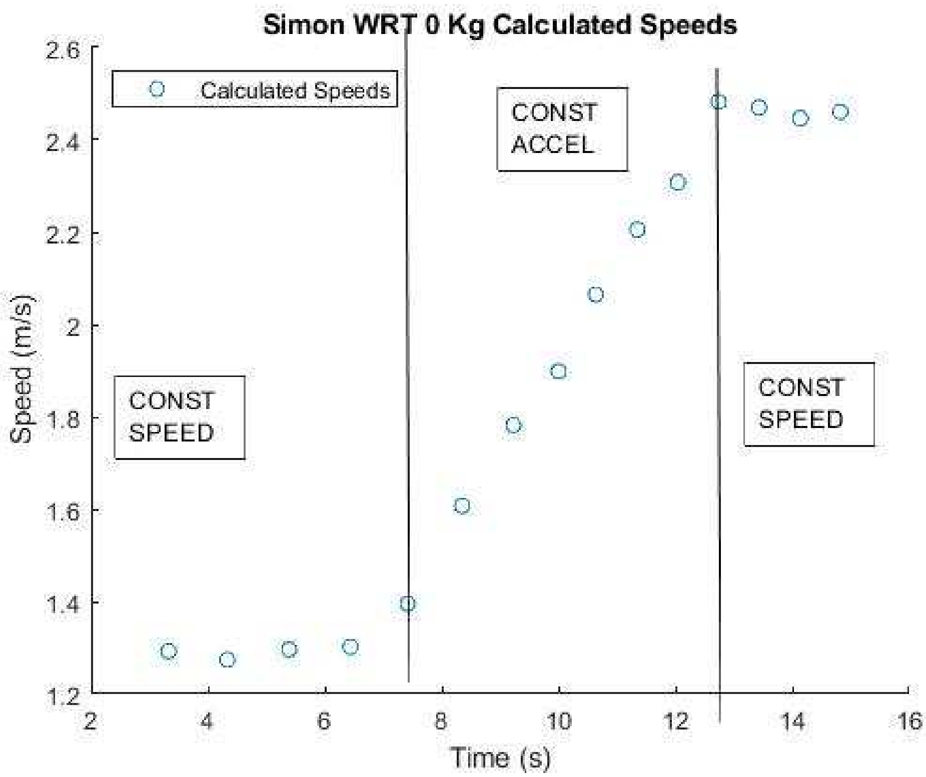

Fig. 102. Calculated speed from Subject 1 Simon's WRT trial with 0 Kg added weight.

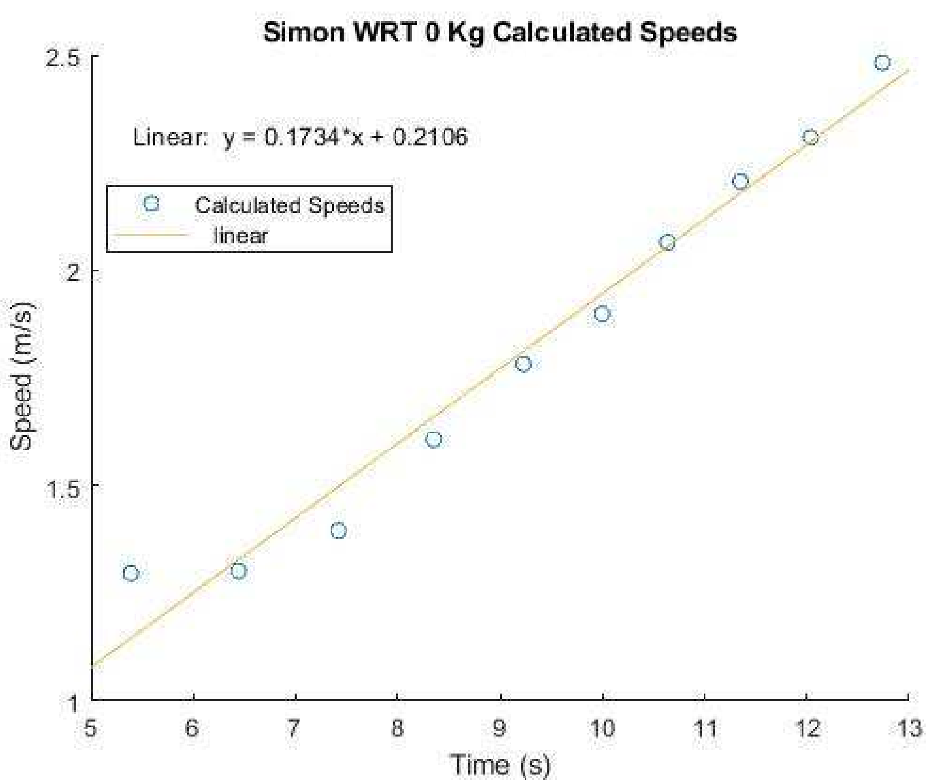

Fig. 103. Zoom from Fig. 102 and linear fitting from constant acceleration zone.

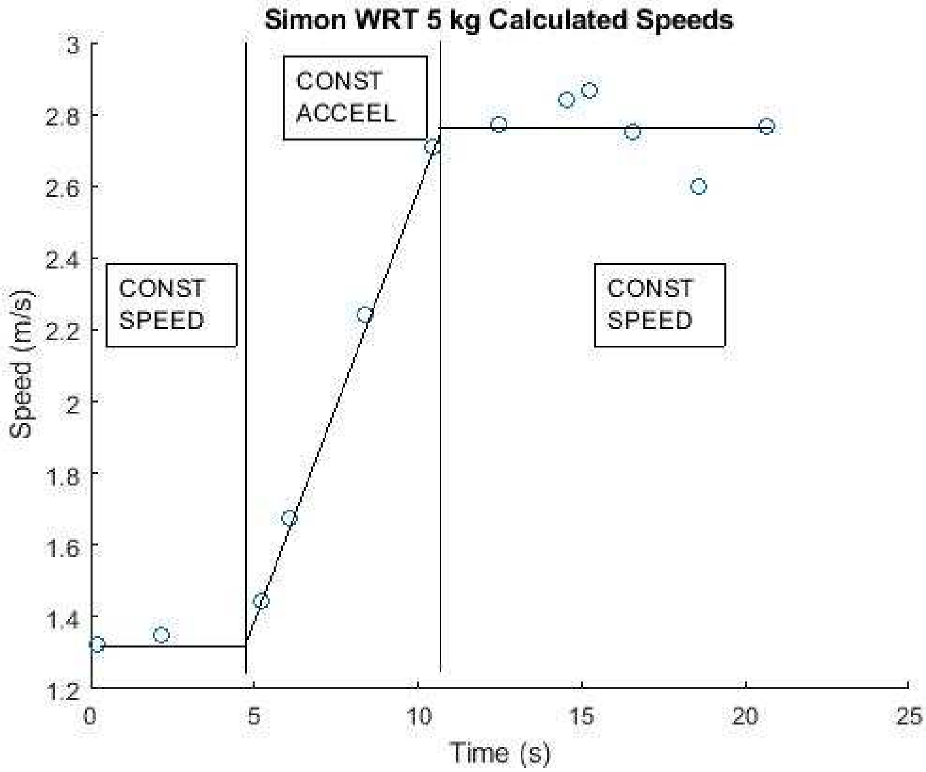

Fig. 104. Calculated speed from Subject 1 Simon's WRT trial with 5 Kg added weight.

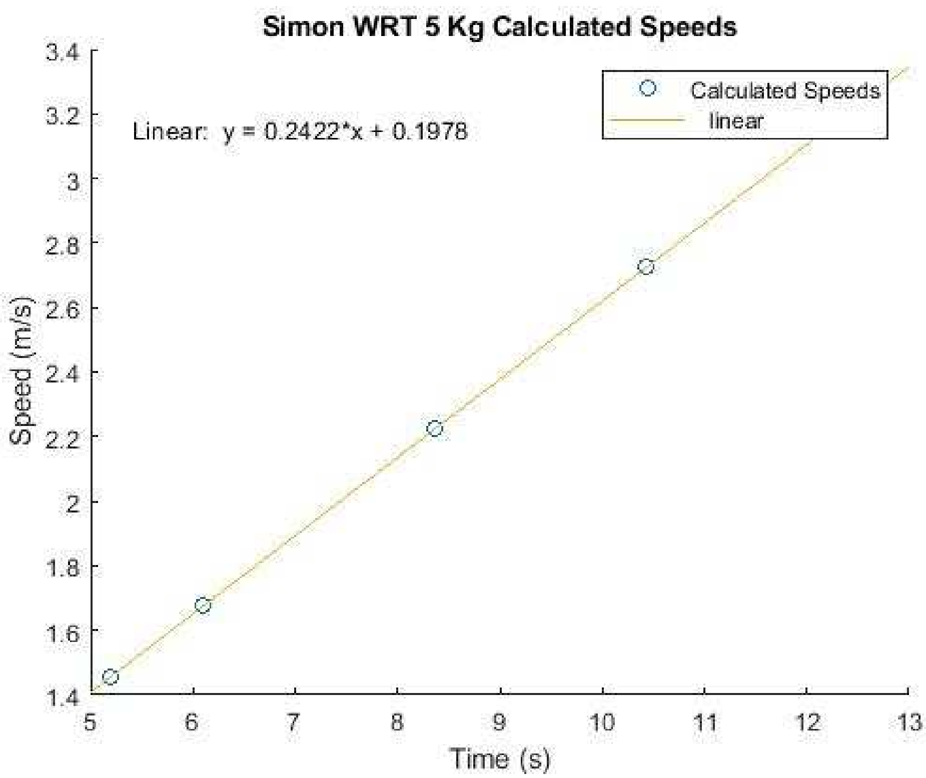

Fig. 105. Zoom from Fig. 104 and linear fitting from constant acceleration zone.

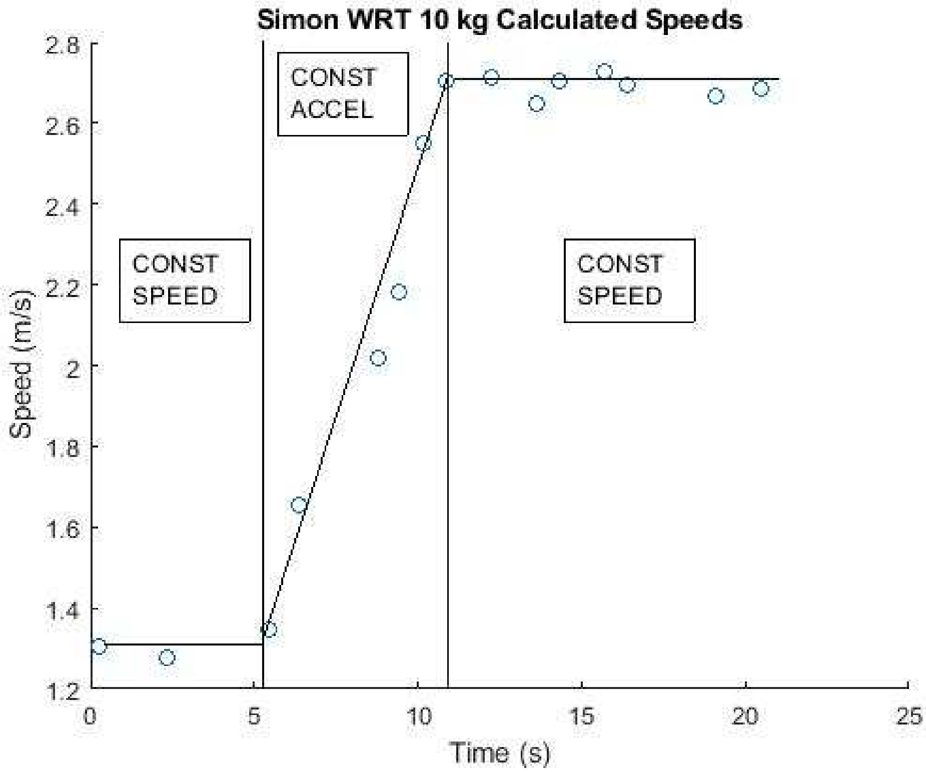

Fig. 106. Calculated speed from Subject 1 Simon's WRT trial with 15 Kg added weight.

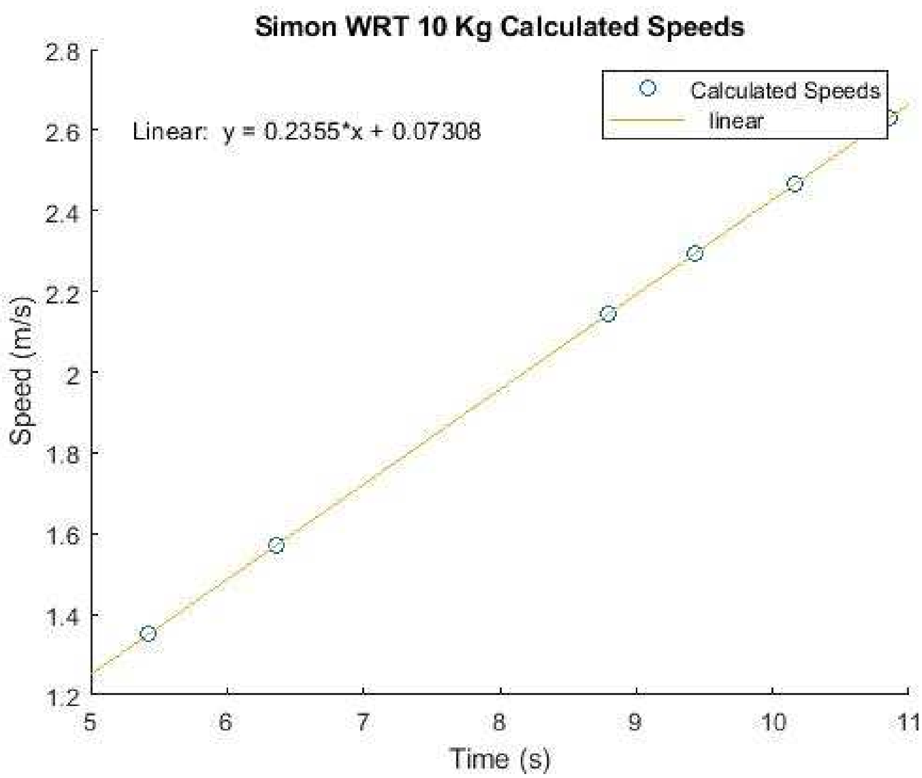

Fig. 107. Zoom from Fig. 106 and linear fitting from constant acceleration zone.

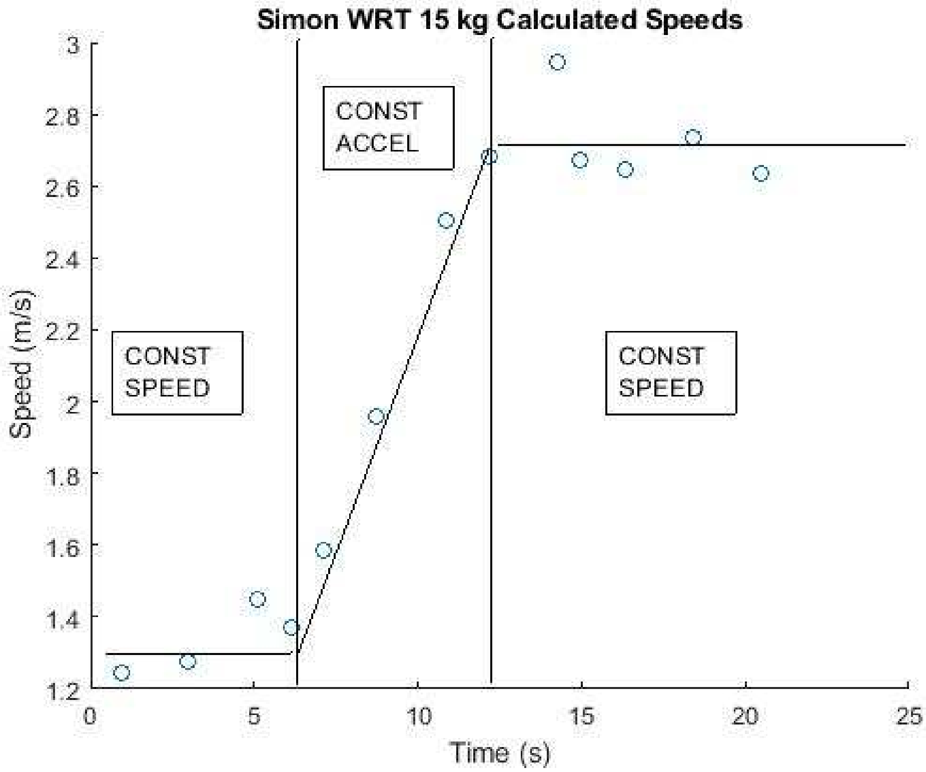

Fig. 108. Calculated speed from Subject 1 Simon's WRT trial without added weight.

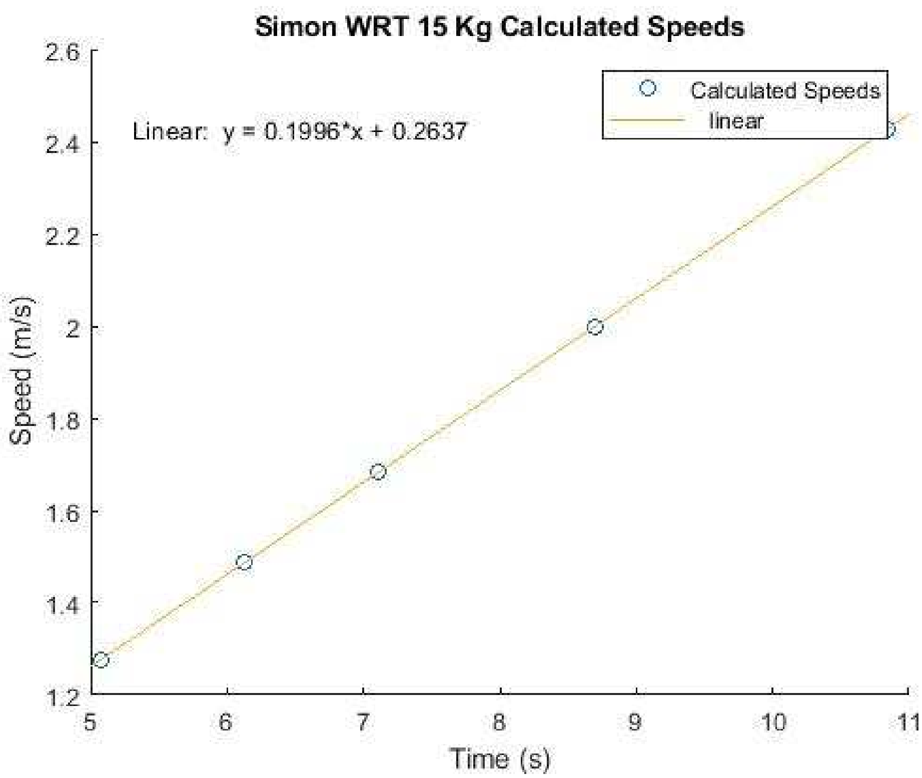

Fig. 109. Zoom from Fig. 108 and linear fitting from constant acceleration zone.

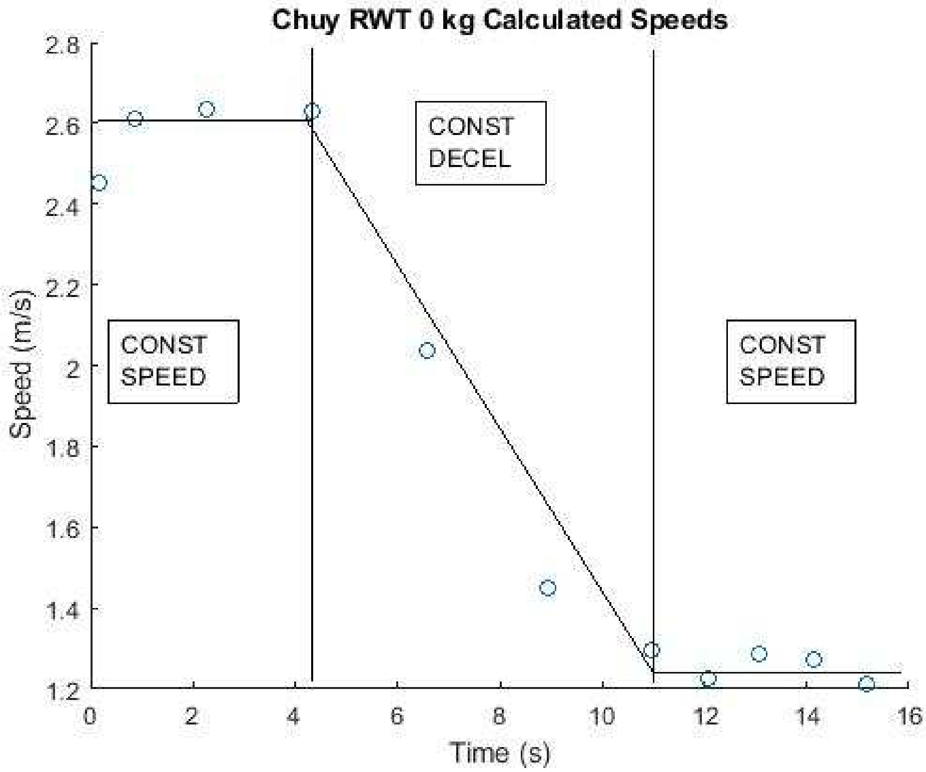

Fig. 110. Calculated speed from Subject 2 Chuy's RWT trial without added weight.

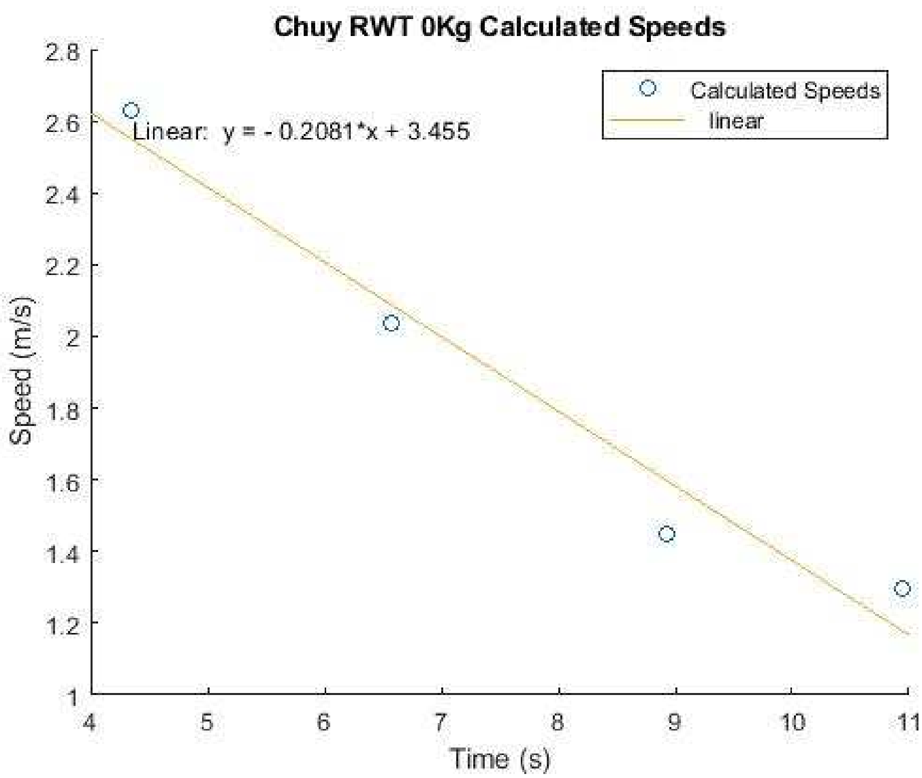

Fig. 111. Zoom from Fig. 110 and linear fitting from constant acceleration zone.

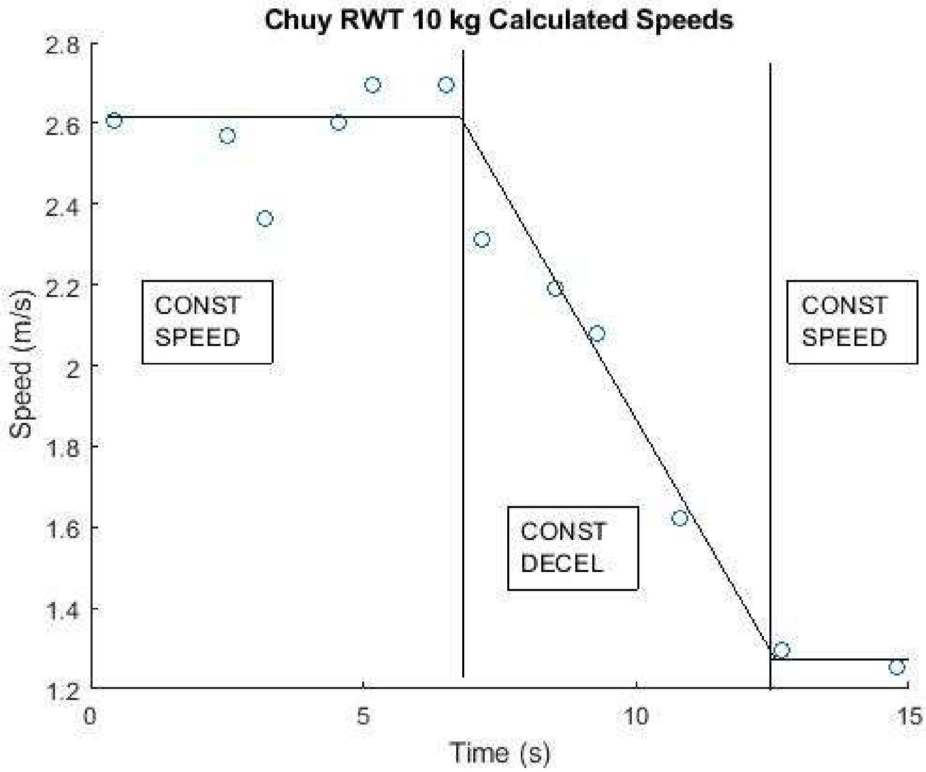

Fig. 112. Calculated speed from Subject 2 Chuy's RWT trial with 10 Kg added weight.

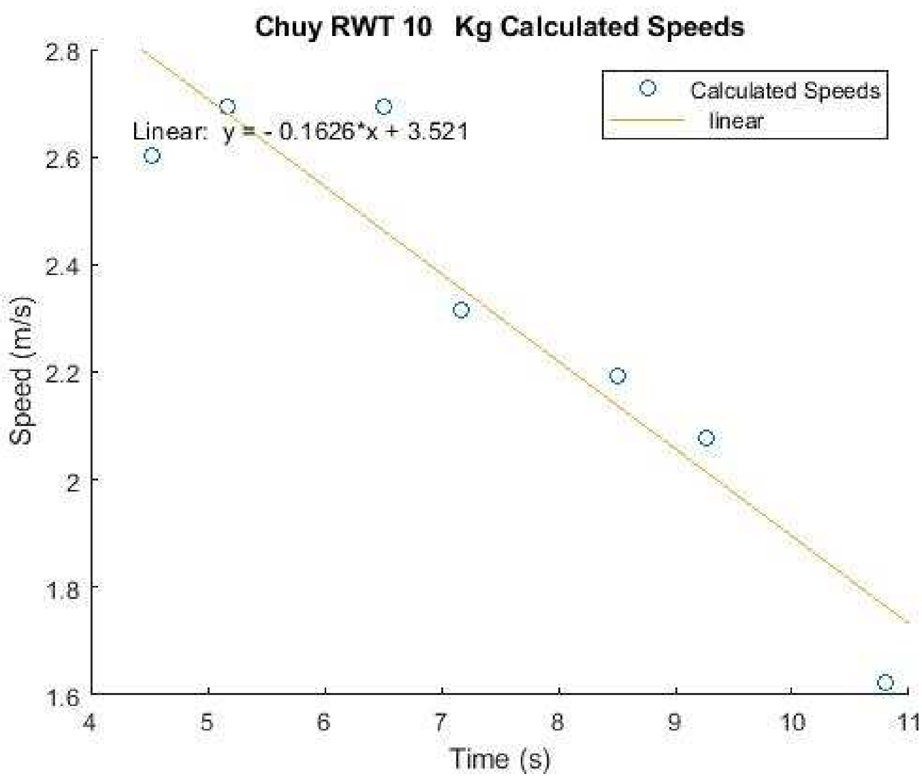

Fig. 113. Zoom from Fig. 112 and linear fitting from constant acceleration zone.

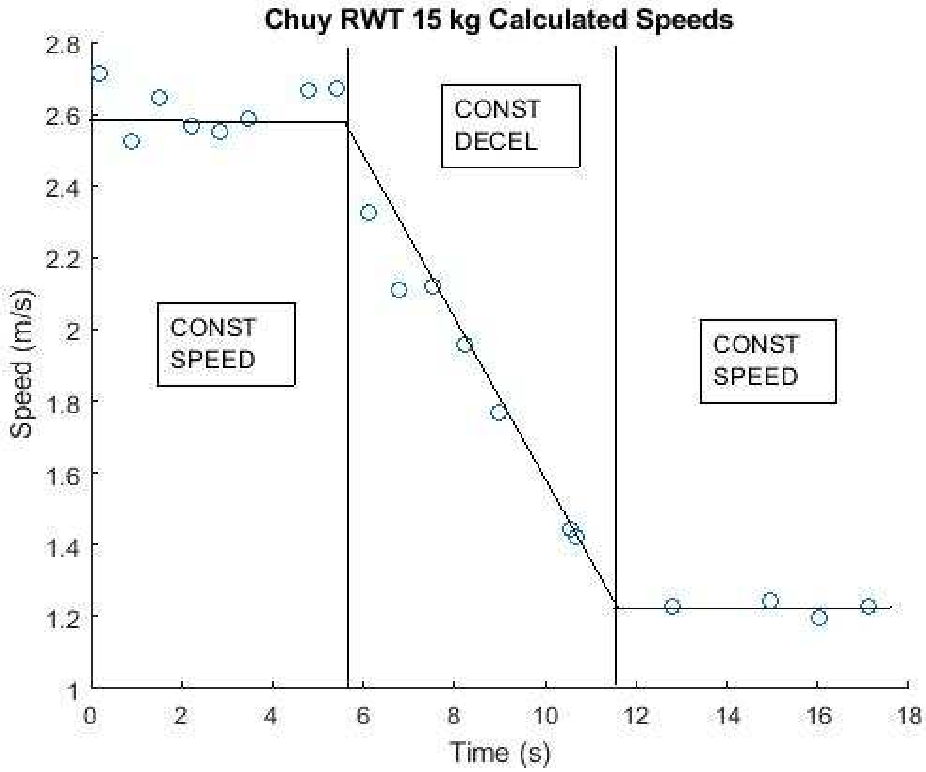

Fig. 114. Calculated speed from Subject 2 Chuy's RWT trial with 15 Kg added weight.

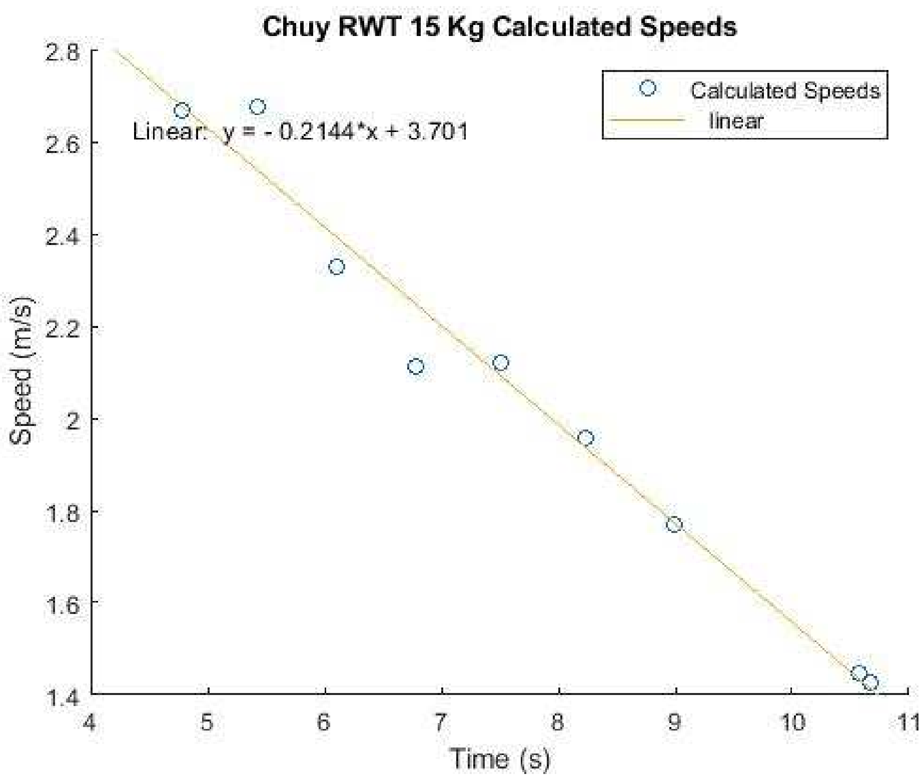

Fig. 115. Zoom from Fig. 114 and linear fitting from constant acceleration zone.

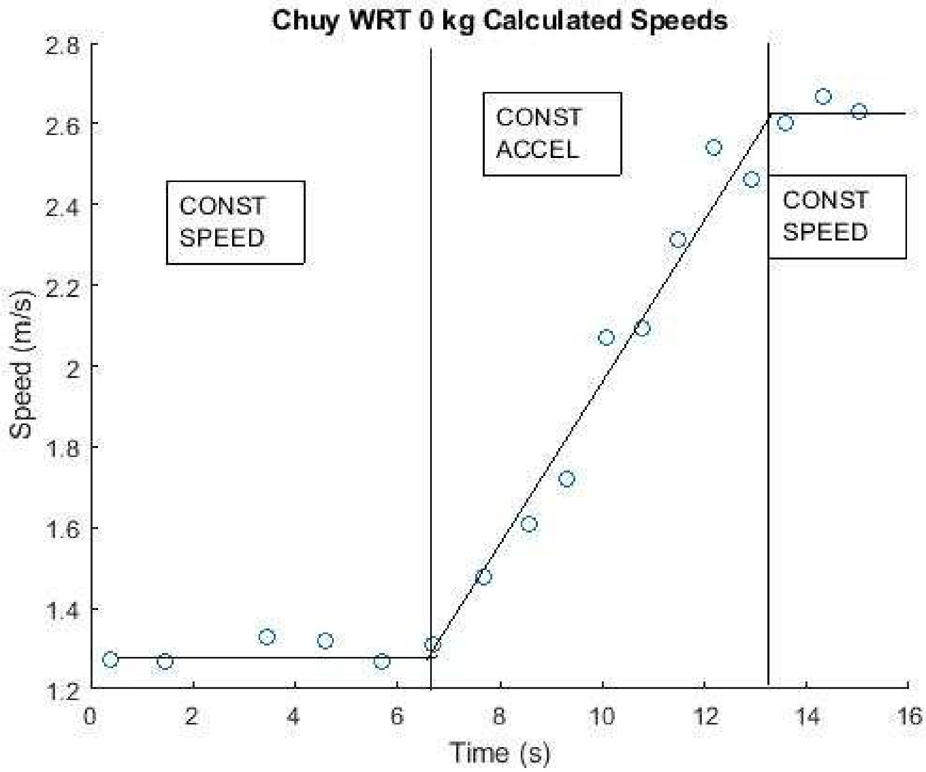

Fig. 116. Calculated speed from Subject 2 Chuy's WRT trial without added weight.

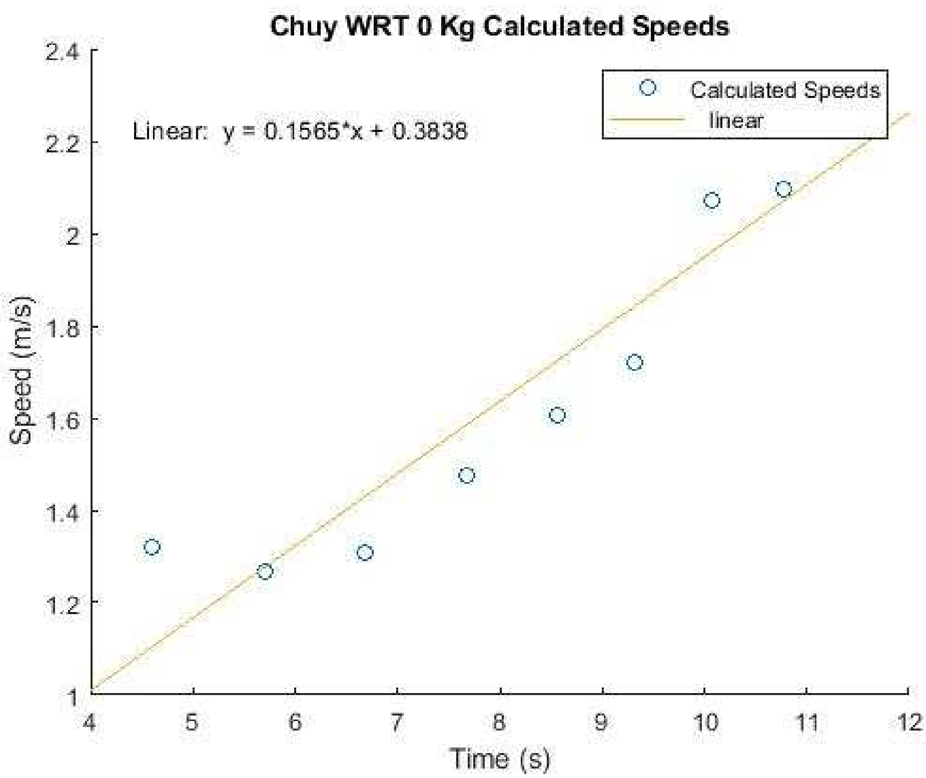

Fig. 117. Zoom from Fig. 116vand linear fitting from constant acceleration zone.

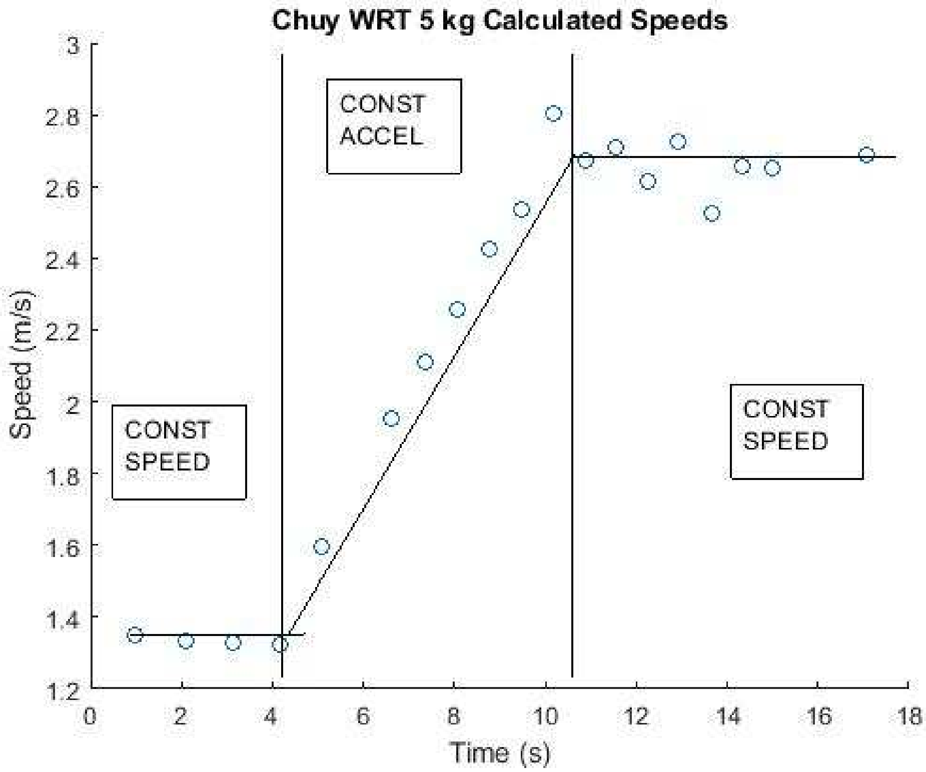

Fig. 118. Calculated speed from Subject 2 Chuy's WRT trial with 5 Kg added weight.

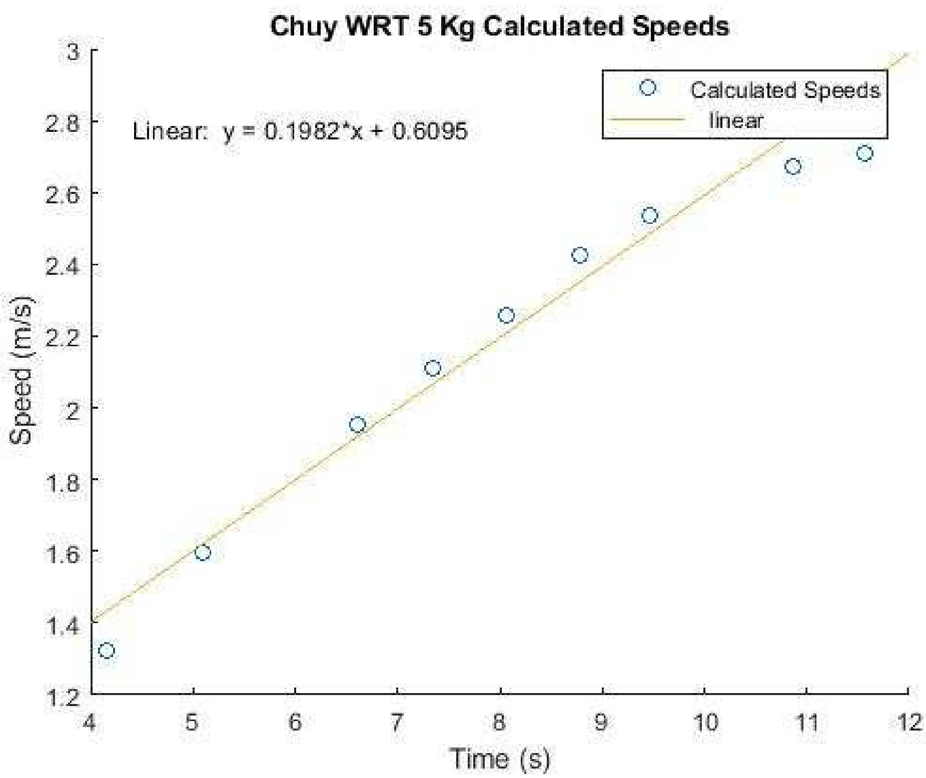

Fig. 119. Zoom from Fig. 118 and linear fitting from constant acceleration zone.

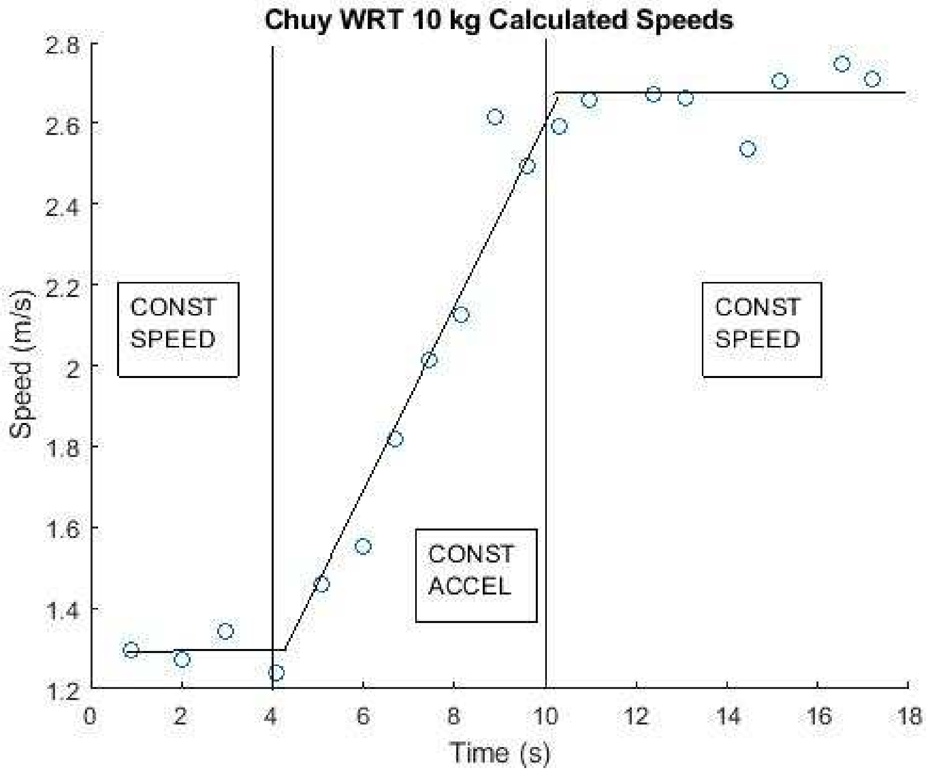

Fig. 120. Calculated speed from Subject 2 Chuy's WRT trial with 10 Kg added weight.

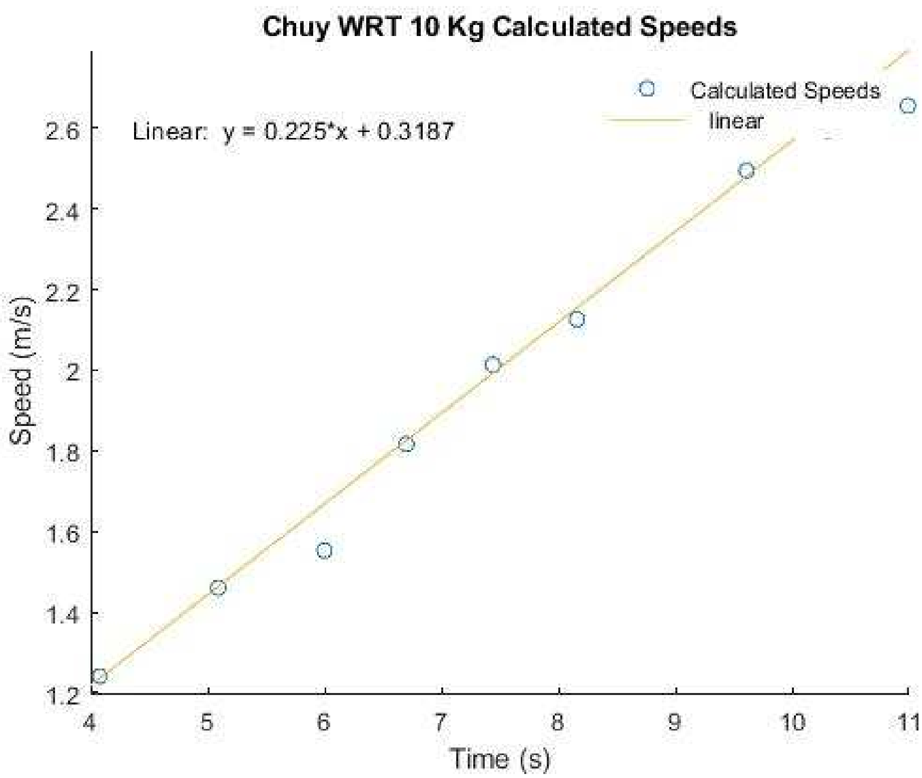

Fig. 121. Zoom from Fig. 120 and linear fitting from constant acceleration zone.

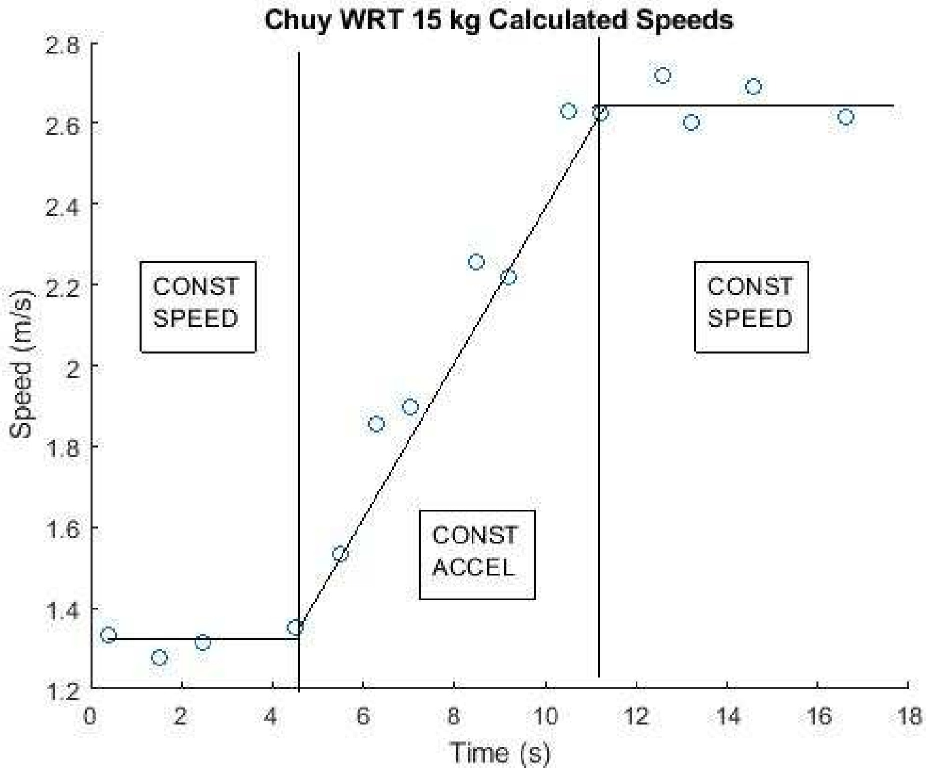

Fig. 122. Calculated speed from Subject 2 Chuy's WRT trial with 15 Kg added weight.

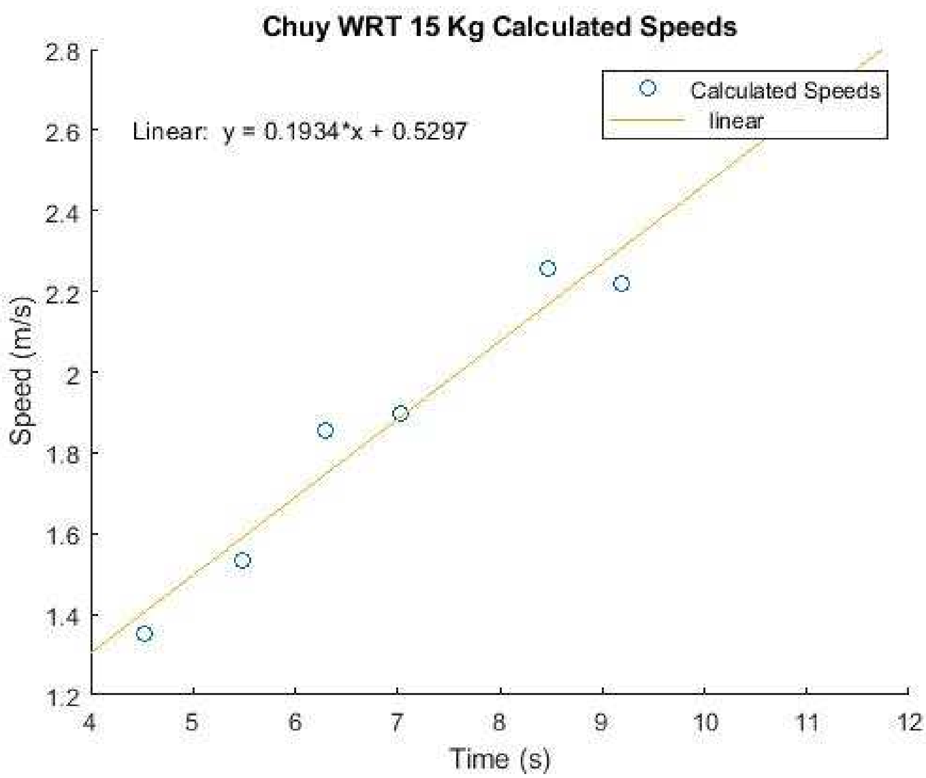

Fig. 123. Zoom from Fig. 122 and linear fitting from constant acceleration zone.

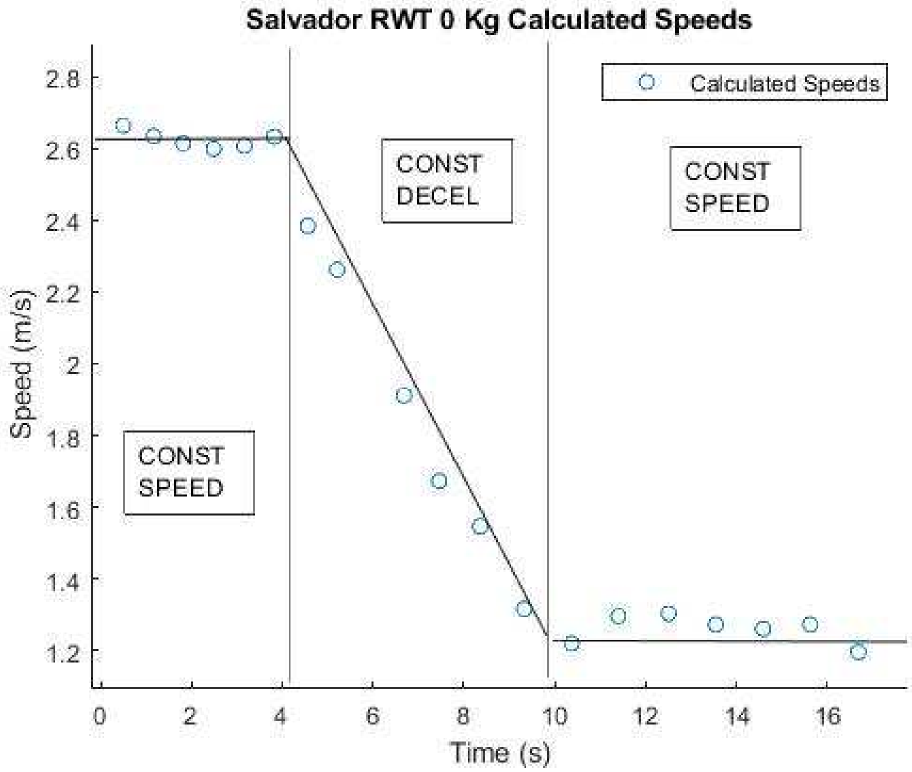

Fig. 124. Calculated speed from Subject 3 Salvador RWT trial with 0 Kg added weight.

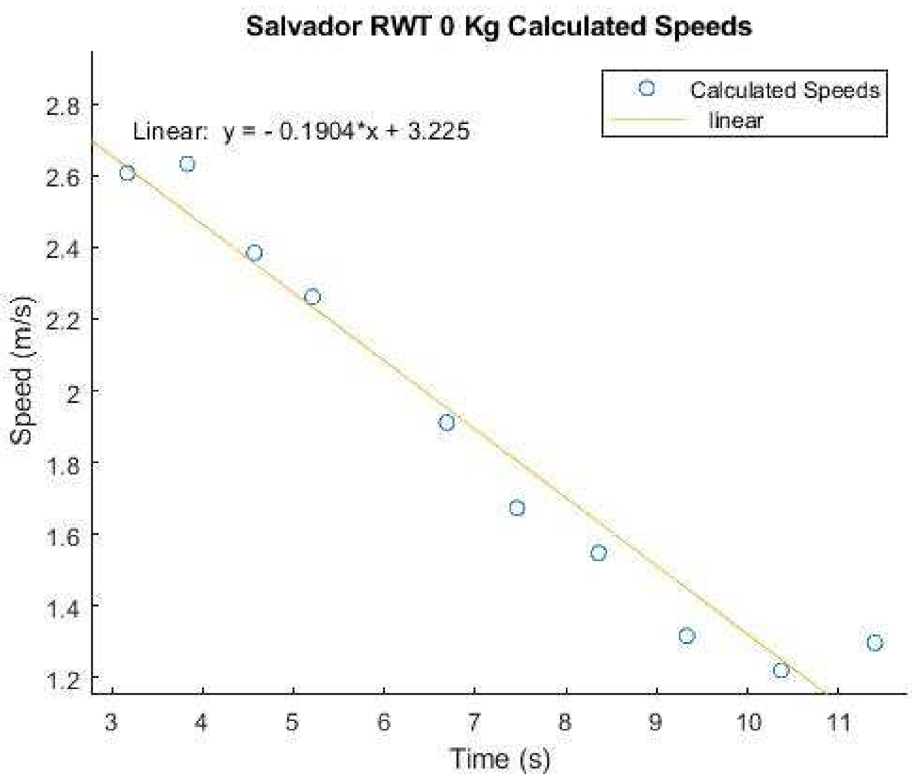

Fig. 125. Zoom from Fig. 124 and linear fitting from constant acceleration zone.

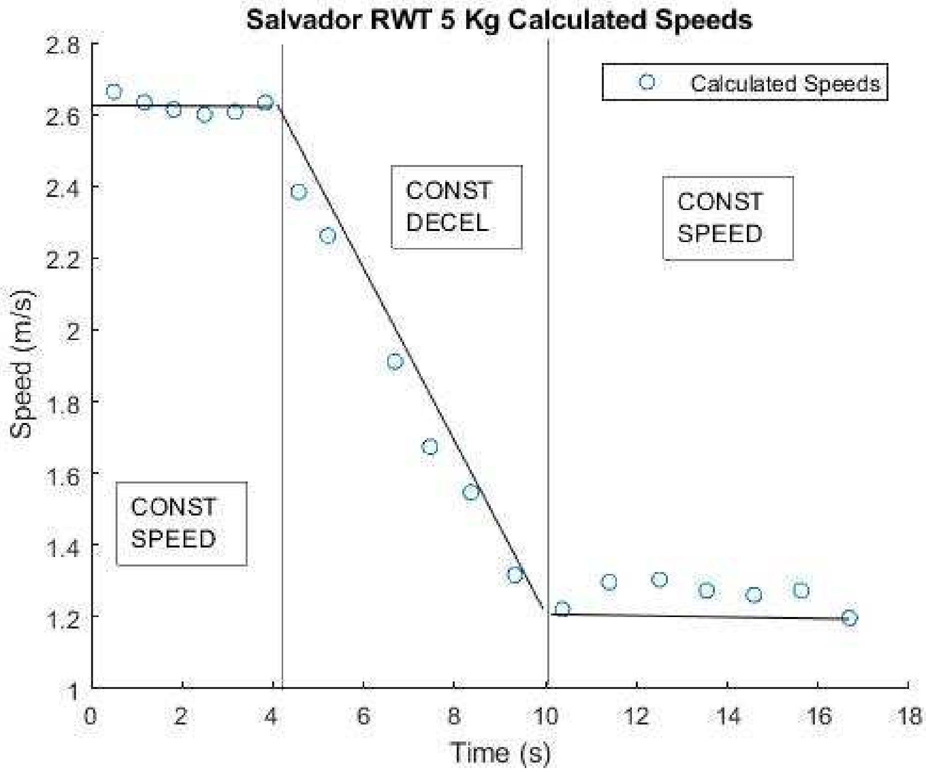

Fig. 126. Calculated speed from Subject 3 Salvador RWT trial with 5 Kg added weight.

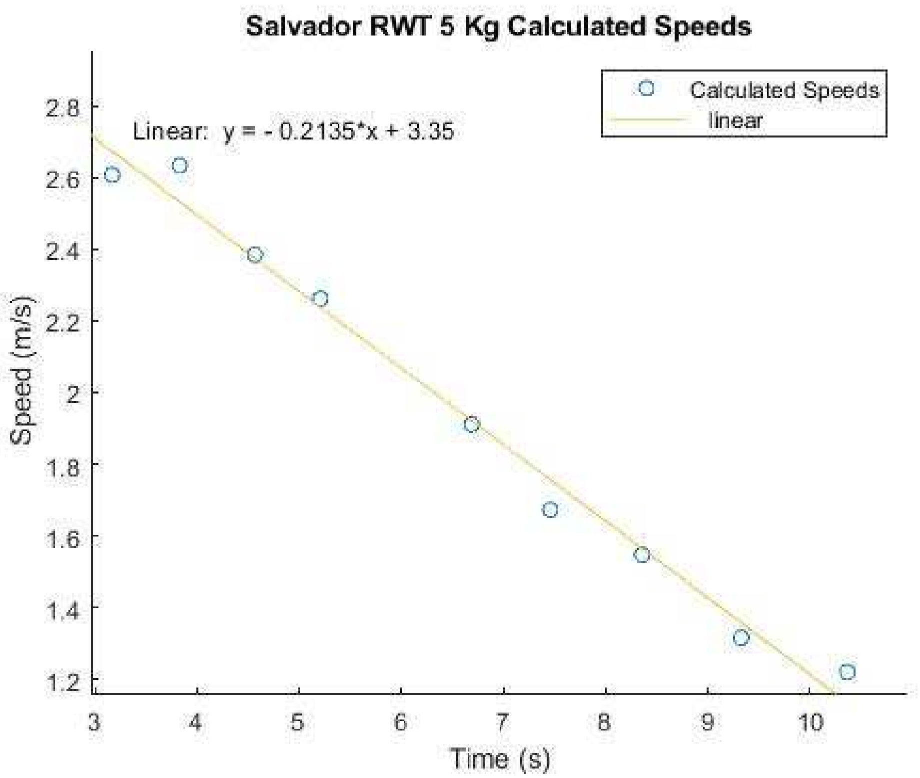

Fig. 127. Zoom from Fig. 126 and linear fitting from constant acceleration zone.

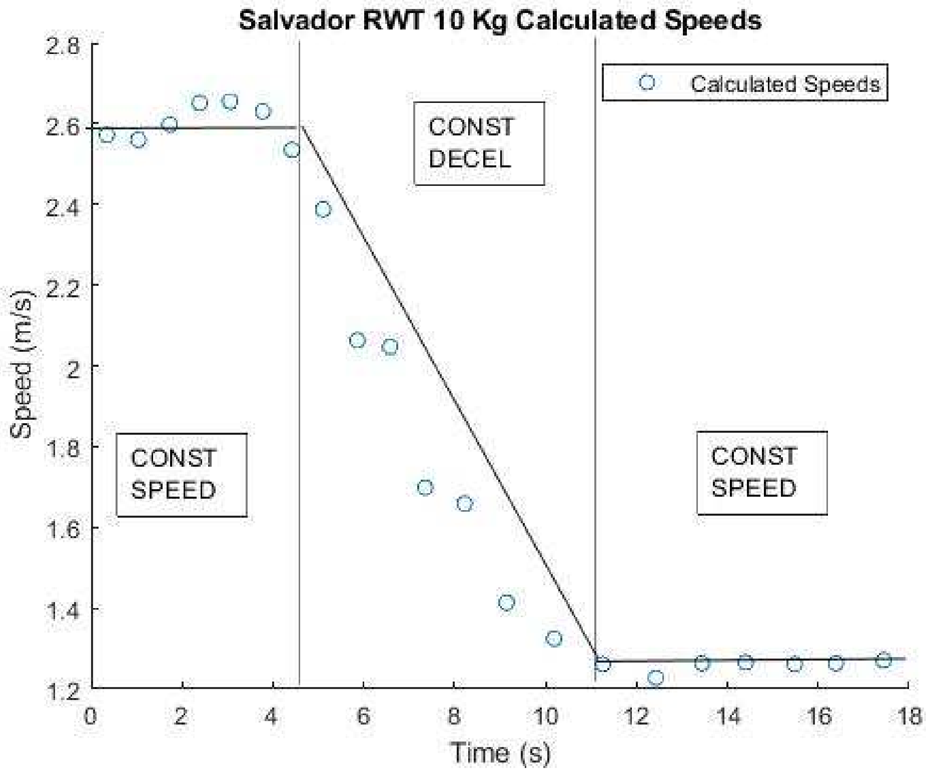

Fig. 128. Calculated speed from Subject 3 Salvador RWT trial with 10 Kg added weight.

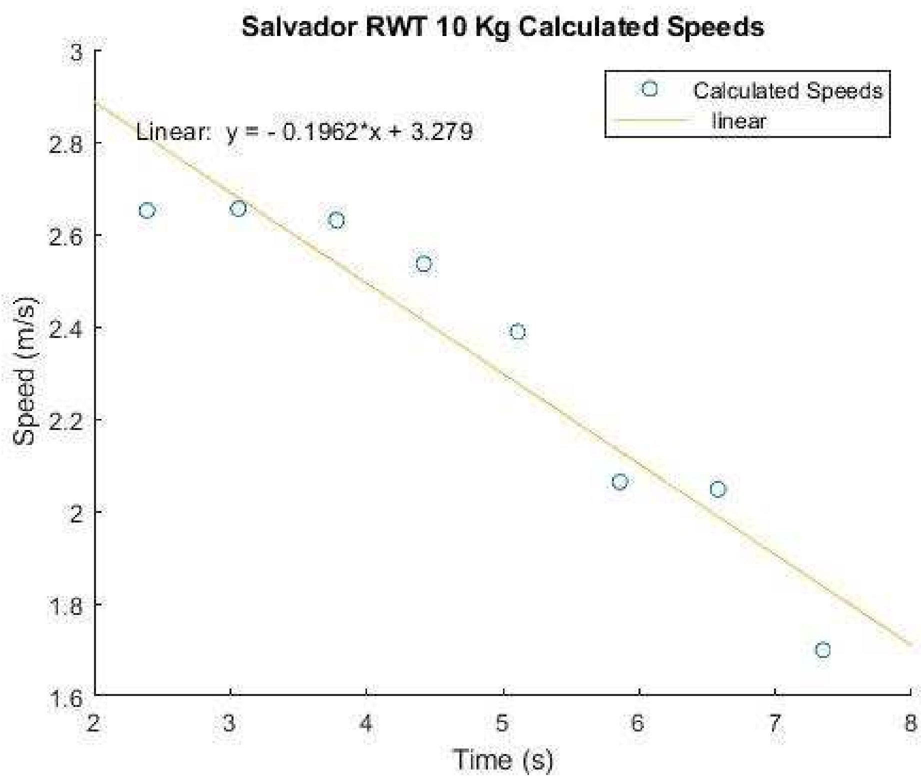

Fig. 129. Zoom from Fig. 128 and linear fitting from constant acceleration zone

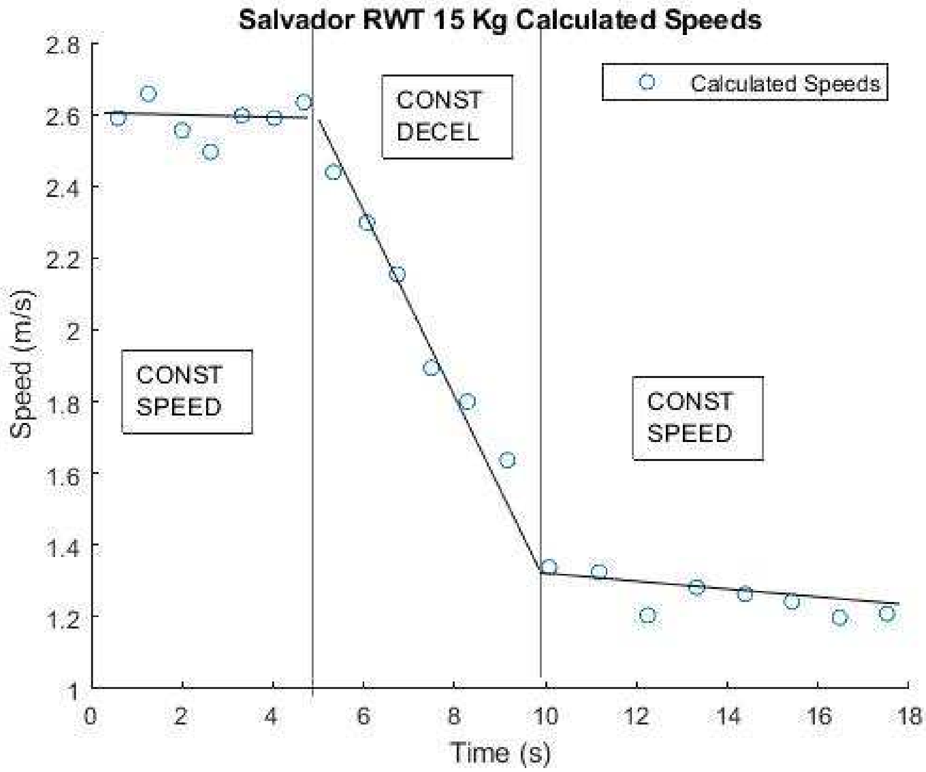

Fig. 130. Calculated speed from Subject 3 Salvador RWT trial with 15 Kg added weight.

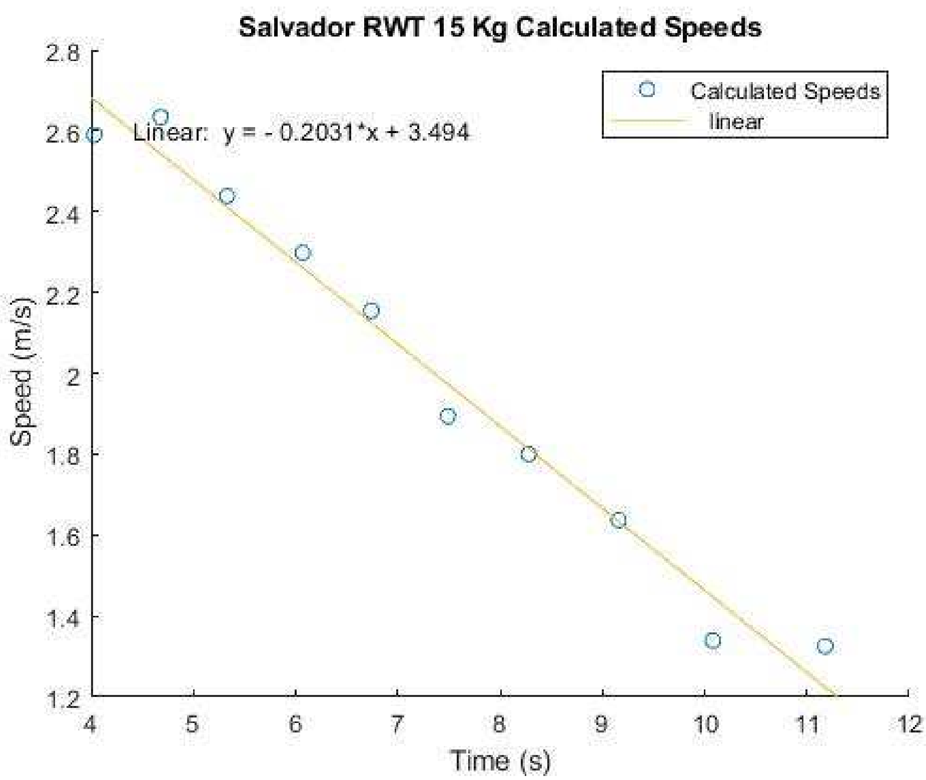

Fig. 131. Zoom from Fig. 130 and linear fitting from constant acceleration zone

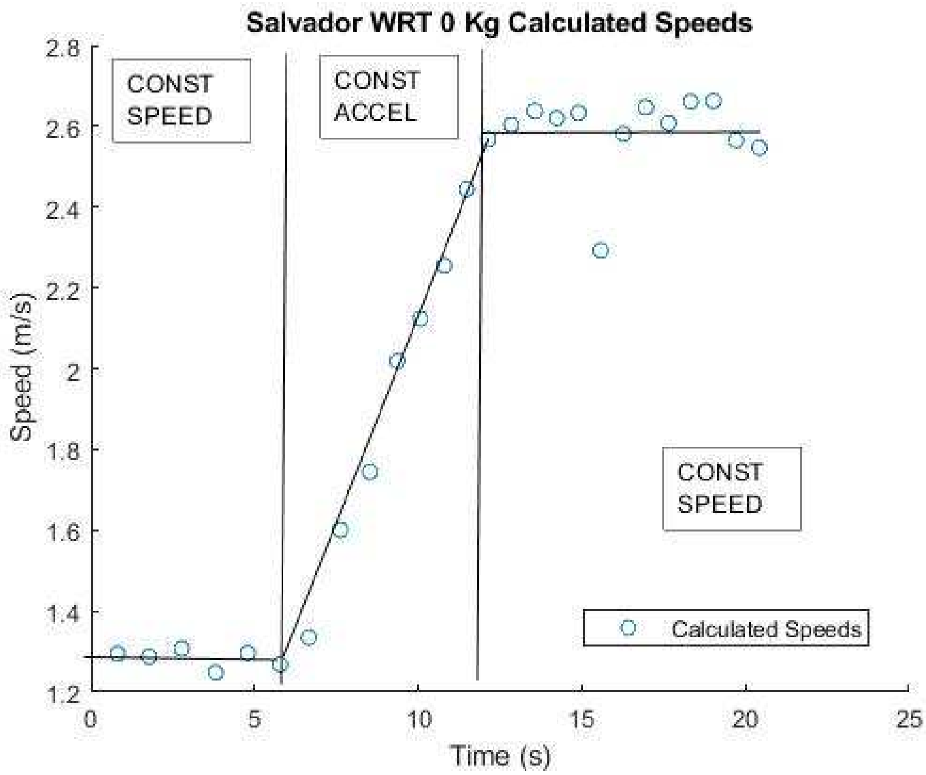

Fig. 132. Calculated speed from Subject 3 Salvador WRT trial with 0 Kg added weight

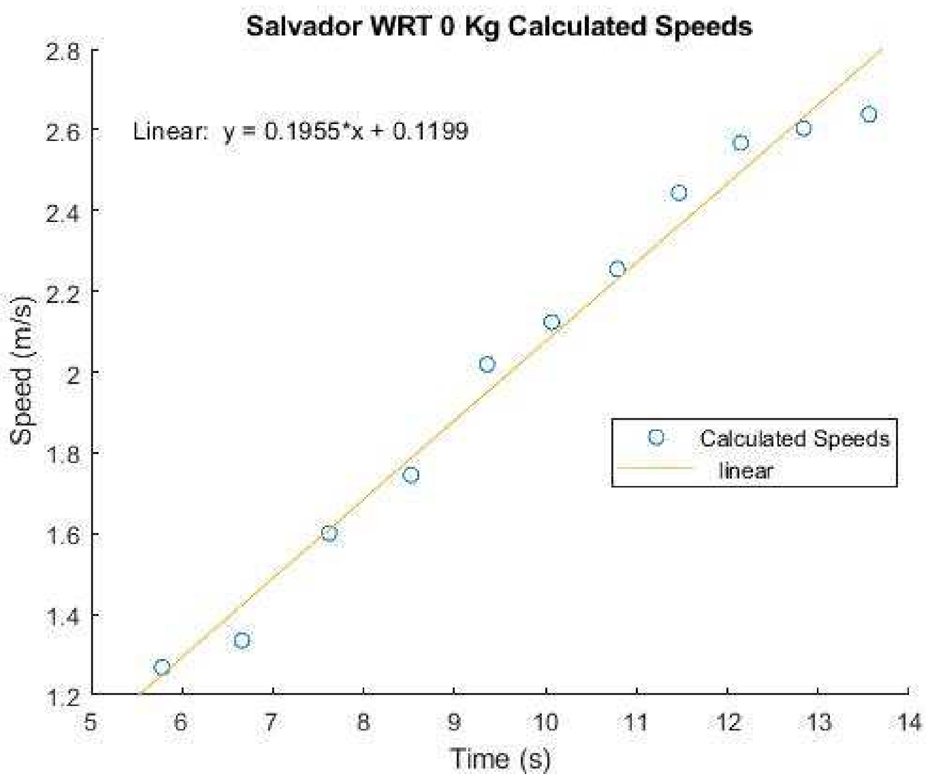

Fig. 133. Zoom from Fig. 132 and linear fitting from constant acceleration zone

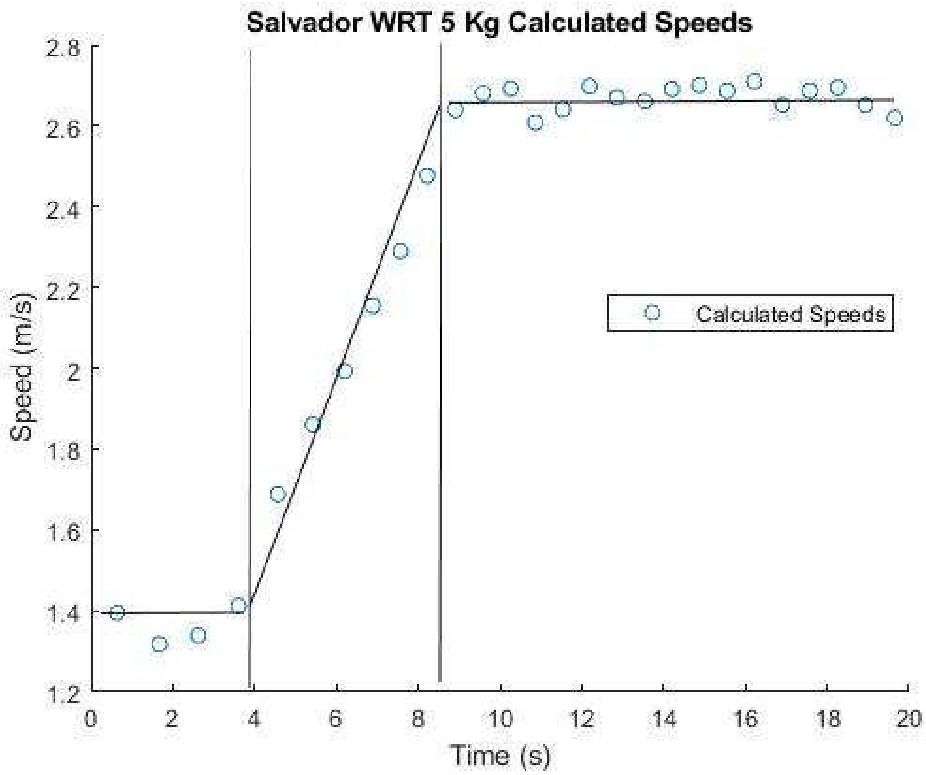

Fig. 134. Calculated speed from Subject 3 Salvador WRT trial with 5 Kg added weight

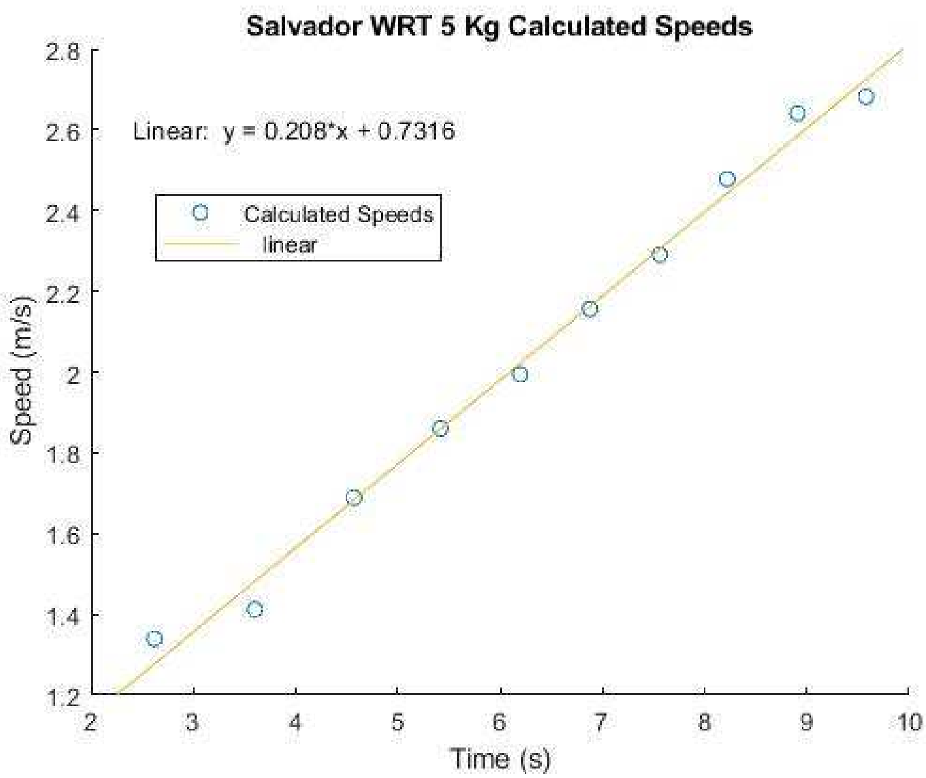

Fig. 135. Zoom from Fig. 134 and linear fitting from constant acceleration zone

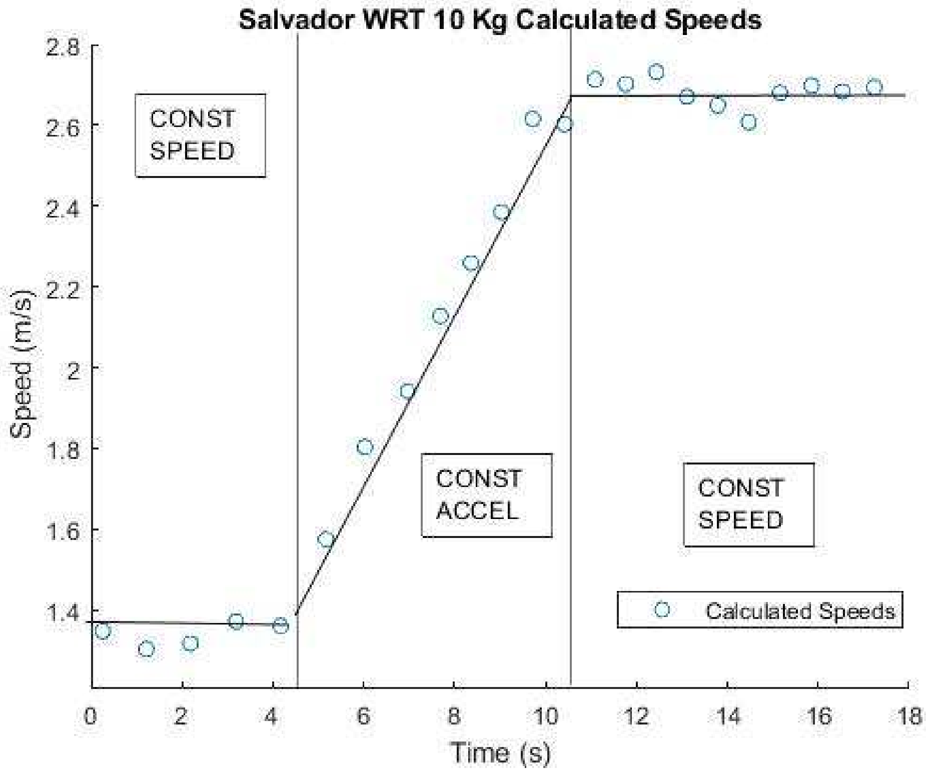

Fig. 136. Calculated speed from Subject 3 Salvador WRT trial with 10 Kg added weight

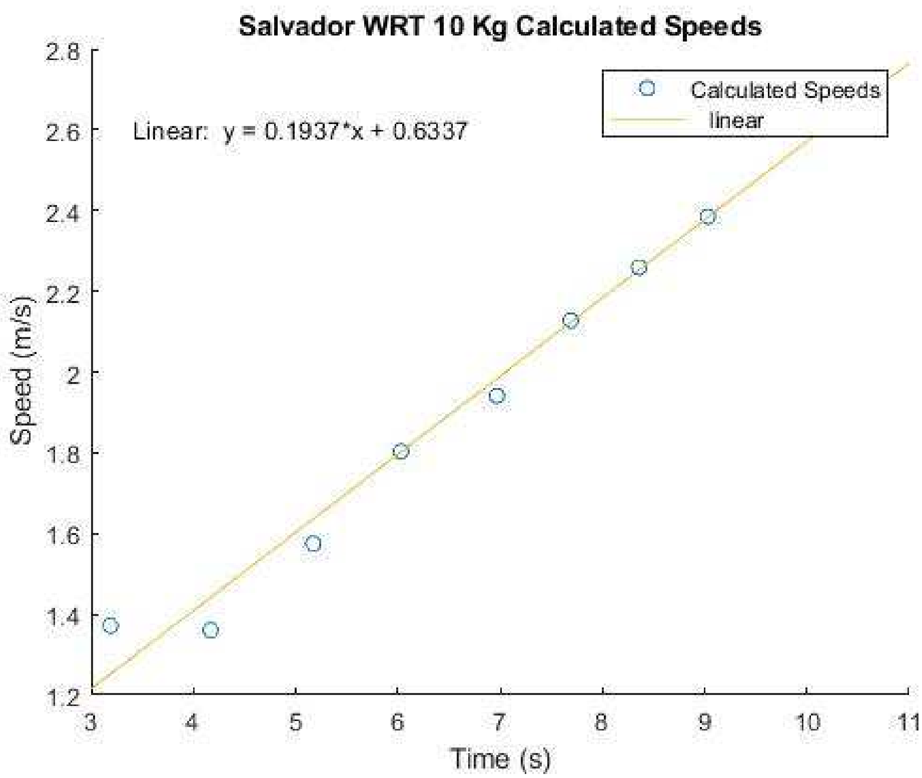

Fig. 137. Zoom from Fig. 136 and linear fitting from constant acceleration zone

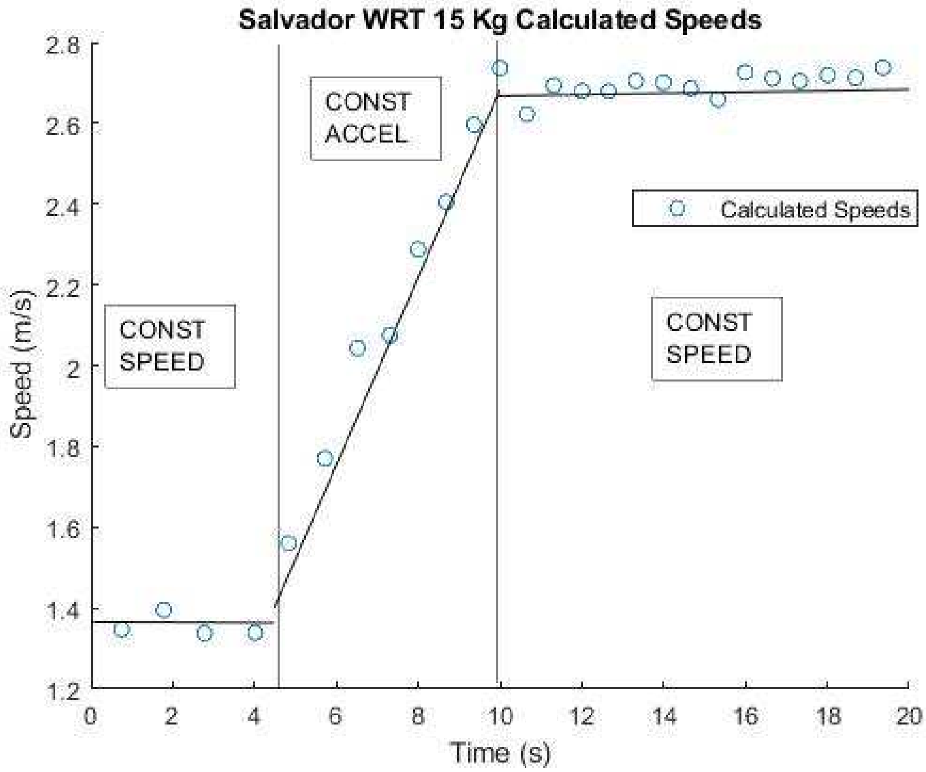

Fig. 138. Calculated speed from Subject 3 Salvador WRT trial with 15 Kg added weight

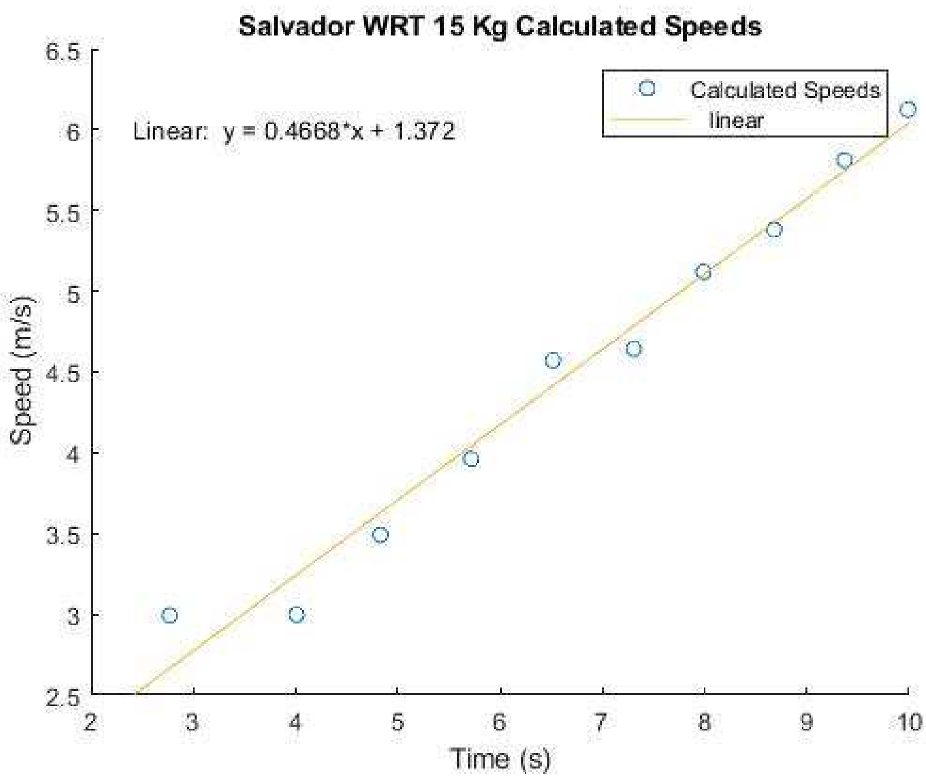

Fig. 139. Zoom from Fig. 138 and linear fitting from constant acceleration zone

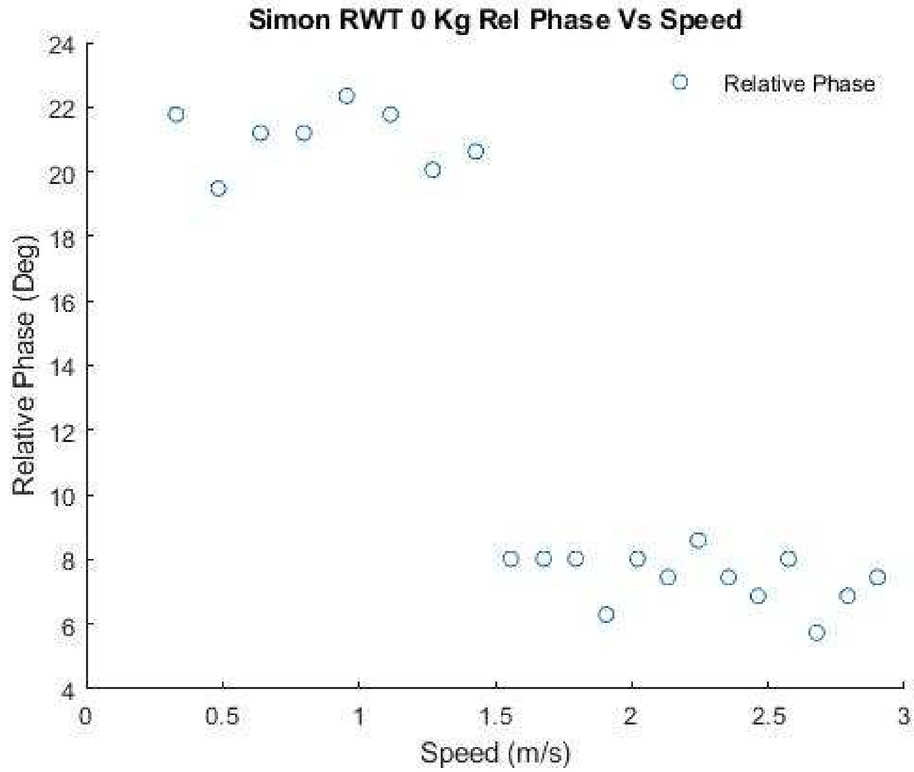

Fig. 140. Subject 1 Simon relative phase vs speed on the RWT trial without added weight.

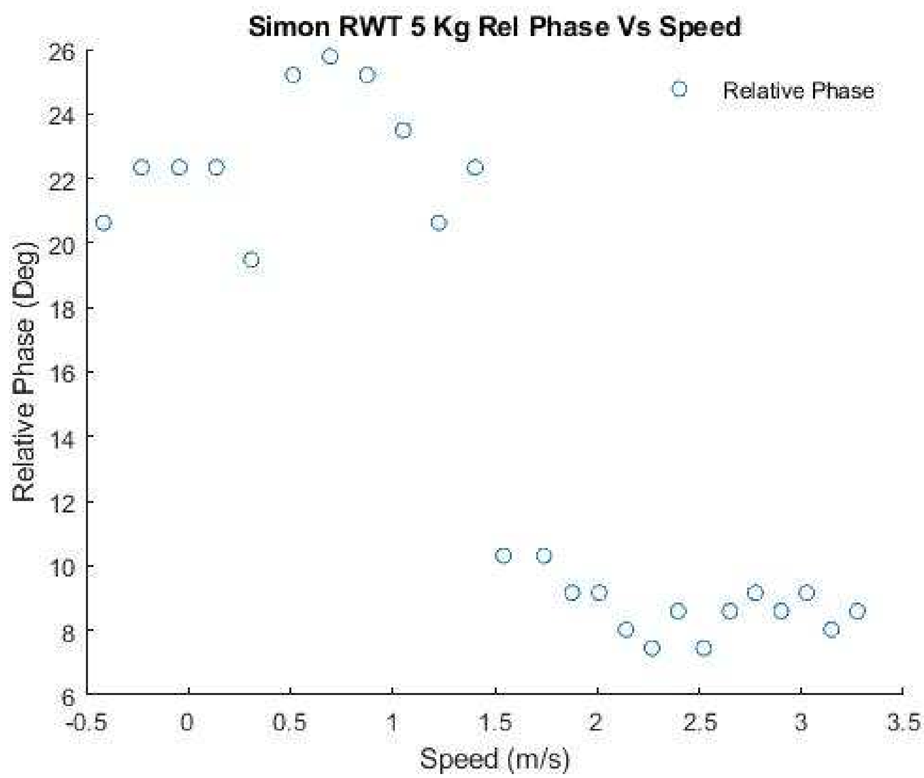

Fig. 141. Subject 1 Simon relative phase vs speed on the RWT trial with 5 Kg added weight.

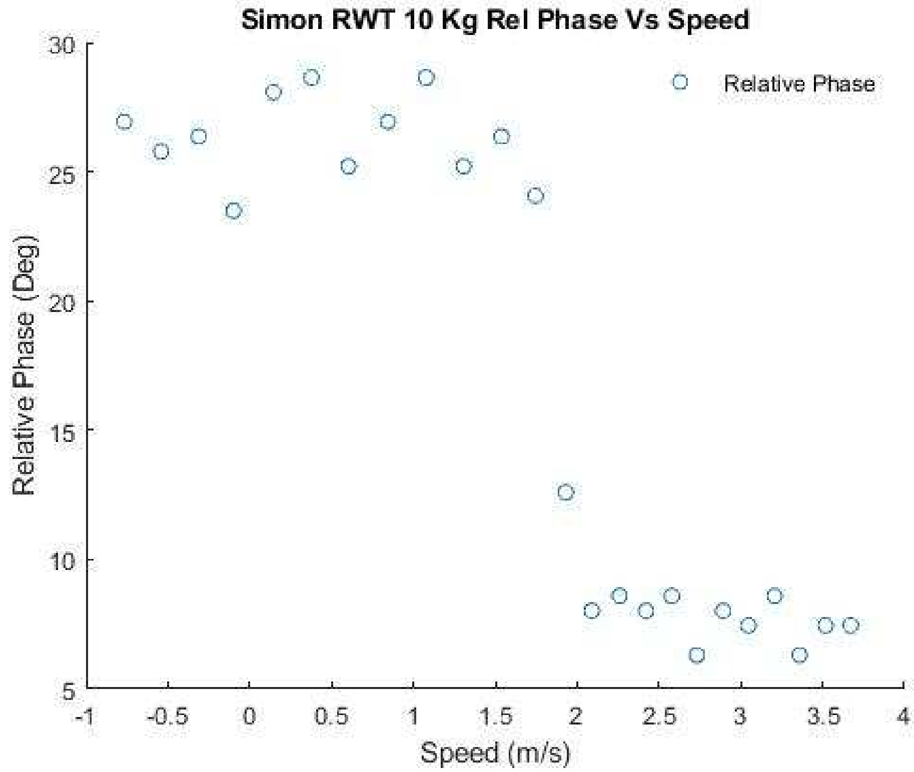

Fig. 142. Subject 1 Simon relative phase vs speed on the RWT trial with 10 Kg added weight.

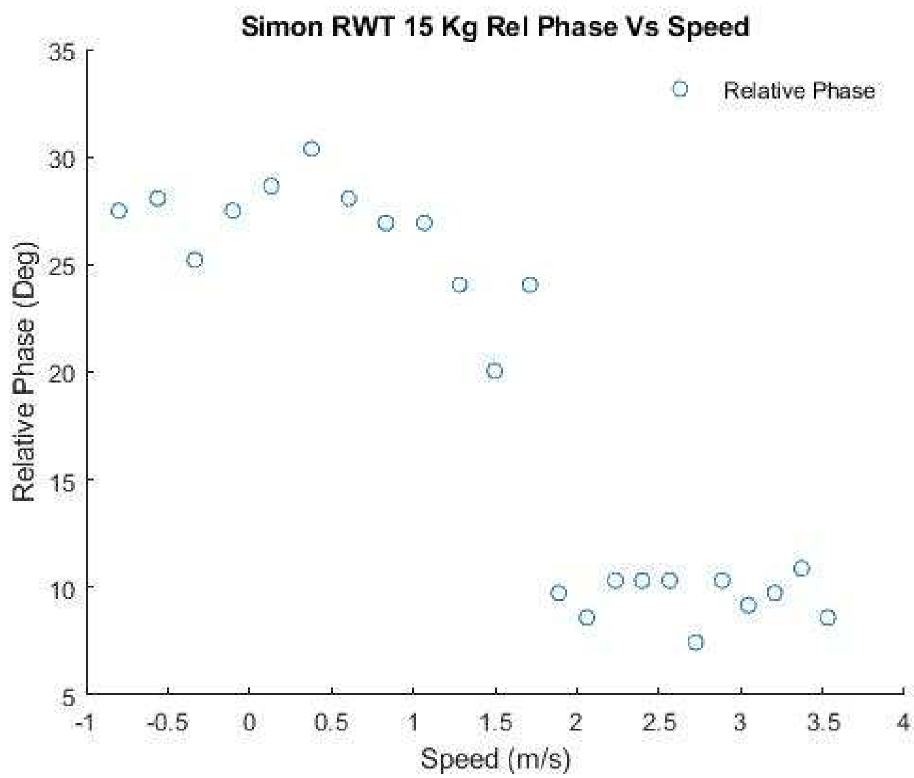

Fig. 143. Subject 1 Simon relative phase vs speed on the RWT trial with 15 Kg added weight.

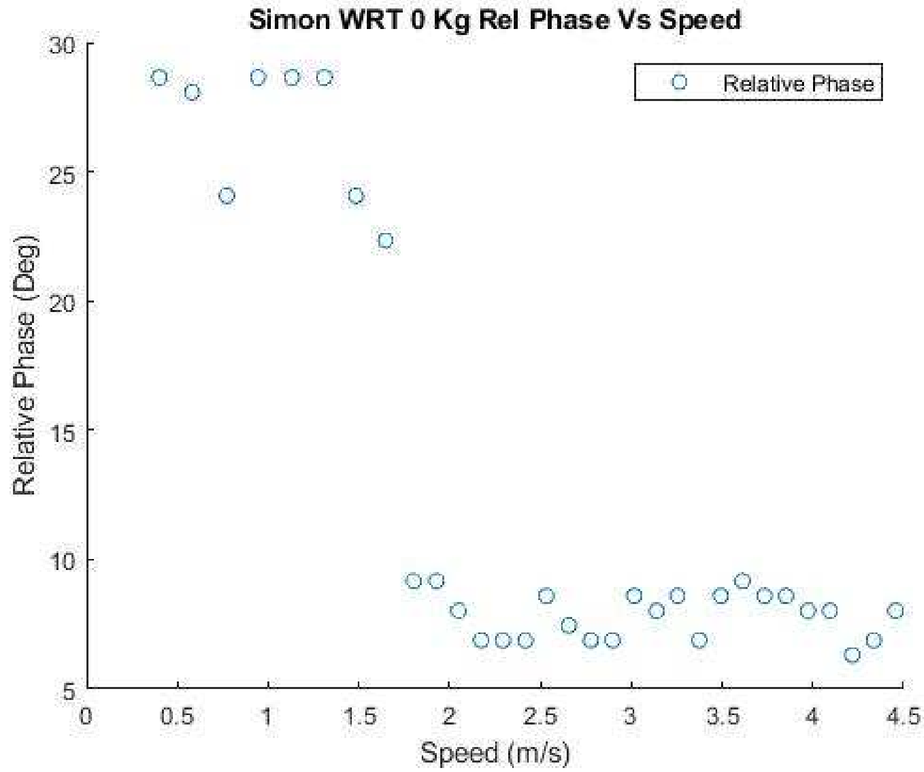

Fig. 144. Subject 1 Simon relative phase vs speed on the WRT trial without added weight

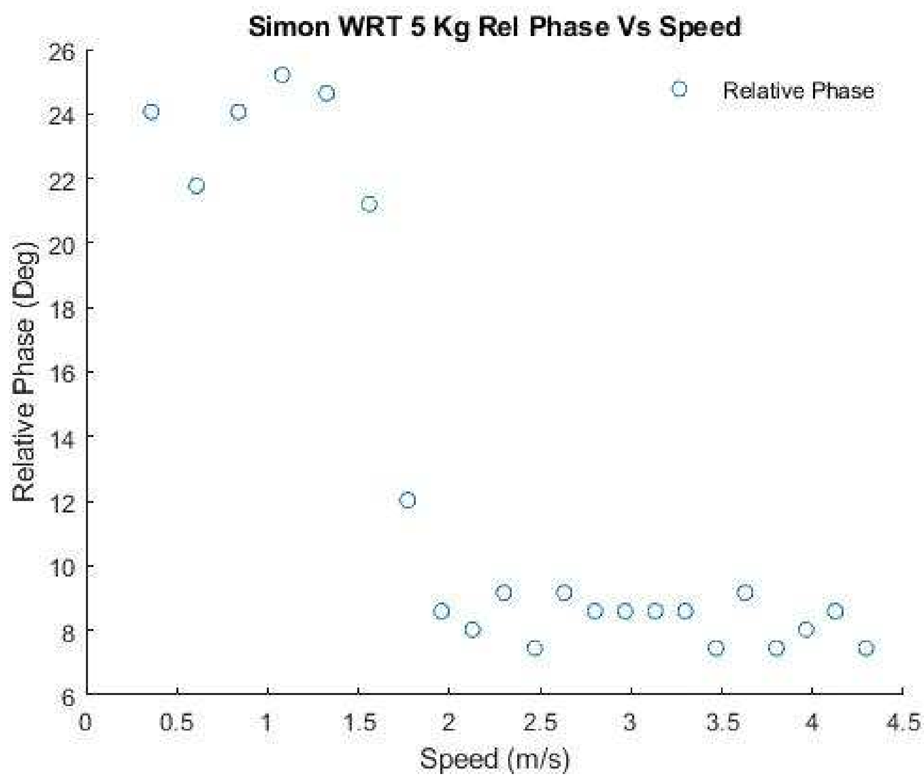

Fig. 145. Subject 1 Simon relative phase vs speed on the WRT trial with 5 Kg added weight.

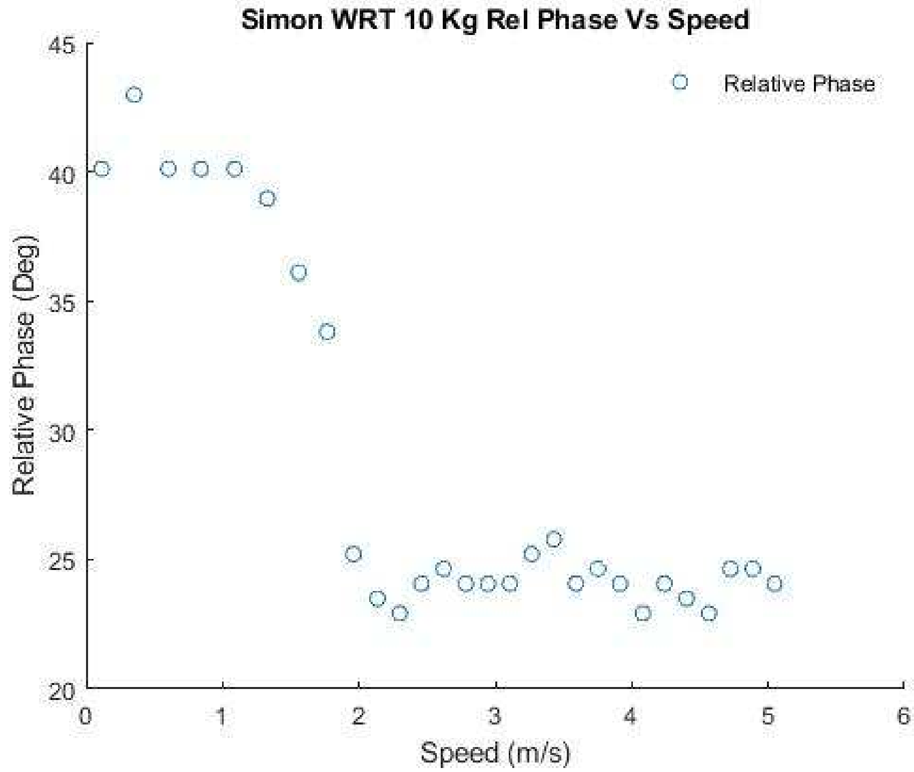

Fig. 146. Subject 1 Simon relative phase vs speed on the WRT trial with 10 Kg added weight.

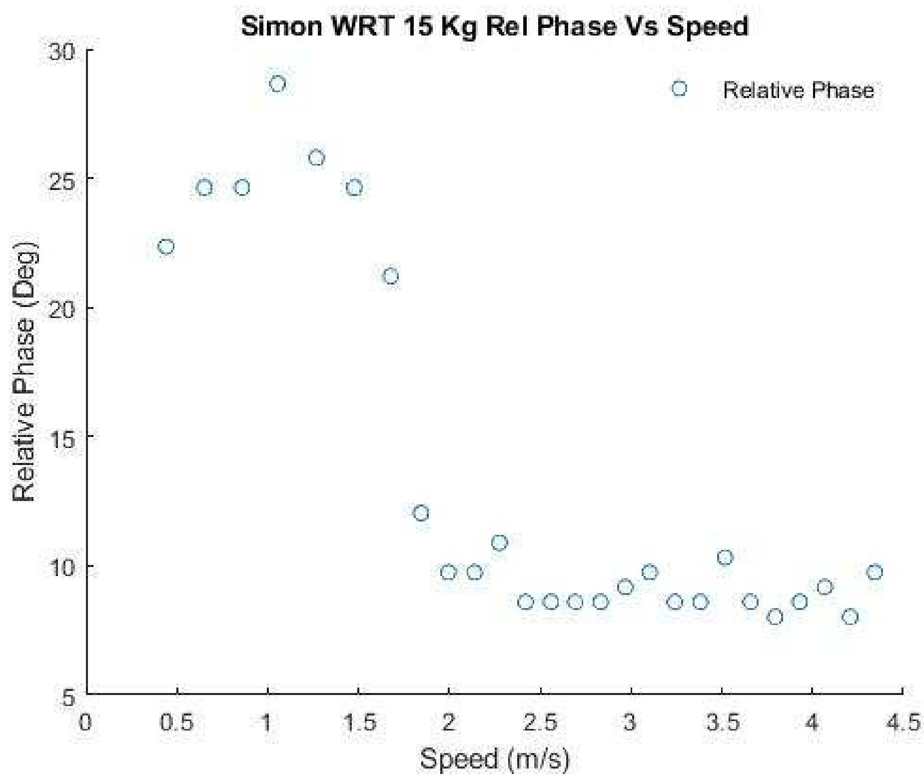

Fig. 147. Subject 1 Simon relative phase vs speed on the WRT trial with 15 Kg added weight

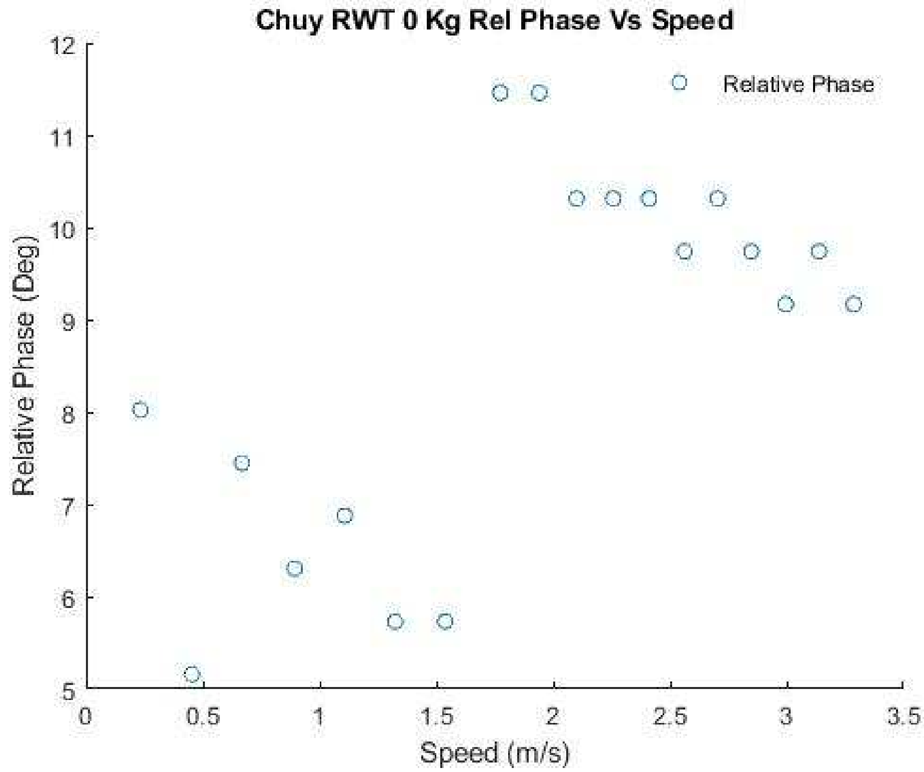

Fig. 148. Subject 2 Chuy relative phase vs speed on the RWT trial without added weight.

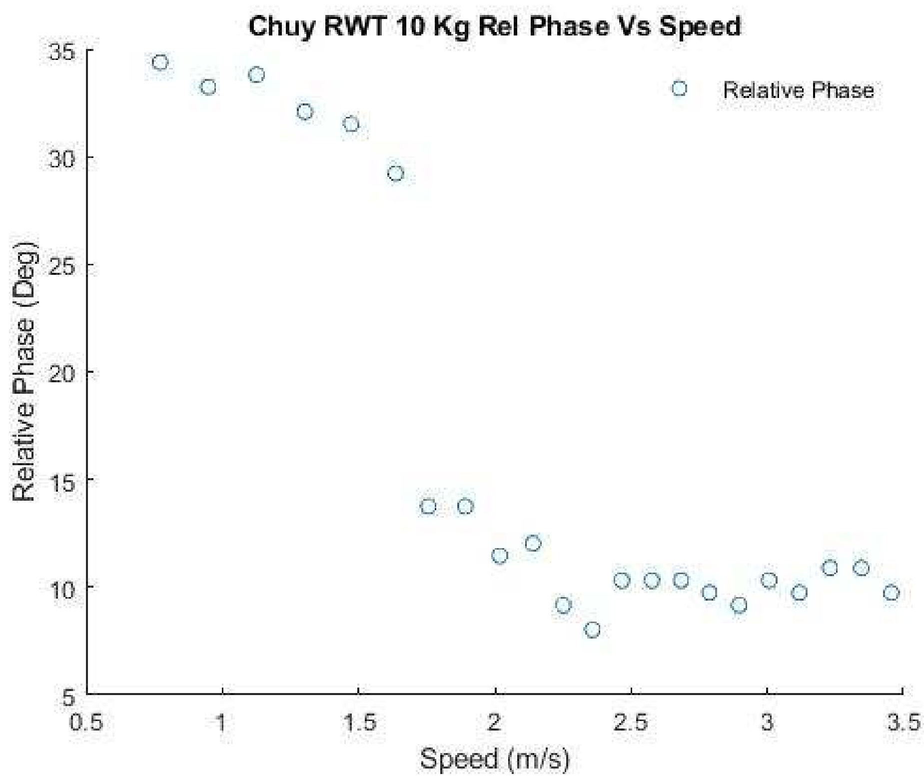

Fig. 149. Subject 2 Chuy relative phase vs speed on the RWT trial with 10 kg added weight.

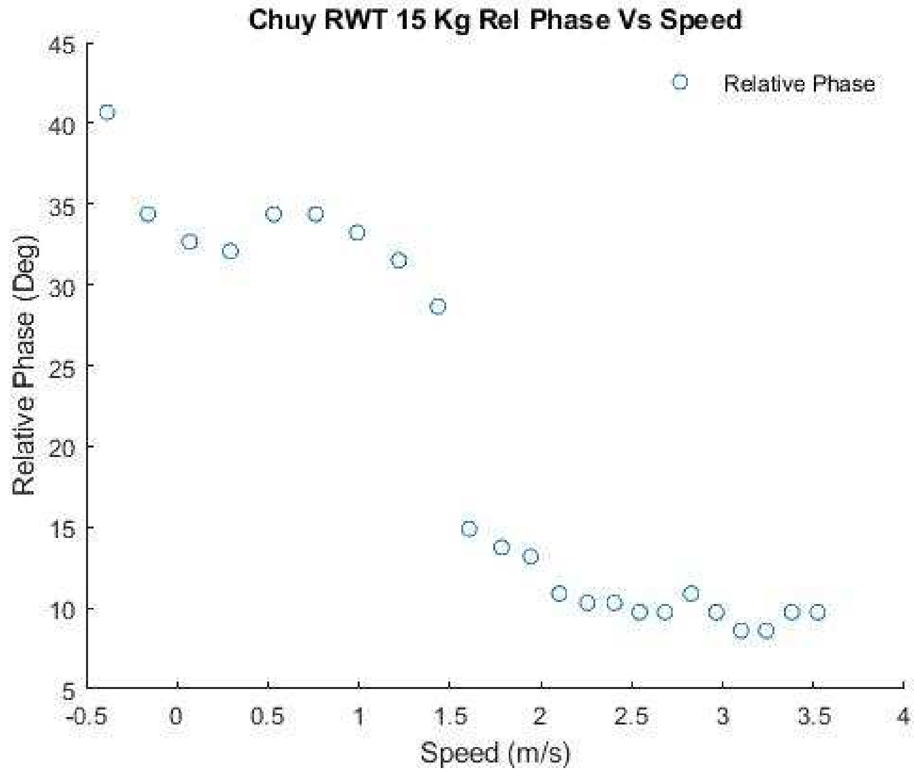

Fig. 150. Subject 2 Chuy relative phase vs speed on the RWT trial with 15 Kg added weight.

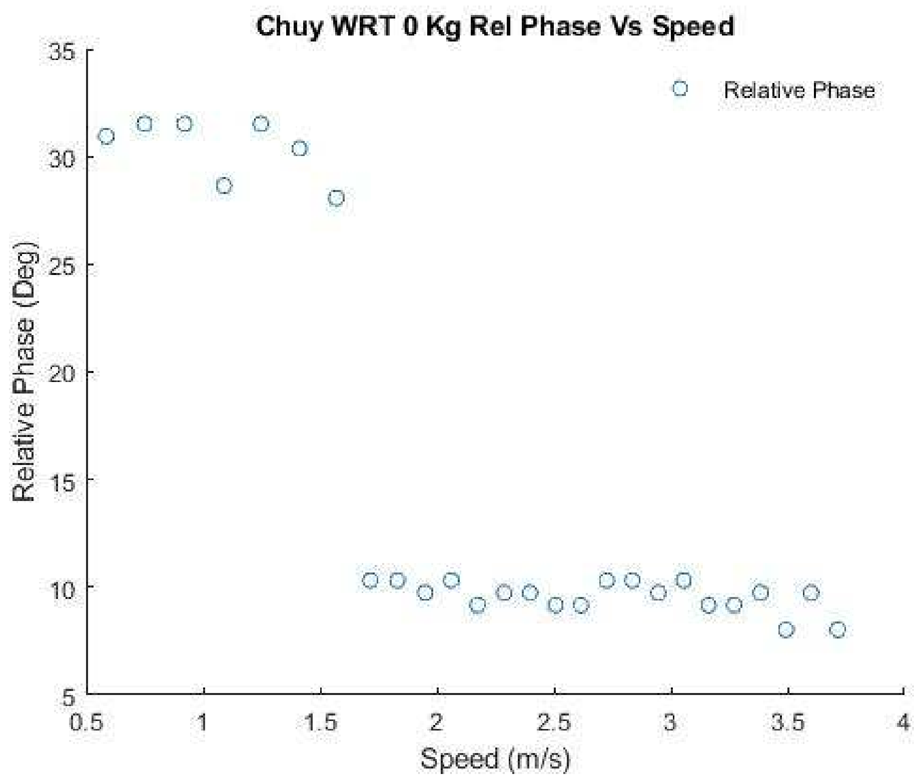

Fig. 151. Subject 2 Chuy relative phase vs speed on the WRT trial without added weight.

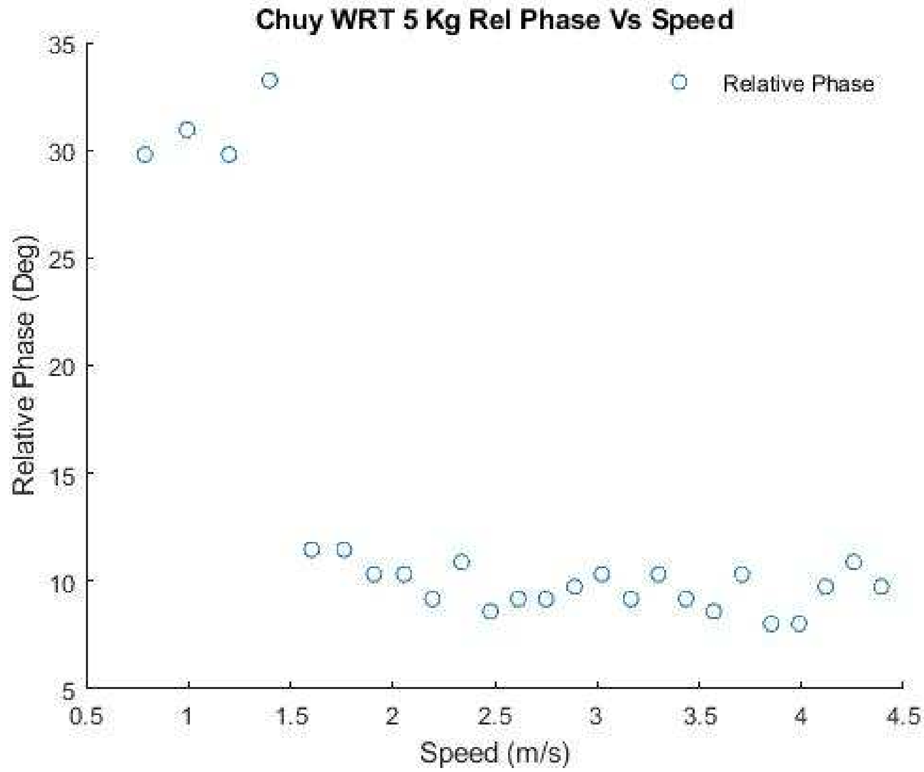

Fig. 152. Subject 2 Chuy relative phase vs speed on the WRT trial with 5 Kg weight.

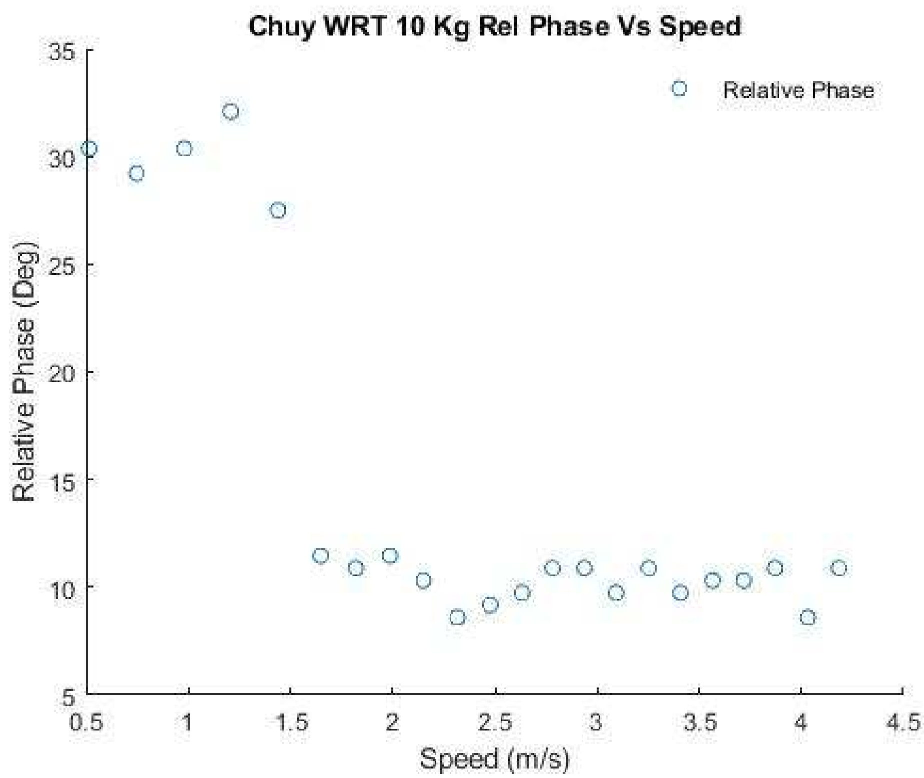

Fig. 153. Subject 2 Chuy relative phase vs speed on the WRT trial with 10 Kg added weight.

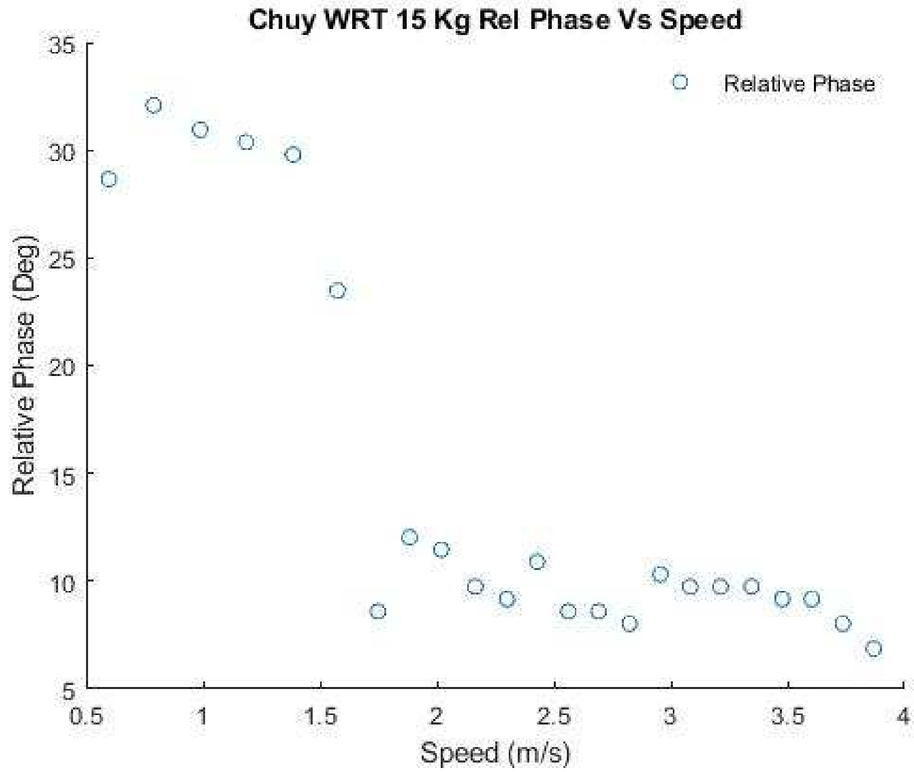

Fig. 154. Subject 2 Chuy relative phase vs speed on the WRT trial with 15 Kg added weight.

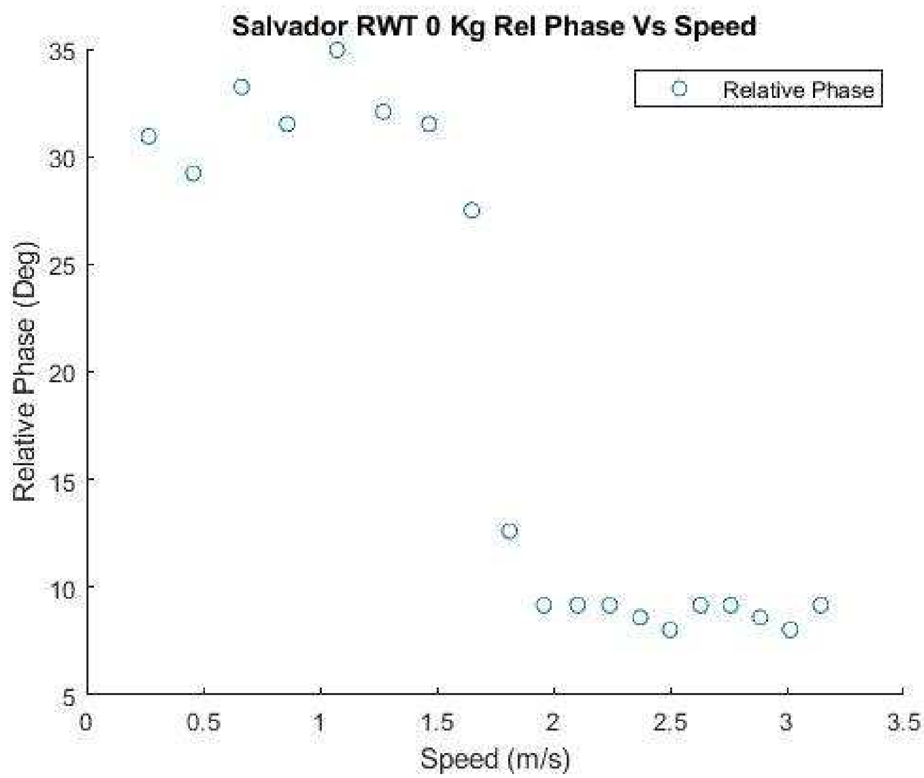

Fig. 155. Subject 3 Salvador relative phase vs speed on the RWT trial without added weight.

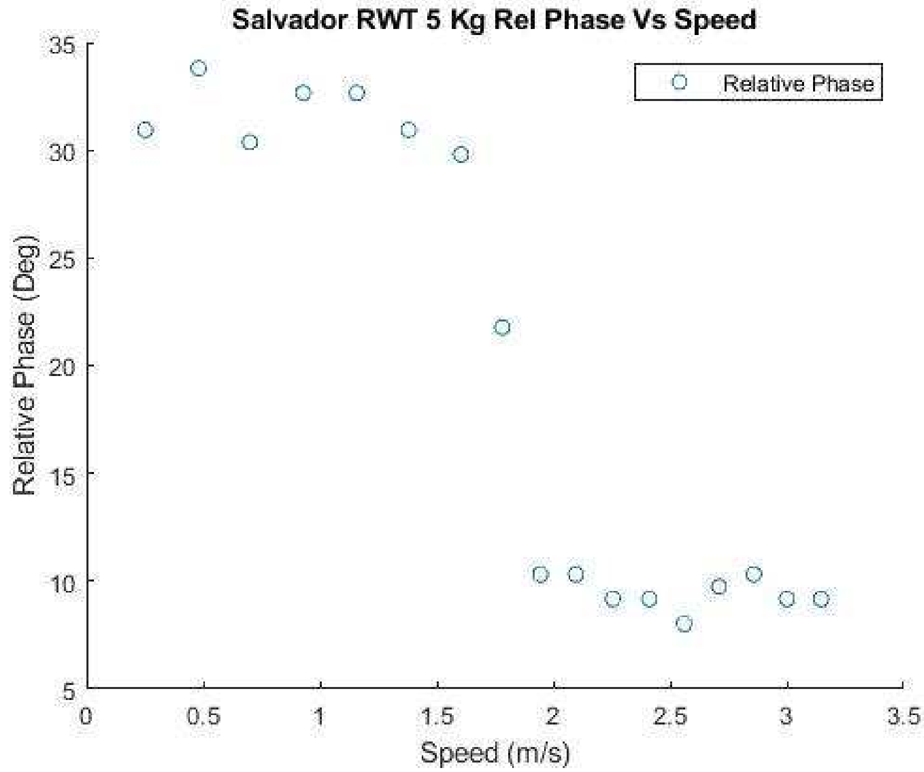

Fig. 156. Subject 3 Salvador relative phase vs speed on the RWT trial with 5 Kg added weight.

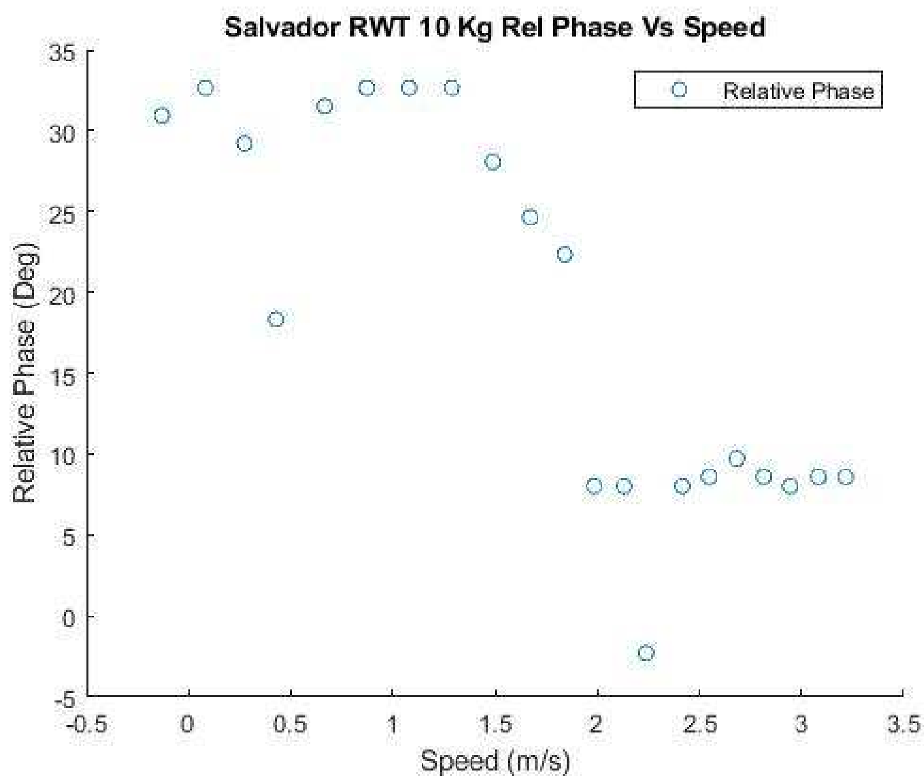

Fig. 157. Subject 3 Salvador relative phase vs speed on the RWT trial with 10 Kg added weight.

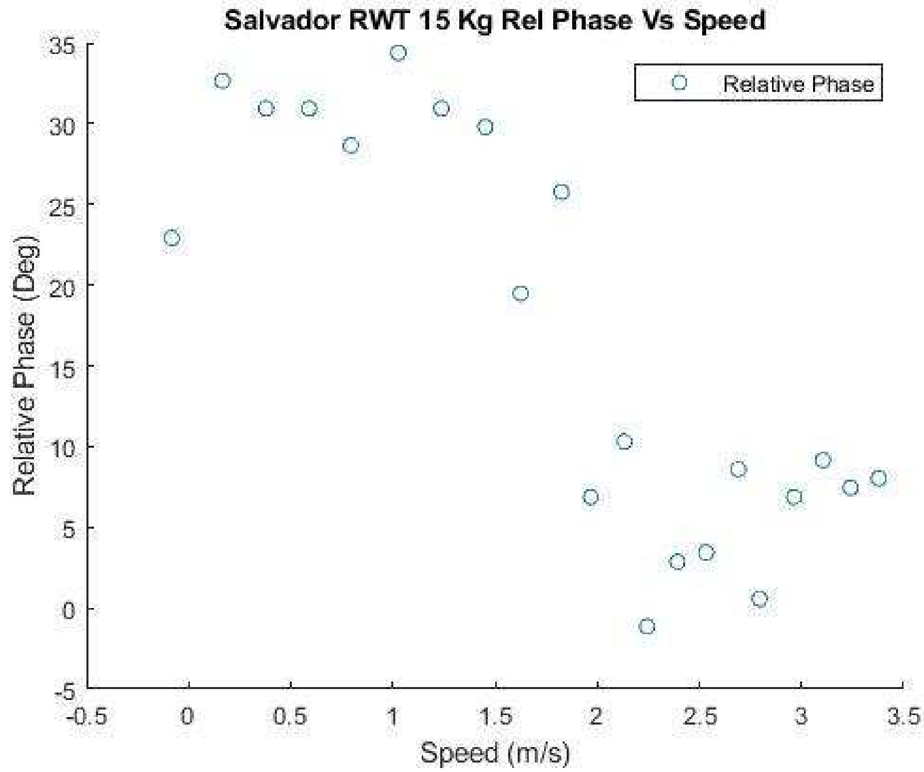

Fig. 158. Subject 3 Salvador relative phase vs speed on the RWT trial with 15 Kg added weight.

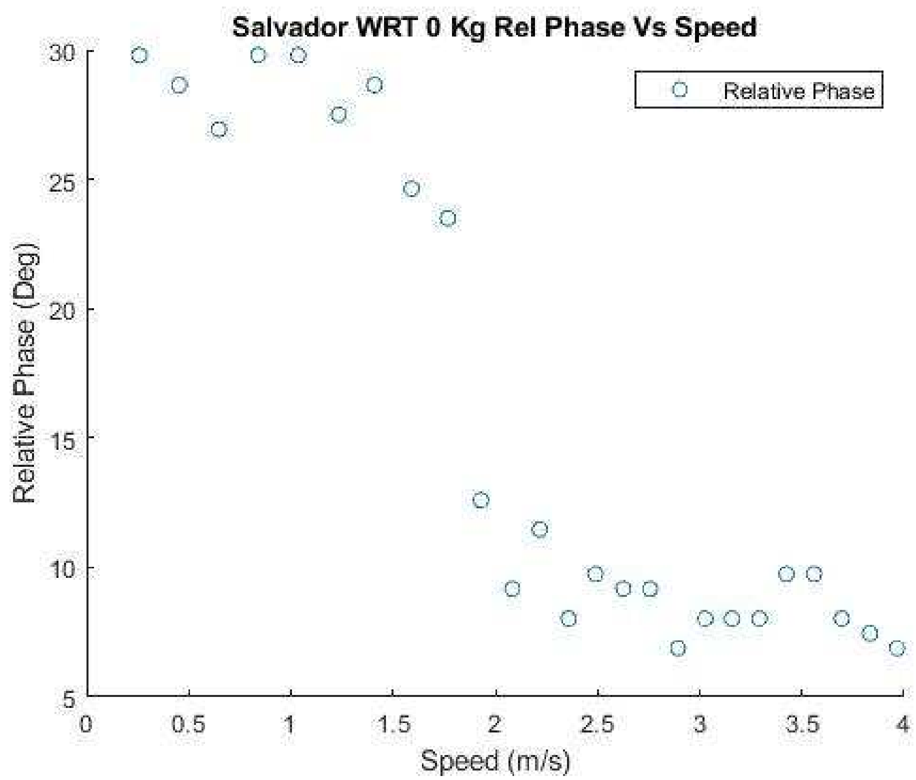

Fig. 159. Subject 3 Salvador relative phase vs speed on the WRT trial without added weight.

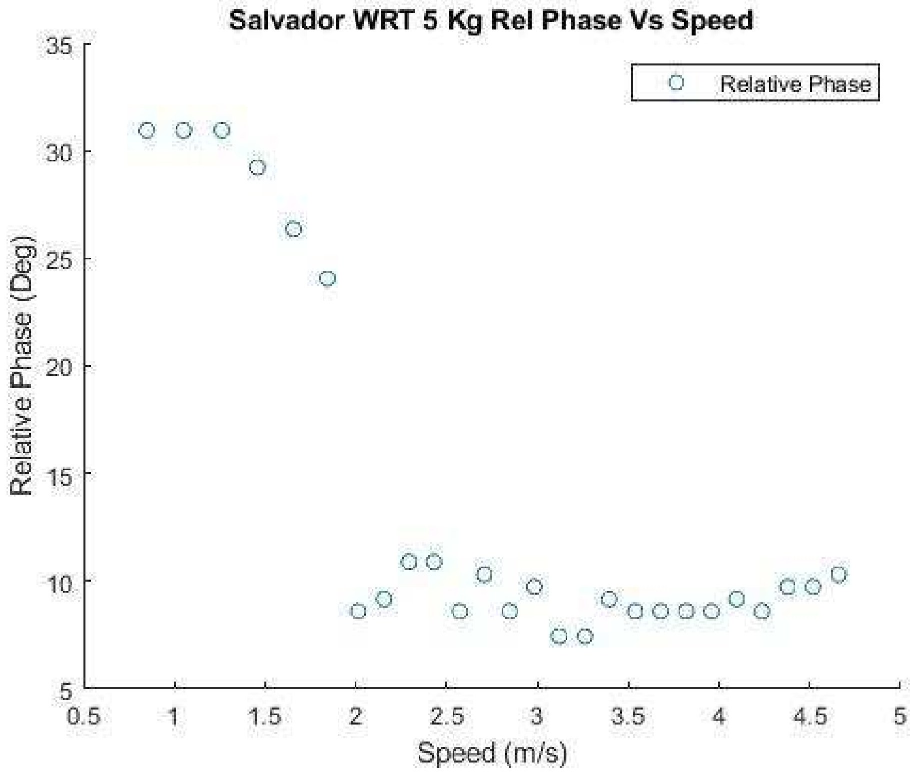

Fig. 160. Subject 3 Salvador relative phase vs speed on the WRT trial with 5 Kg added weight.

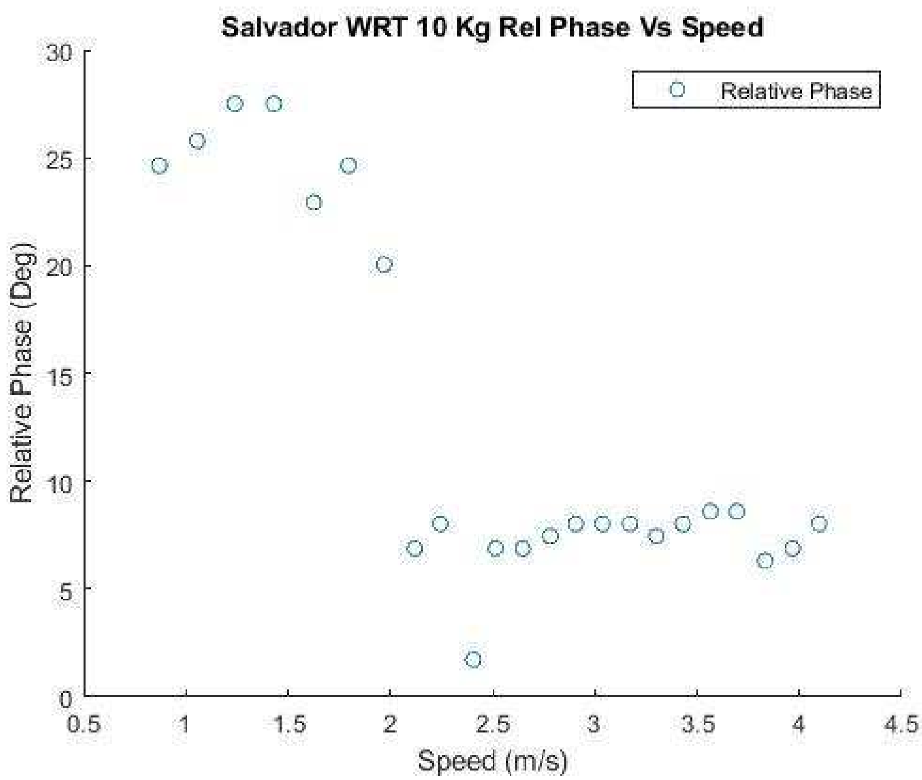

Fig. 161. Subject 3 Salvador relative phase vs speed on the WRT trial with 10 Kg added weight.

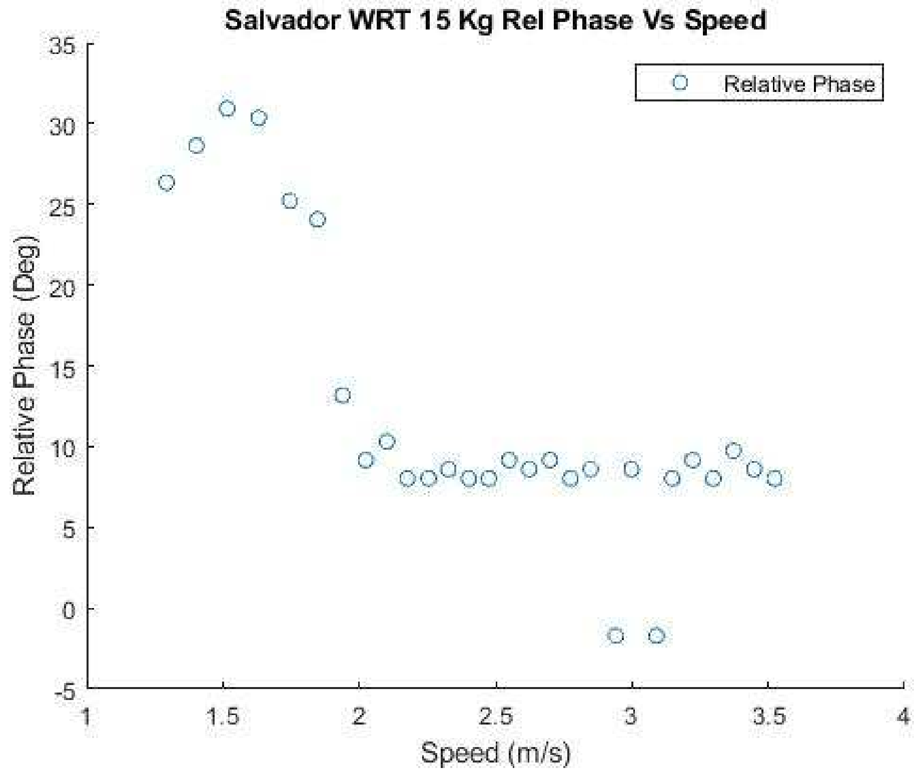

Fig. 162. Subject 3 Salvador relative phase vs speed on the WRT trial with 15 Kg added weight.

BIOGRAPHICAL SKETCH

Salvador Baruch Alcorta Bautista was born in October 23rd 1991. He has a Bachelors in Mechatronics Engineering in Reynosa, at the Univesidad Tecnologica de Tamaulipas Norte from 2012, and a Master of Science in Mechanical Engineering, specialized on Biomechanics from the University of Texas Rio Grande Valley, earned on August 2021. His permanent email is Salvador.alcorta.bautista@gmail.com.

Salvador has been working on the automation and manufacturing industry since January 2012, with experience in machinery design, manufacturing processes, metal working and has started his own company in Mexico.